

Umetco Minerals Corporation



P.O. BOX 1029
GRAND JUNCTION, COLORADO 81502
☎ (970) 245-3700

December 3, 2001

ATTENTION: Document Control Desk
Mr. Melvyn Leach, Chief
U. S. Nuclear Regulatory Commission
Fuel Cycle Licensing Branch, NMSS
Mail Stop T-8A33
Two White Flint North
11545 Rockville Pike
Rockville, MD 20852-2738
Attn: Elaine Brummett

RE: **Gas Hills, Wyoming License Number SUA-648, Docket #40-0299**
ACL Application Revisions

Dear Mr. Leach:

Enclosed please find three copies of revised pages to *Final Application for Alternate Concentration Limits For Gas Hills, Wyoming, May 2001*, submitted to the NRC by Umetco via letters dated May 11, 2001 and May 18, 2001. These revisions are submitted to address various hydrological and geochemical concerns of the NRC staff and are summarized in the attached table.

A *Groundwater Monitoring Plan* has been incorporated into the ACL application as Appendix M. The monitoring plan is also being provided to DOE for review (under separate cover).

NRC approval of the *ACL Application* will result in various amendments to Umetco's radioactive materials license referenced above. Accordingly, Umetco proposes the following language for amendment of license conditions 10B, 35, and 59.

License Condition 10B – EDIT existing LC 10B as follows:

- B. *Provide by September 30th of each year, a current organizational chart and details of the authority and responsibility of each level of management, noting any changes. This submittal will be included in the groundwater ~~corrective-action~~ monitoring review, due each September 30th.*

License Condition 35 – REPLACE existing LC 35 with the following:

Alternate Concentration Limits (ACLs) contained in Umetco's submittals dated May 11, 2001, May 18, 2001, July 30, 2001 and December 3, 2001, have been approved for this site. The licensee shall implement a groundwater compliance monitoring program containing the following:

- A. *Conduct monitoring as described in the Groundwater Monitoring Plan (Appendix M) in the December 3, 2001 submittal referenced above. The licensee shall submit monitoring data by September 30th of each year.*
- B. *Comply with the following ACLs in the western flow regime at Point of Compliance (POC) wells MW1 and MW21A:*

Rec'd copy from
NMSS
12/12/01
NMSSOIPublic

Arsenic = 1.8 mg/l, beryllium = 1.64 mg/l, gross alpha = 3,338 pCi/l, lead-210 = 35.4 pCi/l, nickel = 13.0 mg/l, combined radium-226 and 228 = 250 pCi/l, selenium = 0.161 mg/l, thorium-230 = 57.4 pCi/l, and uranium-natural = 11.9 mg/l.

- C. Comply with the following ACLs in the southwestern flow regime at Point of Compliance (POC) wells GW7 and GW8:

Arsenic = 1.36 mg/l, beryllium = 1.70 mg/l, gross alpha = 6,223 pCi/l, lead-210 = 46.7 pCi/l, nickel = 9.34 mg/l, combined radium-226 and 228 = 353 pCi/l, selenium = 0.53 mg/l, thorium-230 = 44.8 pCi/l, and uranium-natural = 34.1 mg/l.

- D. The licensee shall use, at a minimum, the following lower limits of detection for water quality analysis in mg/l, unless otherwise noted: arsenic = 0.01, beryllium = 0.01, nickel = 0.01, selenium = 0.005, total dissolved solids = 10, sulfate = 1.0, chloride = 1.0, iron = 0.1, pH = 0.1 (standard units), natural uranium = 0.0015, combined radium-226 and 228 = 1.0 pCi/l, thorium-230 = 1.0 pCi/l, lead-210 = 1.0 pCi/l, and gross alpha = 5.0 pCi/l.

License Condition 59 – EDIT existing LC as follows:

59. The licensee shall complete site reclamation in accordance with the approved reclamation plan ~~and groundwater corrective action plan~~, as authorized by License Condition Nos. 35, 54 and 58 in accordance with the following schedules:

- B. Reclamation, to ensure required longevity of the covered tailings ~~and groundwater protection~~, shall be completed as expeditiously as is reasonably achievable, in accordance with the following target dates for completion:

- 1) Placement of erosion protection as part of reclamation to comply with Criterion 6 of Appendix A of 10 CFR Part 40:

For the Inactive Impoundment – December 31, 2002.

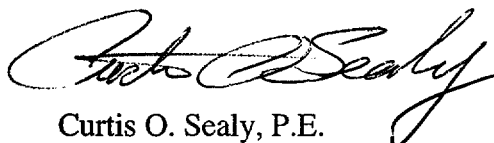
For the A-9 Impoundment – December 31, 2004.

For the Heap Leach Impoundment – December 31, 2001.

- 2) ~~Projected completion of groundwater corrective actions to meet performance objectives specified in the groundwater corrective action plan – December 31, 2001.~~

If you or your staff have any questions, please call me at (970) 256-8836 or Mr. Tom Gieck at (970) 256-8889.

Sincerely,



Curtis O. Sealy, P.E.
General Manager

COS:TEG:ses
Enclosures

c: **With enclosure:**
Wyoming DEQ (Mark Moxley – Letter Only)
Wyoming DEQ (Roberta Hoy)
BLM Casper (Bob Specht)
BLM Lander (Fred Georgeson)

Attachment 1 – Table of November 2001 Edits Gas Hills ACL Application

All CHANGED pages reflect new date of November 2001. UNCHANGED pages retain May 2001 date.

Page #	Edit
Cover	CHANGED date
Exec Summary	1 st paragraph: DELETED “received after review of the draft submittals, dated February 1999 and January 2001”
Exec Summary	11 th paragraph: DELETED “below background levels at the point of exposure” & ADDED “levels that are protective of human health and the environment”
Exhibit A	ADDED
Contents i – iii	CHANGED according to text changes
Contents vii	ADDED Appendix M Monitoring Plan
1-1	4 th paragraph 3 rd line: DELETED “below” & ADDED “within the range of”
1-7	5 th paragraph 5 th line: ADDED “within the range of”
1-7	6 th paragraph 2 nd line: ADDED “within the range of”
2-6	Last paragraph: CHANGED “Susquehana” TO “Susquehanna”
2-8	Last paragraph: DELETED “valves” & ADDED “values”
2-9	1 st paragraph 5 th line: CHANGED “(Figures G-15)” TO “(Figure G-15)”
2-9	1 st paragraph 7 th line: CHANGED “(Figure 3.17)” TO “(Figure G-17)”
2-10	2 nd paragraph 6 th line: CHANGED “MW10D” TO “MW10”
2-10	2 nd paragraph 7 th line: CHANGED “abandonedment” TO “abandonment”
2-10	5 th paragraph 5 th line: CHANGED “drilled recently drilled” TO “drilled”
2-10	Last paragraph 2 nd line: DELETED “ulations.” after 1979
2-11	1 st paragraph: CHANGED spacing because of last paragraph change on 2-10
2-12	Last paragraph 4 th line: DELETED “MW7”
2-12	Last paragraph last line: CHANGED “MW10B” to “MW10D”
2-16	2 nd paragraph 5 th line: CHANGED “because does not” TO “because it does not”
2-17 thru 2-25	DELETED original 2.2.2 (& its subsections) & ADDED new 2.2.2 and 2.2.3, 2.2.4, 2.2.5, 2.2.6; those changes caused shift in pagination (FROM 2-17 through 2-25 TO 2-17 through 2-24)
2-23(was 2-24)	Section 2.3.2 1 st line: CHANGED “at or below background” TO “within the range of background values”
2-23 (was 2-24)	Section 2.3.2 6 th line: CHANGED “at or below background levels” TO “within background range”
2-23 (was 2-25)	Section 2.3.3 5 th line: CHANGED “at or below background” TO “within the range of background values”
3-5	4 th paragraph last line: CHANGED “MW21” to “MW21A”
3-5	5 th paragraph 3 rd line: ADDED “reduction in tailings seepage and subsequent”
3-14	5 th paragraph 7 th line: CHANGED “at a specified” TO “at specified”
3-14	6 th paragraph 8 th & 9 th lines: ADDED “within the range of”
4-1	1 st paragraph 8 th line: DELETED “at or” & ADDED “within the range of”
4-1	2 nd paragraph 8 th line: DELETED “below” & ADDED “within the range of”
4-1	CHANGED: “4.1 METHODOLOGY” to “4.1 Methodology”
4-2	CHANGED: “4.2 RESULTS” TO “4.2 Results”
4-4	Last paragraph 2 nd line: DELETED “below” & ADDED “to within the range of”
4-5	DELETED 3 rd paragraph & ADDED new 3 rd , 4 th , 5 th , 6 th paragraphs; (old 4 th paragraph became 7 th paragraph)
Table 2-9	CHANGED Modeled Values in 3 rd & 5 th columns; ADDED “Maximum” to 3 rd & 5 th columns; DELETED Non-Licensed Constituents portion; CHANGED end note re: composite parameters
Table 2-10	CHANGED values in 3 rd & 5 th columns (POE Values); CHANGED “Background” TO “Background Range” in 3 rd & 5 th columns; DELETED comments column; CHANGED end notes
Table 2-14	CHANGED values in 2 nd column (Maximum Modeled Value at POE Locations)
Appendix B	REPLACED entirely
Appendix C	REPLACED text (tables remain the same); REPLACED Figures C-39 through C-46 with C-39 through C-48
Appendix M	ADDED

**Final
Application for
Alternate Concentration Limits
For
Gas Hills, Wyoming**

Umetco Minerals Corporation
2754 Compass Drive, Suite 280
Grand Junction, Colorado 81506

November 2001

EXECUTIVE SUMMARY

Umetco Minerals Corporation is submitting the following application to revise groundwater protection standards at its facility in Gas Hills, Wyoming. The document supports Alternate Concentration Limits at the Points of Compliance that are protective of human health and the environment at the Point of Exposure. This document has been revised to incorporate responses to the U. S. Nuclear Regulatory Commission comments.

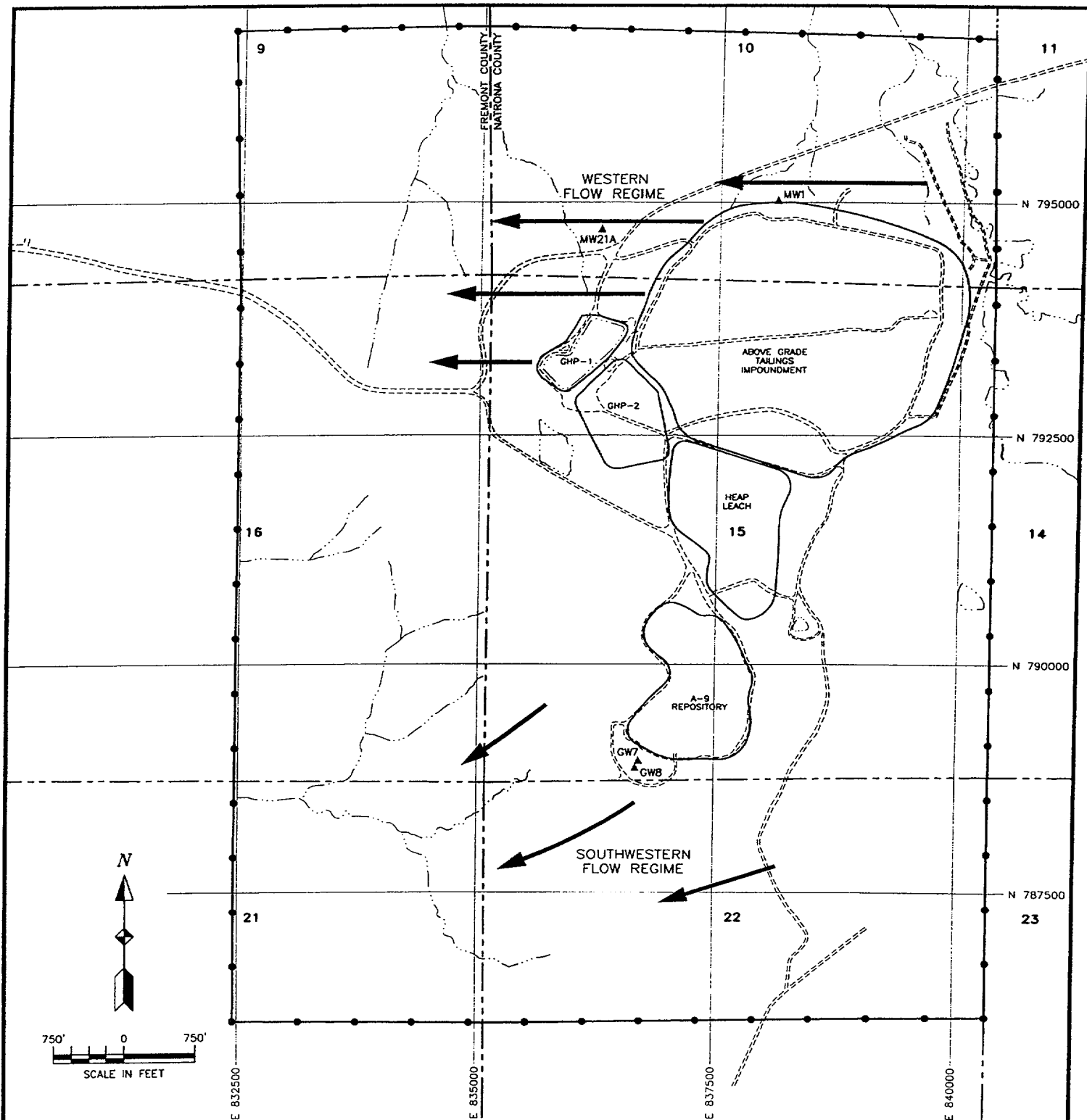
Umetco is requesting Alternate Concentration Limits for two flow regimes in the Wind River aquifer (see Exhibit A) as follows:

- A western flow component in the deep, reducing portion of the aquifer, and
- A southwestern flow component in the shallow, oxidized portion of the aquifer.

The Western Flow Regime underflows the Above Grade Tailings Impoundment. Point of Compliance wells MW1 and MW21A monitor radial and westerly flow from the Above Grade Tailings Impoundment, respectively. The Southwestern Flow Regime underflows the A-9 Repository. Point of Compliance wells GW7 and GW8 monitor groundwater quality in the vicinity of the A-9 Repository.

Revised groundwater protection standards are justifiable for the following reasons:

- The present groundwater protection standards are not representative of ambient conditions.
- The occurrence of widespread ambient contamination is a result of naturally-occurring uranium mineralization and the effects of mining and reclamation activities not related to milling operations.
- The naturally-occurring conditions and impacts from mining and reclamation are indistinguishable from groundwater impacts associated with milling.
- It is technically impracticable and economically infeasible to remediate groundwater to present groundwater protection standards. Corrective action alternatives would require between 80 and 200 years of extraction and treatment at net present value costs of \$30 to \$100 million. Furthermore, additional corrective action would not improve water quality from its current class of use because of widespread ambient contamination.
- The Alternate Concentration Limit values at the Points of Compliance will be reduced by natural attenuation to levels that are protective of human health and the environment.
- The proposed Alternate Concentrations Limits are As Low As Reasonably Achievable.
- The U. S. Department of Energy has accepted the proposed site boundaries for the Umetco Gas Hills facility, pending approval of the Alternate Concentration Limits by the U. S. Nuclear Regulatory Commission, resolution of property and title issues, and any other outstanding issues that may arise.



LEGEND:

- — PROPOSED LONG TERM CARE BOUNDARY
- GW8 ▲ — POINT OF COMPLIANCE MONITOR WELLS
- ← — GROUNDWATER FLOW DIRECTION
- — SECTION LINE
- 15 — SECTION DESIGNATION
- N 787500 — UMETCO SITE 2500' GRID SYSTEM
- UNPAVED ROAD
- SURFACE WATER

UMETCO MINERALS CORPORATION

PLAN VIEW

GAS HILLS SITE

APRIL 2001

EXHIBIT A

Contents

1.0 GENERAL INFORMATION.....	1-1
1.1 Introduction.....	1-1
1.2 Facility Description.....	1-1
1.2.1 Physiography and Meteorology.....	1-2
1.2.2 Mining History.....	1-2
1.2.3 Milling History.....	1-2
1.3 Extent of Groundwater Contamination.....	1-4
1.3.1 Geology.....	1-4
1.3.2 Hydrology	1-4
1.3.3 Geochemistry	1-6
1.4 Current Groundwater Protection Standards	1-7
1.5 Proposed Alternate Concentration Limits.....	1-7
1.6 Proposed Long-Term Care Boundary	1-7
2.0 HAZARD ASSESSMENT.....	2-1
2.1 Source Term and Contaminant Characterization.....	2-1
2.1.1 Naturally-Occurring Mineralization.....	2-1
2.1.1.2 Impacts from Mining and Reclamation	2-3
2.1.2 Mill-Related Constituents	2-5
2.1.2.1 Mill and Heap Leach Operations	2-5
2.1.2.2 Chemical Composition of Tailings	2-6
2.1.2.3 Indicator Parameters	2-7
2.1.2.4 Distribution of Constituents.....	2-7
2.1.2.5 Vertical Distribution of Constituents	2-9
2.1.2.6 Evaluation of the HW4	2-10
2.1.2.7 Constituent Seepage Rates	2-10
2.2 Transport Assessment.....	2-11
2.2.1 Hydrologic Assessment.....	2-11
2.2.1.2 Hydrostratigraphic Units.....	2-12
2.2.1.3 Groundwater Flow Direction and Hydraulic Gradient.....	2-13

Contents

2.2.1.4	Aquifer Properties	2-15
2.2.1.5	Groundwater Velocity	2-15
2.2.1.6	Groundwater Flow Model	2-16
2.2.2	Geochemical Assessment	2-17
2.2.3	Geochemical Model Code	2-18
2.2.4	Model Development	2-18
2.2.5	Model Simulations	2-19
2.2.6	Transport Modeling of Chloride and Sulfate	2-20
2.3	Exposure Assessment	2-20
2.3.1	Water Resource Classification and Uses	2-21
2.3.1.1	Area Description and Land Use	2-21
2.3.1.2	Current Water Resource Uses	2-21
2.3.1.3	Potential Future Groundwater Uses	2-22
2.3.1.4	Potential Future Uses of Hydraulically Connected Surface Water ..	2-22
2.3.2	Evaluation of Human Health Hazards	2-23
2.3.3	Evaluation of Environmental Hazards	2-23
2.3.3.1	Potential Effects on Aquatic and Terrestrial Wildlife Life	2-23
2.3.3.2	Potential Effects on Agricultural Crops and Plants	2-23
2.3.3.3	Potential Adverse Effects on Physical Structures	2-24
3.0	CORRECTIVE ACTION ASSESSMENT	3-1
3.1	Summary of the Corrective Action Program	3-1
3.1.1	A-9 Repository Groundwater Recovery System	3-2
3.1.2	AGTI Groundwater Recovery System	3-2
3.2	Corrective Action Program Evaluation	3-3
3.2.1	A-9 Repository Groundwater Recovery System Evaluation	3-3
3.2.2	Above Grade Tailings Impoundment Groundwater Recovery System Evaluation	3-4
3.3	ALARA Analysis for the Existing CAP	3-5
3.3.1	Estimated Exposure Duration	3-5
3.3.2	Exposed Population	3-6

Contents

3.3.3	Estimated Average Constituent Concentrations	3-6
3.3.4	Calculation of Collective Averted Dose from Ingestion of Groundwater	3-6
3.3.5	Calculated Averted Cost per Person-Rem	3-7
3.4	Calculated Benefits of 100 Percent Effective CAP	3-8
3.4.1	Estimated Collective Averted Dose for 100 percent effective CAP	3-8
3.4.2	Present Worth of Collective Averted Dose for 100 percent effective CAP...	3-9
3.4.3	Benefit from Averted Dose for 100 percent Effective CAP	3-10
3.5	Feasibility of Alternate Corrective Actions	3-11
3.5.1	Corrective Action Alternatives	3-11
3.5.2	Cost Analysis of Corrective Action Alternatives.....	3-13
3.6	As Low As Reasonably Achievable Demonstration	3-14
4.0	PROPOSED ALTERNATE CONCENTRATION LIMITS	4-1
4.1	Methodology	4-1
4.2	Results.....	4-2
4.2.1	Southwestern Flow Regime	4-2
4.2.2	Western Flow Regime.....	4-3
4.3	Summary	4-4
4.3.1	Proposed Implementation Measures	4-5
5.0	REFERENCES.....	5-1

Appendices

Appendix A	Ambient Groundwater Quality Characterization
Appendix B	Geochemical Model
Appendix C	Numerical Groundwater Flow Model
Appendix D	Water Rights Search Documentation
Appendix E	Basis for Alternate Concentration Limits
Appendix F	Correspondence Associated with Site Transfer
Appendix G	Isoconcentration Maps
Appendix H	Time Versus Concentration Data for Deep Well Completions
Appendix I	Water Quality Data for DW3, HW3, and HW4
Appendix J	Constituent Concentrations in the Point of Compliance Wells
Appendix K	Analysis of Impact from Power Resources Incorporated In Situ Leach Uranium Mine Operations
Appendix L	Cost Tables for Alternative Corrective Actions
Appendix M	Monitoring Plan

1.0 GENERAL INFORMATION

1.1 Introduction

Umetco Minerals Corporation (Umetco) submits this application to revise groundwater protection standards (GWPS) for its facility in Gas Hills, Wyoming. This document supports the establishment of Alternate Concentration Limits (ACLs) as being protective of human health and the environment at the proposed point of exposure (POE). This application was prepared in accordance with 10 CFR 40, Appendix A (Criteria 5B(5) and 5B(6)) and generally follows *Staff Technical Position Alternate Concentration Limits for Title II Uranium Mills* (NRC 1996). Upon acceptance and approval of the ACLs, Umetco proposes to eliminate the groundwater corrective action program (CAP) that is being conducted in accordance with U.S. Nuclear Regulatory Commission (NRC) Source Materials License SUA-648, Docket No. 40-0299, Condition 35.

Staff Technical Position Alternate Concentration Limits for Title II Uranium Mills (NRC 1996) states that in making the present and potential hazard finding, the NRC will consider 19 factors related to potential adverse effects on water quality for the site. Table 1.1 lists these 19 factors, and provides text references for each factor to be addressed.

The CAP was implemented to abate milling impacts to groundwater by reducing constituent concentrations at point of compliance (POC) wells to the GWPS set forth in License SUA-648. However, ambient groundwater conditions render the current GWPS at the POC wells impractical and unattainable. Mineralization, mining, and reclamation activities have caused widespread ambient groundwater contamination that is unrelated to but inseparable from milling impacts. The characterization of ambient groundwater quality is presented in Appendix A.

These ambient conditions make reduction of constituent concentrations to the current GWPS technically impracticable at the POC wells in the Wind River aquifer; however, geochemical and hydrologic processes reduce constituent concentrations to values within the range of background that are protective of human health and the environment at the proposed POE. The proposed POE is the proposed long-term care boundary (LTCB). Geochemical and groundwater flow models were used to evaluate the effects of these processes on the distribution and movement of constituents. The results of the geochemical modeling are provided in Appendix B and the results of the groundwater flow model are presented in Appendix C. Appendix D contains information on the water rights search. The basis for the proposed ACLs used in the geochemical model is presented in Appendix E. Copies of correspondence regarding the site transfer are in Appendix F.

1.2 Facility Description

Gas Hills is located in Fremont and Natrona Counties, Wyoming, approximately 60 miles east of Riverton in a remote area of central Wyoming (Figure 1.1). The site lies within the Gas Hills Uranium District of the Wind River Basin, in portions of Sections 10, 15, 16, and 22, Township 33 North, Range 89 West. The Restricted Area (RA), including tailings disposal and heap leach area, consists of approximately 542 acres, of which Umetco owns 280 acres. The site plan map,

1.4 Current Groundwater Protection Standards

The GWPS established in 1989 in Source Materials License SUA-648, Condition 35 were based on short-term monitoring conducted approximately ten years ago from background wells LA2 and MW2 (Figure 1.18). The GWPS listed in Table 1.3 are currently applied to the two POC wells in the vicinity of the AGTI (MW1 and MW21A), and the two POC wells in the vicinity of the A-9 Repository (GW7 and GW8).

Background water quality is defined as follows:

“...the chemical quality of water that would be expected at a site if contamination had not occurred from the uranium milling operation. Ambient contamination from uranium mineral bodies, mining operations, or other human activities are considered as part of the background water quality.” (NRC 1993)

The GWPS currently prescribed in the license do not account for the widespread ambient contamination present at Gas Hills resulting from mineralization and mining activities.

1.5 Proposed Alternate Concentration Limits

Based on the results of the hazard assessment and analytical data from the site monitoring network, Umetco has developed site-specific ACLs that are protective of human health and the environment at the POE and are “As Low As Reasonably Achievable” (ALARA). The proposed ACLs are presented in Table 1.4. The hazard assessment indicates geochemical conditions result in attenuation of constituent concentrations to within the range of background levels before reaching the proposed POE, regardless of whether these constituents are derived from mineralization, mining, or milling activities.

The location of the POE was selected to ensure a sufficient distance for attenuation of licensed constituents to within the range of background levels. The distance from the POC to the POE was based on the results of the geochemical and groundwater flow models (Appendices B and C respectively). Additional information supporting the proposed ACLs is provided in Section 4.0.

1.6 Proposed Long-Term Care Boundary

The LTCB coincides with the POE determined from the results of the geochemical (Appendix B) and groundwater models (Appendix C). The land to be transferred to the U.S. Department of Energy (DOE) for long-term surveillance and maintenance is shown on Figure 1.19. The legal description of the area within the LTCB is as follows:

All of Section 15, the north half of Section 22, the northeast quarter of Section 21, the east half of Section 16, the southeast quarter of Section 9, and the south half of Section 10, Township 33 North, Range 89 West, 6th Principal Meridian.

The Uranium Mill Tailings Radiation Control Act (UMTRCA) of 1978 (42 USC § 7901) as amended, provides for reclamation and regulation of uranium mill tailings at two categories of mill tailings sites, *i.e.*, Title I and Title II. Title I includes former uranium mill sites that were unlicensed, as of January 1, 1978, and essentially abandoned. Title II includes uranium mill sites

Acid leaching of sandstone uranium ores contributed sulfuric acid to the tailings piles (Merritt 1971). Sodium chlorate and manganese dioxide were added to the process as oxidizers to bring the solution to an Eh between 0.400 and 0.425 volts. Additionally, ammonia gas was used as a neutralizer and ammonium nitrate was used as an eluant in the resin in pulp ion exchange process. Sodium chlorate, used as an oxidizer in later years resulted in maximum chloride concentrations in the process solution of 7,030 mg/l.

Mill tailings were placed in two areas: the AGTI and the A-9 Repository. During ore processing from 1960 to 1984, approximately 16 million tons of tailings were placed in the AGTI and the A-9 Repository.

Placement of tailings in the AGTI began in 1960. In 1969, the impoundment was expanded approximately 12 acres to the east, and in 1972 an additional 27 acres was added to the north in 1972. In 1974, the impoundment was expanded 55 acres to the east. The AGTI expansions are shown on Figure 2.6. The AGTI was used until 1979.

Tailings were placed in the A-9 Repository from December 1979 until 1984. During that period, approximately 1.6 million cubic yards of tailings were placed in the A-9 Repository. Additionally, between 1988 and 1990, 1.8 tons of tailings from the DOE Riverton Title I site were placed in the A-9 Repository. Based on review of the environmental assessment prepared by DOE June 1987, the Riverton tailings did not contribute to groundwater quality at the Gas Hills site. Specifically, the following factors were noted.

- Milling ceased in 1963, therefore the tailings dewatered approximately 25 years before placement at Gas Hills.
- A deposit of cobbly alluvium underlies the entire pile. The alluvium was relatively thick, ranging from 14 to 18 feet. Transport of tailings liquid was facilitated by the permeability of this underlying formation.
- The moisture content of the tailings averaged 6 percent.

2.1.2.2 Chemical Composition of Tailings

Approximately 465,000 tons of tailings slurry, containing 20 to 30 percent solids by volume (NRC 1980a), were discharged annually into the AGTI. Groundwater quality representative of chemical characteristics of the tailings placed in the AGTI is shown in Table 2.3. After tailings placement into the AGTI ceased in 1979, the impoundment was stabilized by placement of engineered cover materials. The AGTI and the adjacent heap leach area comprise approximately 215 acres.

The A-9 Repository was lined with a 3-foot compacted clay layer and equipped with a decant system to dewater the tailings. Tailings were placed into the A-9 Repository between 1980 and 1984. The chemical composition of tailings in the A-9 Repository is listed in Table 2.1. The impacts of the Susquehanna tailings in the A-9 Repository are minimal because the tailings were placed dry and capped with an interim cover.

Regimes. HW4 is used to monitor environmental conditions in perched water that represents the upgradient extent of the Southwestern Flow Regime. The “hot spot” identified at HW4 is limited in extent both vertically and laterally and will not impact groundwater quality at the POC wells. The basis for determining the ACLs is provided in Section 4.

In the Western Flow Regime, the highest concentrations for licensed constituents were generally observed at wells MWI43, MWI64, MWC55, and MW67 (Figures E-1 through E-9). These wells are located along the central and western parts of the AGTI. Typically the highest concentrations of selenium occurred at POC well MW1 with the exception of MW67 (Figure E-8).

For the Southwestern Flow Regime, the highest concentrations for the radionuclide constituents were generally observed at POC well GW7, and monitor well MW7 (Figures E-12, 13, 14, 16, 18). MW7 is located along the northern extent of the A-9 Repository. The highest concentrations for nickel and beryllium were recorded at GW3 and MW61 (Figures E-11 and E-15). The highest values for arsenic were observed at well PW7, which is located cross-gradient of the A-9 Repository and is considered a background well (Figure E-10). Selenium was highest at GW5 and RW2 (Figure E-17). The concentration plots did not indicate significant upward trends for any of the constituents although there was a sharp increase in radionuclide concentrations at POC well GW7 around 1996-97 followed by a gradual decrease (Figures E-10, 12, 13, 14, 16, 18).

Isoconcentration maps were developed from water quality data for the Southwestern and Western Flow Regimes. These maps are presented for arsenic, beryllium, nickel, selenium, lead-210, radium-226+228, thorium-230, natural uranium, and chloride for 1990, 1995, and 2000. The maps are included in Appendix G. When interpreting the maps, it must be noted that the data sets for each of the time periods are not identical. For example, installation of a new monitoring well between two of the reporting periods may cause the appearance of a significant change in the direction or rate of movement of a constituent plume.

As in the concentrations plots, the isoconcentration maps for the Western Flow Regime show the highest concentrations for arsenic, beryllium, nickel, natural uranium and radium-226+228 are generally beneath the western and central portions of the AGTI (Figures G-1 through G-5). The highest concentrations of selenium and lead-210 are found beneath the northern portion of the AGTI (Figures G-6 and G-7). Thorium-230 concentrations are sporadic, both temporally and spatially, and do not define a consistent plume (Figure G-8).

Monitor wells MW28 and MW71B are located directly downgradient and west of the AGTI. None of the licensed constituents were detected above the GWPS in either of these wells. Chloride has also been historically low at these locations (Figure G-9). These factors provide evidence that milling-related impacts have not reached these wells. However, because of ambient conditions radium-226+228 concentrations at these two wells and at MW77 located further to the west, exceed the Class III groundwater standard of 5 picoCuries per liter (pCi/l). The radium values confirm that ambient water quality downgradient of the site does not meet WDEQ classifications for domestic, agricultural, or livestock use.

For the Southwestern Flow Regime, the isoconcentration maps are also generally consistent with the data observed in the concentration trend plots. With the exception of HW4 as previously discussed, the highest concentrations of beryllium, lead-210, radium-226+228, thorium-230, and natural uranium are found in the vicinity of the POC well GW7 (Figures G-10 through G-14). Elevated arsenic concentrations are present in the vicinity of background location PW7 (Figure G-15). Selenium is highest at GW5 and RW2 (Figure G-16) and nickel is more diffusely distributed with highest concentrations at PW1 (Figure G-17). Chloride concentrations have generally been highest in the vicinity of GW5 (Figure G-18).

2.1.2.5 Vertical Distribution of Constituents

Mineralization, mining/reclamation, and mill-related impacts are limited to the uppermost portion of the groundwater where oxidizing conditions are present. In the vicinity of the site, the thickness of the Wind River Formation exceeds 300 feet. In the deep, more reducing portions of the aquifer, groundwater is not impacted. Evaluation of groundwater quality data from monitor wells completed in the deeper portions of the Wind River aquifer (MW28, MW30, MW70B, and MW71B) indicates that licensed constituents do not exceed current GWPS (Table 2.4) and vertical migration is not occurring (Figure 2.7 and 2.8). Concentration trend plots for the licensed constituents are included in Appendix H. Chloride would provide the earliest indication of milling-related impacts because it is non-reactive and does not attenuate. Chloride trend plots illustrate that there has been no significant increase in any of the four wells and that concentrations are low and within the range of background (Figure 2.7).

Recent well replacements provide additional comparative data between the Western and Southwestern Flow Regimes in the area of the A-9 Repository. In 1999, monitor wells MW6, MW7, and MW10, which had been completed above and/or across the mudstone aquitard, were abandoned and replaced with MW6D, MW7D, and MW10D. The replacement wells were completed beneath the mudstone unit (US Environmental Services 1999). Monitor well MW24D, installed adjacent to existing wells MW24 and DW4 (which were not abandoned), was also completed beneath the mudstone. DW4 is also a deep completion. A comparison of chloride data from the deep- and shallow-completed wells indicates that chloride concentrations are much higher in the shallow wells (Figure 2.8). Chloride levels are very low in most of the deep-completed wells with the exception of MW7D. Injection of treated water in the vicinity of MW7 between 1991 and 1995 resulted in a localized increase in the water table of approximately 80 feet (Figure 2.9). The increased hydraulic head in the area of MW7 may have forced shallow groundwater into the deeper aquifer system beneath the mudstone. The low chloride levels indicate that milling-impacted groundwater has not migrated into the deeper portions of the Wind River Aquifer except in areas where artificially induced vertical gradients may have temporarily facilitated such movement. The recharge mound associated with injection has dissipated and migration of milling-related constituents into the deeper portions of the Wind River Aquifer in the area of the A-9 Repository has ceased.

2.1.2.6 Evaluation of the HW4

Anomalously high concentrations of arsenic, beryllium, nickel, lead-210, thorium-230, natural uranium and sulfate have been detected in monitor well HW4. The increase in constituent concentrations at HW4 started gradually in early 1993 and then rapidly between mid-1997 and early 1998 (Appendix I). Field pH has been measured between 2 and 3 s.u. since 1993. The specific cause of the increase has not been determined although the source may be residual tailings seepage, experimental heap leach liquor, or laboratory leach field liquor. Regardless of the source, water level and water quality data demonstrate the limited vertical and lateral extent of the high concentrations.

Saturated thickness in HW4 is less than 10 feet and has been steadily declining since the well was installed in 1984 (Appendix I). The decline in water levels indicates that there is no source of recharge to the perched water zone. The perched zone does not extend to the north and terminates a few hundred feet to the west. Monitor well HW3, the nearest downgradient monitoring point to HW4 completed above the mudstone, has a saturated thickness of approximately 5 feet. The saturated thickness at monitor well MW10, located approximately 2500 feet west and southwest of HW4, was less than 5 feet at the time of its abandonment in 1999. The limited saturated zone, coupled with declining water levels, indicates a finite and diminishing volume of shallow groundwater above the mudstone north of the A-9 Repository.

As shown in the isoconcentration maps, constituent concentrations measured in surrounding monitor wells are typically an order of magnitude less than HW4 (Appendix G, Figures G-10 through G-18). Furthermore, HW3, located closest to HW4 and completed above the mudstone, is near or below the GWPS for all of the constituents, with the exception of nickel. This indicates that lateral migration from HW4 has been limited and has not reached HW3.

Monitor well DW3 is located adjacent to HW4 but is completed beneath the mudstone. Water quality data from DW3 indicates that all licensed constituents, except for radium 226+228, are below GWPS (Appendix H). Note that radium 226+228 was not anomalously high at HW4. The data confirm that the HW4 "hot spot" has not impacted the deeper aquifer.

Previous attempts to pump water from HW4 have provided minimal quantities of water. The well typically pumps dry within a matter of minutes (at rates of approximately 1 gpm) and then takes several days to recover. In order to determine if the low yield from this well is caused by poor or damaged well construction or is the result of intrinsic aquifer characteristics, an offset well was drilled. The replacement well was located within ten feet of HW4 and was drilled to the top of the mudstone unit (total depth of 144 feet). No groundwater was encountered in the borehole during drilling. Subsequent attempts to measure the water level in the borehole a week after drilling indicated the well was still dry. The lack of saturated conditions within 10 feet of HW4 confirms the limited extent of the "hot spot".

2.1.2.7 Constituent Seepage Rates

Based on water balance calculations seepage rates for the AGTI reached a maximum of approximately 100 gallons per minute (gpm) in 1979. Seepage declined rapidly following closure of the AGTI. Current seepage rates are estimated to be between 20 and 30 gpm based on

modeling (SMI 1997). The model indicates continuous decline in seepage rates to less than 1 gpm within the next 10 to 20 years. Stabilization of the tailings and placement of an engineered clay cover over the AGTI have eliminated infiltration of surface water.

The 1998 seepage rate for the A-9 Repository was estimated at 3.3 gpm (Shepherd Miller, Inc. 1998). Continued pumping under the current CAP will extract seepage from the A-9 Repository, but will also continue to import constituents related to natural-occurring conditions and mining activities.

2.2 Transport Assessment

The transport assessment evaluated potential migration pathways for regulated constituents. Key components were hydrologic and geochemical factors that control solute transport. The hydrologic component defines the rate and direction of groundwater flow within the aquifer. The geochemical component considers the reduction in solute concentrations that occur along groundwater flowpaths. The Wind River aquifer directly below the Gas Hills site was the focus of this assessment because it is the uppermost aquifer and no other aquifers are impacted by mill-related constituents.

The nearest aquifers above the Wind River are the Miocene Split Rock, Oligocene White River, and the Eocene Wagon Bed Formations. These formations are found in outcrops along the Beaver Divide several miles to the south and are topographically 500 to 1,000 feet or more above the water levels observed at Gas Hills. The presence of the topographic divide indicates that groundwater from the site can not reach the post-Wind River aquifers to the south. Therefore, aquifers above the Wind River were not evaluated in this transport assessment.

Mineralization, mining/reclamation, and mill-related impacts are limited to the uppermost occurrence of groundwater where oxidizing conditions are present. In the deep, more reducing portions of the aquifer, groundwater is not impacted. Evaluation of groundwater quality data from monitor wells completed in the deeper portions of the Wind River indicates that vertical migration is not occurring (as discussed in Section 2.1.2). For this reason, aquifers beneath the Wind River aquifer are not considered in this assessment.

The direction of groundwater flow from the site is predominately west and southwest as shown on Figure 1.16. The Wind River Formation is truncated by Paleozoic rocks of the Granite Mountains south of the site. To the west and northwest, the Wind River Formation pinches out against the Cretaceous Cloverly Formation, Cody Shale, Frontier Formation and Mowry Shale, the Jurassic Nugget Sandstone, Sundance and Morrison Formations, and the Triassic Chugwater Formation. All of these formations are considered aquitards with the exception of the Cloverly Formation and the Nugget Sandstone. Those formations receive recharge west of the site on the flanks of the Dutton Basin Anticline and discharge into the Wind River Formation. Consequently, because groundwater does not discharge into any other aquifers within several miles of the site, the transport assessment focused on evaluating the Wind River aquifer.

2.2.1 Hydrologic Assessment

Direction and velocity of groundwater flow are critical hydrologic factors that determines solute transport. Determination of the groundwater flow direction is based on water-level data that are

routinely collected from an extensive monitor well network (Figure 1.18). The velocity of groundwater flow depends on hydraulic conductivity, hydraulic gradient, and porosity.

The hydraulic conductivity and porosity are intrinsic properties of the aquifer matrix and do not vary with time. Hydraulic conductivity estimates are derived from pumping tests. Porosity estimates are derived from core data and literature. Hydraulic gradient varies in time and space depending on changes to the groundwater flow regime. Under normal non-stressed conditions, changes in hydraulic gradients within an aquifer tend to be minor and occur gradually. When a groundwater flow regime is stressed (due to extraction, injection, mine dewatering, mounding from seepage, etc.) hydraulic gradients may change abruptly, resulting in measurable changes in groundwater flow velocity and direction.

2.2.1.2 Hydrostratigraphic Units

As previously described, two flow regimes, or hydrostratigraphic units, are defined and characterized for purposes of the ACL application. The Southwestern Flow Regime includes the upper portion of the Wind River Formation and is present beneath the A-9 Repository. It is characterized as a shallow unconfined system with a southwesterly flow direction and a saturated thickness typically less than 20 feet. This shallow flow system generally occurs within 150 feet of the ground surface and contains most of the ore-grade uranium mineralization. Oxidizing conditions prevail in the vicinity of the A-9 Repository, becoming more reducing away from the site. The Southwestern Flow Regime is absent beneath the AGTI and west of the site. The Southwestern Flow Regime, where present, is separated from the Western Flow Regime by a mudstone unit.

The mudstone unit is an aquitard that acts as a confining unit between the Southwestern and Western Flow Regimes. The base of the mudstone unit is the top of the Western Flow Regime. The mudstone varies from 20 to 40 feet in thickness across the site and dips to the south-southwest at approximately 1 degree. The mudstone unit crops out in surface drainages along the north side of the AGTI.

The Western Flow Regime includes the lower portion of the Wind River Formation and lies beneath the mudstone unit. The Western Flow Regime is characterized as a deeper, more reducing system, a saturated thickness on the order of 300 feet, and a general flow direction to the west. The Western Flow Regime is confined in areas to the south where the Southwestern Flow Regime is present. It is unconfined to the north, where the Southwestern Flow Regime is absent.

Hydrogeologic cross sections illustrate the absence of saturated conditions in the upper portion of the Wind River Formation north of the A-9 Repository and west of the AGTI (Figure 2.10). The north-south cross section (A-A') shows saturated conditions in the Southwestern Flow Regime (above the mudstone unit) in the vicinity of the A-9 Repository (wells MW24, MWI54, and MW7D). Note that the shallow water table is depressed in the vicinity of MW24 as a result of pumping under the CAP. Saturated conditions do not exist above the mudstone unit at the AGTI (wells MWC46, MWI66, MWC47A, MWC48, and MWC49). Between the A-9 Repository and the AGTI there is a transitional area where a perched water table is present above the mudstone (wells MW10 and MW10D). On the east-west cross section, the first occurrence of

presented in Table 2.5. Under current conditions, the calculated velocity of groundwater beneath and immediately west of the AGTI is between 0.04 to 0.3 ft/d. The travel time for groundwater beneath the western edge of the AGTI to reach monitor well MW77 (a distance of 3,800 ft) using the range of velocities, is between 34 and 2,600 years.

An estimate of groundwater velocity in the vicinity of the AGTI can be made indirectly by using water quality data from monitor wells MW28, and MW25. Chloride was present at monitor well MW25 at a concentration of 125 mg/l in March 1988. At that time, the chloride concentration at MW28 was 8 mg/l. As recently as January 1999, the chloride concentration at MW28 was 6 mg/l. Chloride is considered a conservative constituent because it does not chemically react in groundwater and should not be attenuated as it moves along a groundwater flowpath. Therefore, the levels of chloride observed at MW25 should eventually reach MW28 (with some minor attenuation due to dispersion and dilution). The distance between the two wells is approximately 400 feet. The time period from March 1988 to January 1999 is approximately 3,950 days. Chloride concentrations at MW28 have remained steady from March 1988 to January 1999 indicating that groundwater carrying the elevated chloride has not reached MW28. The distance of 400 feet divided by 3,950 provides an upper bound for groundwater velocity of 0.1 ft/d.

2.2.1.6 Groundwater Flow Model

A groundwater flow model was developed to evaluate groundwater flowpaths and velocities, mining impacts on the flow system, and the effectiveness of the current corrective action, as well as alternative corrective actions at the Gas Hills site. Additionally, the groundwater flow model was used to analyze the fate and transport of non-reactive conservative constituents, chloride and sulfate.

Three-dimensional analysis of groundwater flow and advective transport in the Wind River aquifer system was performed using MODFLOW (McDonald 1988), a finite difference groundwater flow model and MODPATH (Pollock 1989 and 1994), a particle-tracking model, both developed by the United States Geological Survey. Development and calibration of the model is described in Appendix C. The model was initially calibrated to current site hydrologic conditions. The calibrated model was then used for further analysis. Results of the model are summarized in the following paragraphs.

Variability in groundwater flowpaths and velocity was addressed using a probabilistic or stochastic modeling approach (Appendix C). One hundred simulations were performed using the stochastic model. Hydraulic conductivity was randomly varied over a range of 0.01 to 5 ft/d. In an effort to evaluate model simulations that were representative of the site hydrologic system, only the twenty simulations with the best fit to calibration statistics were selected for further analysis. Particle tracking was performed on those simulations to identify the range of flowpaths and groundwater velocity.

The range of flowpaths determined from the stochastic models was used to determine placement of the POE along potential groundwater pathways. All groundwater leaving the site via either the Southwestern or Western Flow Regime eventually intercepts a plane 2,600 feet west of the site. This plane was selected as the proposed west edge for the LTCB.

The average and maximum groundwater velocities for flowpaths in each of the twenty simulations for each flow regime were calculated (Appendix C). The maximum velocity calculated for the Western Flow Regime was 0.33 ft/d and the average of the twenty simulations was 0.15 ft/d. The maximum velocity calculated for the Southwestern Flow Regime was 0.28 ft/d and the average was 0.1 ft/d. The maximum velocities of 0.33 ft/d and 0.28 ft/d were used as an upper limit for the geochemical speciation model for the Western and Southwestern Flow Regimes, respectively. Geochemical model simulations were also run for both the Western and Southwestern Flow Regimes using a more typical and representative groundwater velocity of 0.167 ft/d as described in Section 2.2.2.

The average and minimum travel times to reach the LTCB from the downgradient edge of the AGTI and A-9 Repository for each stochastic simulation and each flow regime were also calculated (Appendix C). The minimum and average travel times for the Western Flow Regime were 30 and 101 years, respectively. The minimum travel time for the Southwestern Flow Regime was 40 years and the average was 139 years.

The groundwater flow model was also used to assess impacts on the flow system resulting from mining activities west, south, and east of the site (Appendix C). Of particular concern are the hydraulic properties of backfilled material used to reclaim many of the mines in the area. As previously discussed, there were no mine pits within the proposed LTCB that penetrated groundwater downgradient of the AGTI or A-9 Repository. However, some mines upgradient and east of the site penetrated groundwater and were reclaimed by backfilling. A sensitivity analysis was conducted to determine the impacts these mines might have on groundwater flow direction and velocity. Results of the sensitivity analysis indicate there were no perturbations to groundwater flow outside the range previously determined from the stochastic model simulations. Groundwater velocities also were within the range of the stochastic simulations.

The effectiveness evaluation of the CAP and the analysis of alternative corrective action are addressed in Section 3.0.

The groundwater flow (MODFLOW) and solute transport (MT3D, Zheng 1990) models were used to evaluate the reduction in concentrations of sulfate and chloride between the POC and POE as a result of advective processes. Description of the model is provided in Appendix C, and the results are summarized in Section 2.2.2. The groundwater flow and transport model was used because attenuation of these non-reactive constituents is not adequately addressed by the geochemical speciation model (PHREEQC). PHREEQC is used to evaluate migration and attenuation of constituents that are influenced and controlled by redox conditions and the neutralization capacity of the aquifer matrix (Section 2.2.2 and Appendix B).

2.2.2 Geochemical Assessment

The geochemistry of Wyoming type roll-front uranium deposits has been extensively studied and Gas Hills has been used as a type location for roll-front deposits (DeVoto 1978, Harshman 1974, King and Austin 1966). These studies have provided site-specific information on mineral phases and groundwater characteristics in the vicinity of ore zones, especially pH and Eh, which are two of the most important factors that control the solubility of the hazardous constituents. Figure 2.18 summarizes these conditions determined by Harshman (1966) for ore deposits at Gas Hills

and Shirley Basin, Wyoming. The Eh values range from +300 to -300 millivolts and the range of pH is from 4 to 8, depending on position relative to the ore deposit. The information summarized by Harshman (1966) is consistent with field measurements collected in 1998 to determine site specific redox conditions. Measurements were made for the ferrous/ferric iron redox couple, the sulfide/sulfate sulfur redox couple, and Eh using a platinum electrode. Sulfide/sulfate measurements were generally most consistent with Harshman's model of redox conditions, and Eh values indicated an increase in reducing conditions with distance from the site, where the lowest values occurred in areas containing ore deposits (Figure 2.19).

Data regarding site-specific redox conditions, in addition to recent groundwater results from monitoring wells, were used as input to the site geochemical model. The model is based on knowledge of groundwater compositions and geochemically reactive aquifer components present at Gas Hills, and utilizes geochemical principles based on the site conceptual geochemical model (Geraghty & Miller, Inc. 1996). The geochemical speciation and transport model PHREEQC was used to predict the concentrations of arsenic, beryllium, nickel, selenium, lead-210, radium-226+228, thorium-230, and natural uranium at the Point of Exposure (POE) for a 1,000-year period. Gross alpha concentrations at the POE were calculated based on the modeled concentrations of the alpha contributors (excluding uranium and radon).

2.2.3 Geochemical Model Code

The computer code PHREEQC (Parkhurst 1995) was chosen for this study to model chemical speciation, mass transfer, and mass transport (see Appendix B for modeling details). The geochemical model simulates advection and chemical reactions as water moves through a one-dimensional column, for distances simulating transport between the POCs and the POE. Dispersion is accounted for using a longitudinal dispersivity value of 50 m, and source reduction is also accounted for based on results of previous dewatering studies of the tailing impoundments (Appendix B). The MINTEQ database (Allison et al 1991) was used for this study because it contains several uranium species and phases applicable to Gas Hills conditions. Thermodynamic data for thorium were imported from the EQ3/6 database (Wolery 1992) and radium data were taken from Langmuir and Riese (1985). PHREEQC uses ion-association and Debye Huckel expressions to account for the non-ideality of aqueous solutions. The ion-exchange model assumes that the thermodynamic activity of an exchange species is equal to its equivalent fraction. The surface complexation module uses the diffuse double layer (Dzombak and Morel 1990) and the non-electrostatic surface complexation models (Davis and Kent 1990).

2.2.4 Model Development

A geochemical model was developed to simulate hazardous constituent transport along two pathways: (1) the Western Flow Regime POC to POE and (2) the Southwestern Flow Regime POC to POE. Because unique conditions are present in the two flow regimes, each was modeled separately. A local mudstone unit separates the Southwestern Flow Regime from the deeper Western Flow Regime. The southwestern flow is toward a proposed in-situ leach operation. The Western Flow Regime moves into regionally reduced portions of the Wind River aquifer. Both models assume a porosity of 15 percent, a hydraulic conductivity of one foot per day (ft/d) and a hydraulic gradient of 0.025, resulting in a groundwater velocity of 0.167 ft/d.

The model uses the AGTI as the primary source of mill-derived fluids associated with the Western Flow Regime. The model grid extends from the western edge of the AGTI, through POC well MW21A, and through monitoring wells MW28 and MW77 to the POE, approximately 4,600 feet from the edge of the AGTI. The model grid consists of 46 cells, each representing an aquifer unit 100 feet long (Figure 2.20). The model construction featured the regionally reduced conditions in the Wind River Formation in this area and the presence of an oxidized, carbonate-depleted halo at the downgradient edge of the AGTI. The Southwestern Flow Regime model uses the A-9 Repository as the primary source of mill-derived fluids. The model grid extends from POC well GW7, and through monitoring wells GW8 and MW74 to the POE, approximately 5,400 feet downgradient. The model grid for the Southwestern Flow Regime consists of 54 cells, each representing an aquifer unit 100 feet long (Figure 2.21).

Each cell of the Western and Southwestern Flow Regime model was assigned aqueous properties based on site-specific measurements. Native groundwater compositions from the January 2001 sampling of monitoring wells were used as the initial solutions in the model cells. For the initial source terms, the model conservatively incorporated the 95 percent upper confidence limit of the upper 95th quantile concentration of the hazardous constituents representing monitoring wells in the Upper and Lower Wind River Formation for the Southwestern and Western Flow Regimes, respectively (Appendix E). For the major ions, the input concentrations from the original ACL application were used (99th percentile of concentrations from selected wells). The decaying source terms used as the inflow solutions to the model cells were determined by accounting for decreasing flow rates from the impoundments over time (Appendix B).

The model cells were also assigned mineralogic properties based on site-specific measurements. Prior measurements of cation exchange capacity and total iron content in aquifer solids were used to assign quantities of ion exchange sites and specific adsorption sites to the cells (Appendix B). Although the presence of potentially reactive minerals, especially calcite, has been identified in the Upper and Lower Wind River Aquifer, calcite was omitted as an initial solid phase in the model. Since the native groundwaters are undersaturated with respect to calcite, the chemical composition of the initial groundwater was significantly altered prior to the transport simulations such that they were no longer representative of site conditions. The geochemical model is therefore conservative, by only allowing for cation exchange and surface complexation as attenuation mechanisms. The effects of neutralization by mixing with natural groundwater and reactions with carbonate minerals are thus not simulated in the model.

2.2.5 Model Simulations

Two flow rates were modeled for the Western Flow Regime: 0.167 ft/d and 0.33 ft/d. For these flow rates, the model was assigned 644 and 1,242 shifts, respectively, corresponding to 1,000 years of transport time. For example, at a flow rate of 0.167 ft/d along the Western Flow Regime, 14 pore volumes (PV) will have moved from the POC to the POE (4,600 feet) in 1,000 years. Therefore, $(14 \text{ PV}) \times (46 \text{ cells}) = 644 \text{ shifts}$. Two flow rates were modeled for the Southwestern Flow Regime: 0.167 ft/d and 0.28 ft/d. For these flow rates, the model was assigned 648 and 1,026 shifts, respectively, corresponding to 1,000 years of transport time.

The geochemical modeling results are shown in Table 2.9. Profiles of concentrations of each constituent along the flow path after more than 1,000 years are shown in Appendix B. Concentrations of constituents remain within the range of observed background at the proposed POE after more than 1,000 years despite of the conservative approach taken throughout the model.

2.2.6 Transport Modeling of Chloride and Sulfate

Sulfate and chloride migration and attenuation were evaluated using the groundwater flow and solute transport model as described in Appendix C. These non-hazardous constituents were selected for evaluation because of their non-reactive behavior. It is conservatively assumed that these constituents will provide the “worst-case” scenario (i.e., fastest travel time and minimum attenuation) for migration from the POC to the POE and receptor points beyond the POE.

Model simulations were only run for a period of 400 years because the concentration versus time plots generated from the model output indicate that the peaks for sulfate and chloride will have passed through the POE for both flow regimes within that time. Chloride concentrations remained below the Wyoming Department of Environmental Quality (WDEQ) Class I standard at the POE for both flow regimes throughout the simulated time. Sulfate concentrations remained below the Wyoming Department of Environmental Quality (WDEQ) Class III standard at the POE for both flow regimes throughout the simulated time. The range of background values indicates that ambient groundwater quality for the area is, at best, Class III. Modeling also indicates that migration from the site will not result in an exceedance of the Class III sulfate standard at Iron Springs. Sulfate concentrations at Iron Springs currently range from 500 to 900 mg/l. Modeling indicates a maximum incremental increase of approximately 80 mg/l at Iron Springs. This incremental increase would not alter the existing water quality as the sulfate concentration would remain well below the Class III standard of 3,000 mg/l. Based on the model results, there will be no significant impacts from chloride or sulfate at the POE, Iron Springs or any other more distant springs.

2.3 Exposure Assessment

According to NRC requirements for ACL applications (NRC 1996), the objectives of the exposure assessment are to: 1) identify the maximum permissible levels that are protective of human health and the environment; 2) evaluate human and environmental exposures to hazardous constituents; and 3) demonstrate that the proposed ACLs do not pose substantial present or potential future hazards to human health or the environment. Based on the geochemical model results presented in Section 2.2, combined with the evaluation of ambient groundwater quality provided in Appendix A, the modeled hazardous constituent concentrations at the potential POE are not distinguishable from ambient conditions when the concentrations at the POCs are at or below the proposed ACLs. This finding is demonstrated in Table 2.10, which compares the modeled values at the proposed POE for both the Western and Southwestern Flow Regimes with the corresponding ambient groundwater quality concentrations.

Because mill-related sources at the Gas Hills facility will pose no incremental risks to human health or the environment, a quantitative analysis of potential exposures and human health and environmental hazards is not required. However, because certain elements of the exposure

assessment are still germane, and in general accordance with NRC requirements for ACL applications, this section presents pertinent qualitative information regarding current and potential future land and water resource uses identified for the Gas Hills study area. To facilitate review, the general ACL outline format has been adhered to where possible, but some sections are brief due to lack of relevance.

2.3.1 Water Resource Classification and Uses

A fundamental component of the exposure assessment is the extent to which human or environmental receptors are, or may be, exposed to groundwater or hydraulically connected surface water potentially affected by the site. To assess this endpoint, this section describes existing and potential future land and water uses in the Gas Hills site vicinity.

2.3.1.1 Area Description and Land Use

The Gas Hills uranium district is located in a sparsely populated area covering portions of Natrona and Fremont Counties in central Wyoming. The principal land use surrounding the Gas Hills site is uranium mining, although some land is used for livestock grazing and hunting on a seasonal basis. Soils in the Gas Hills area are classified as generally unsuitable for cultivation (USDA 1973 in NRC 1980a). Consequently, agriculture is not a viable land use.

Most of the land within five miles of the Gas Hills site is public domain under BLM jurisdiction; only a small percentage of land is privately owned. The nearest private residence located five miles northeast (upgradient) of the site, is inhabited on a seasonal basis only. The nearest downgradient residence is approximately 20 miles from the site.

2.3.1.2 Current Water Resource Uses

Table 2.11 summarizes the results of a search of ground and surface water rights in the vicinity of the Gas Hills site (Wyoming State Engineer's Office 1999). Figure 2.22 identifies corresponding land and water uses. The water rights search yielded 178 distinct water uses, the majority of which (59 percent) are permitted for monitoring purposes. The remaining uses are classified as miscellaneous (14 percent), industrial (13 percent), stock watering (12 percent), and irrigation (3 percent). Information documenting the Water Rights Search, including location, status, and water yield data, is provided in Appendix D.

Of particular relevance to this assessment is the fact that all irrigation and stock water uses correspond to surface water sources. The five irrigation uses correspond to the CBC, Diamond Ring, and Cross L ditches located upgradient to the north/northeast of the Gas Hills site (Figure 2.22). Stock watering uses include the Rattlesnake springs/ditches located east of the site and several springs located west of the site (e.g., Iron Spring and Lincoln Spring). These springs have not been impacted by site activities, nor are any site-related water quality impacts expected in the future.

Groundwater in the region is used principally for monitoring, miscellaneous (for example, dewatering), and industrial purposes. No municipal, domestic, irrigation, or stock uses of groundwater in the area were identified (Table 2.11). This reflects the lack of permanent

residents in the area, historical land uses, and/or the local ambient groundwater quality (Appendix A), which is not suitable for domestic or agricultural purposes.

2.3.1.3 Potential Future Groundwater Uses

In defining potential future groundwater uses, the following factors were considered.

- 1) Ambient Groundwater Quality. Widespread ambient contamination within the uppermost aquifer has resulted in groundwater quality that is not compatible with domestic, agricultural, or livestock groundwater uses (Appendix A, Table 2.12). Comparison of ambient levels of constituents with WDEQ groundwater quality standards yields a Class IV (industrial) designation as shown in Table 2.12, this finding applies to radium-226+228 and gross alpha (uranium excluded) for both flow regimes and arsenic for the Southwestern Flow Regime.
- 2) Demographic Projections. The sparse population that characterizes the Gas Hills area is expected to remain stable. This prediction is based on 1997 census projections as well as other factors, including the harsh climate, lack of arable land, and the lack of a foreseeable economic base.
- 3) Institutional Controls on Future Land and Water Use. As shown in Figure 2.22 and documented in Appendix F, 1,920 acres of land will be transferred to the DOE in perpetuity. As part of the DOE long-term surveillance and maintenance requirements, groundwater will be restricted within this land transfer area.

None of the factors identified above are expected to change in the future. A related issue is the fact that PRI recently applied for an in situ mining permit from the Land Quality Division of the State of Wyoming for the area located due south of the Gas Hills facility (PRI 2001; Appendix A, Figure A.1).¹ Proposed operation is scheduled to begin in 2003 and is estimated to continue until 2020. The groundwater to be affected, which includes all ore zones presently known and identified within PRI's permit boundary, will automatically be classified Class V (uranium commercial), as required by Chapter VIII of the Water Quality Division regulations. According to PRI's permit application, the land will be returned to native rangeland for wildlife and livestock grazing after mining is complete (PRI 2001). The aforementioned factors support the assumption that groundwater at and in the vicinity of the Gas Hills site is suitable, at best, for industrial use only. Additional discussion regarding the proposed PRI in situ leach mine operation and potential impacts to groundwater quality is provided in Appendix K.

2.3.1.4 Potential Future Uses of Hydraulically Connected Surface Water

A hydraulic connection exists between groundwater and springs located west of the site (e.g., Medicine Spring, Lincoln Spring, and Iron Spring), some of which, are used for stock watering purposes. However, historical results of biannual surface water samples collected from these

¹The mining permit area will be located in the Gas Hills in all, or parts, of Section 6, T32N, R89W, Sections 21, 22, 27, 28, 29, 31, 32, 33 and 34, T33N, R89W, and Sections 1, 2, 3, 10, 11 and 12, T32N, R90W, Fremont and Natrona Counties, Wyoming, approximately 45 miles southeast of Riverton (PRI 2001).

springs indicate no impacts related to the Gas Hill site. In fact, water quality in some of the springs, in particular Iron Spring, is influenced by acidic conditions associated with naturally-occurring mineralization (Section 2.1.1). Given the lack of demonstrated water quality impacts and the hydrogeological characteristics of the site precluding potential future impacts (Section 2.2), the exposure assessment focuses solely on groundwater-related exposure pathways.

2.3.2 Evaluation of Human Health Hazards

Because the modeled constituent concentrations at the POE are within the range of background values for all parameters (Tables 2.6, 2.10, and 2.12), no adverse human health impacts are anticipated, thereby precluding the need for a quantitative assessment of human health hazards or risks. For reference, Table 2.13 presents information regarding the likelihood of various exposure pathways. [This information is presented irrespective of the geochemical modeling results, which yield levels of hazardous constituents at the POE that are within background range.]

2.3.3 Evaluation of Environmental Hazards

The potential for environmental exposures in the vicinity of the Gas Hills site is expected to be limited due to the lack of permanent surface water bodies, the poor soil quality precluding use of groundwater for irrigation purposes, and the other factors discussed in the preceding sections. Consequently, the environmental hazard evaluation provided below is semi-quantitative in nature. Again, modeled values at the POE are within the range of background values for all parameters, precluding the need for a quantitative assessment. Where available, wildlife benchmark values are provided for comparison purposes only.

2.3.3.1 Potential Effects on Aquatic and Terrestrial Wildlife Life

Based on the physical setting of the Gas Hills site, the only likely exposure pathway for wildlife receptors would be ingestion of water from a stock watering tank supplied by a well and/or ingestion of irrigated forage. The proposed ACLs and the modeled POE hazardous constituent concentrations were compared to benchmarks developed for limiting exposure to wildlife listed in Table 2.14. The benchmarks for radionuclides are based on a limiting dose of 100 millirads per day (Higley 1995). The benchmarks for inorganic constituents are based on No Observed Adverse Effect Levels derived for DOE's Oak Ridge facility site (Sample 1996). As demonstrated in Table 2.14, the modeled concentrations at the proposed POE are orders of magnitude below both the wildlife benchmark values and the WDEQ groundwater standards for livestock.

2.3.3.2 Potential Effects on Agricultural Crops and Plants

The modeled constituent concentrations at the proposed POE are orders of magnitude below the WDEQ standards for agricultural water use, demonstrating that no adverse impacts to crops or plants are anticipated. Note, however, that application of the Class II agricultural limits is not appropriate for the Gas Hills site given the ambient groundwater quality which exceeds these limits for some constituents—in particular, arsenic, gross alpha, and radium-226+228 in both flow regimes, and nickel in the Western and selenium in the Southwestern Flow Regime. Consequently, the Class II standards are presented in Table 2.14 for comparison purposes only.

2.3.3.3 Potential Adverse Effects on Physical Structures

There are no physical structures in the flow path of the groundwater that could be adversely affected by groundwater quality.

- mounds are discontinuous and do not create a hydraulic barrier to groundwater movement across the site.
- **Pumping without injection.** The 1998 water-level elevation map (Figure 2.14) illustrates the effects of extraction on the groundwater flow regime.

Groundwater modeling was used for capture zone analysis. Development and calibration of the model is described in Appendix C. A groundwater model was used to evaluate flowpaths under the pumping with injection operating condition (Figure 3.4). The results of the modeling indicate that hydraulic capture was not established across the AGTI. Groundwater modeling was also used for capture zone analysis of pumping without injection condition. The model results indicate that groundwater beneath the AGTI is not contained by extraction (Figure 3.5).

Evaluation of water quality data from the AGTI POC wells indicates that concentrations have decreased for some constituents but increased for others (Appendix J). At MW21A, the concentrations of radium-226+228, lead-210, thorium-230, and natural uranium have decreased compared to 1990 levels. Radium-226+228 and thorium-230 concentrations have also decreased at MW1. Arsenic and beryllium concentrations increased from 1990 levels at both MW1 and MW21A. Lead-210 has increased at MW1.

Both groundwater flowpath models and water-level data indicate that hydraulic capture was not obtained under either pumping or pumping and injecting programs. Decreasing concentrations for select constituents is attributed to reduction in tailings seepage and subsequent dissipation of the mound below the AGTI and not a result of the CAP.

3.3 ALARA Analysis for the Existing CAP

The following section will provide an ALARA analysis for the existing CAP. The purpose of this section is to provide data that will be used in the assessment of corrective action alternatives. In this analysis, Umetco has chosen to simulate an exposure scenario at the POC wells. This scenario cannot occur at any present or future time because of mandated DOE long-term custodial care.

To date, corrective actions coupled with the dissipation of the groundwater mound have reduced the concentrations of some constituents in POC wells. However, several of the licensed constituents have increased since the CAP was implemented. This ALARA analysis was performed using the measured radionuclide concentrations and calculated doses for the POC wells as the most conservative cases.

3.3.1 Estimated Exposure Duration

The exposure duration for populations consuming water from the POC wells was based on the duration that seepage from the source would continue plus the time period for mill-related hazardous constituents to be flushed from the aquifer. It should be noted that the travel times estimated for the exposure duration differ from the travel times cited under the alternative corrective action assessment. This is because the POC wells are located at different distances

costs were developed for each alternative. A life cycle cost analysis was performed to determine the net present value (NPV) for each of the alternatives.

Costs for the NPV analysis were based on data from the Environmental Remediation Cost Data 2001 (Means) Report, historic Gas Hills site expenditures, cost estimates from vendors, and engineering judgment. Costs were assumed to grow at an annual average inflation rate of 3.2 percent and an annual average discount rate of 5.2 percent. The results are given in 2001 dollars (Table 3.4).

Assumptions for each alternative including cash flows and costs for each year of the project life cycle are included in Appendix L.

Comparing the costs for each option versus the benefit derived shows that each corrective action listed above has a cost greater than the benefit derived value (Table 3.5). Therefore, the only practicable corrective action is institutional controls coupled with the ACL values proposed in this report.

3.6 As Low As Reasonably Achievable Demonstration

Radiation protection regulations mandate that doses be ALARA, taking into account the state of technology, the economics of improvement in relation to benefits to public health and safety, other societal and socioeconomic considerations, and in relation to the utilization of atomic energy in the public interest. License termination, or termination of a CAP, requires that the licensee demonstrate that the applicable dose criteria have been met and that doses are ALARA. Restoration of groundwater potentially impacted by licensed activities requires that hazardous constituent concentration limits be met at specified POC wells. These concentration limits are background concentrations, drinking water concentration limits, or ACLs, which, if met, are protective of human health and the environment.

Section 3.1 and 3.2 have shown that, despite continued optimization efforts, the CAP at Gas Hills has been ineffective in returning constituent levels at the POC wells to the GWPS. Section 3.3 demonstrated that the CAP is not justified based on the ALARA analysis. Section 3.4 has shown using a derived benefit analysis that even a 100 percent effective CAP should cost no more than \$2,515,400. Alternative corrective actions were evaluated in Section 3.5. No reasonable or feasible corrective action was identified that could reduce hazardous constituents at the POC wells in a cost-effective manner. The actions described above, coupled natural attenuation mechanisms at Gas Hills that will reduce hazardous constituents at the POE to within the range of background levels, show that the proposed ACL is ALARA.

It should be noted that it is technically unachievable to restore groundwater quality to the GWPS at the POC wells because of the presence of widespread groundwater constituents that are non-milling derived but inseparable from milling-derived contamination. Groundwater modeling of both the Western and Southwestern Flow Regimes indicates that continued pumping from wells in any type of array or number will enhance constituent mobility from multiple mineralized zones and mining reclamation areas. Regardless, natural attenuation mechanisms without corrective action will prohibit degradation of groundwater quality. The water quality will be protective of human health and the environment at the proposed POE as described in Section 2.0.

4.0 PROPOSED ALTERNATE CONCENTRATION LIMITS

The proposed ACLs are protective of human health and the environment. As demonstrated in Section 3.0, the proposed ACLs meet ALARA. Furthermore, the evaluation of widespread ambient groundwater contamination shows that continued corrective actions will have little or no effect on water quality. The hazard assessment (Section 2.0) demonstrates that geochemical conditions result in attenuation of constituent concentrations within short distances from the potential sources, regardless of whether the constituents are derived from mineralization, mining, or milling activities. Results of geochemical and groundwater flow modeling indicate attenuation of constituent concentrations to levels within the range of background levels at the proposed POE (Figure 4.1).

An analysis was conducted to provide an estimate of the maximum concentrations that may occur at the POC wells for both the A-9 Repository and the AGTI in the future. These maximum concentrations were then evaluated using the geochemical model to determine the degree of attenuation and reduction along the flowpath to the POE. The revised geochemical model is provided as Appendix B. Geochemical modeling using input values representative of maximum concentrations that may be observed at the POC wells indicates that the proposed ACLs are protective of human health and the environment at the POE. The model also shows that concentrations at the POE will be within the range of background values established for the area, as described in Appendix A. The results of the analysis provide the basis for revised ACLs. The methods used in the analysis and the resulting values are described in the following sections.

4.1 Methodology

The determination of the ACLs consisted of the following:

- 1) Water quality data for each flow regime (southwestern and western) were ranked for the following licensed constituents: arsenic, beryllium, nickel, selenium, lead-210, radium-226+228, thorium-230, natural uranium, and gross alpha. Only data collected after 1992 were included in the ranking. The ranking determined which monitoring wells consistently recorded the highest concentrations for each constituent.
- 2) Concentration trend plots were developed for those wells with consistent highest values that were also hydraulically upgradient or crossgradient of the POC wells. This was done to identify and eliminate outliers from the data and to evaluate trends. Based on the trend plots, wells were selected as representative of the highest concentrations within the flow regime for each of the constituents.
- 3) A statistical evaluation of data from the wells with the highest values was performed to determine the mean, standard deviation, and upper 95th quantile of the data set. The 95 percent upper confidence limit (UCL) was then calculated for the upper 95th quantile of each data set. The 95 percent UCL was selected to provide assurance that the ACLs will not be exceeded at the POC wells.

In some cases, the wells that consistently provided the highest observed concentrations for a specific constituent were actually the POC wells. For instance, POC well GW7 had the highest concentrations for the Southwestern Flow Regime for the radionuclides. In other cases, wells upgradient of the POCs represented the maximum observed concentrations. Attenuation of constituents is expected along the flowpath from upgradient wells to the POC. However, the attenuation will not be of the scale anticipated further downgradient from the POC because the geochemical environment is different (oxidizing versus reducing). Therefore, selection of the 95 percent UCL of the 95th quantile for data from either the POCs or from wells hydraulically upgradient of the POCs is appropriate. These ACLs, as revised, are representative of the maximum concentrations that may occur at the POC wells and are protective of human health and the environment, as shown with the geochemical modeling efforts.

4.2 Results

4.2.1 Southwestern Flow Regime

The water quality data ranking for the Southwestern Flow Regime is provided for arsenic, beryllium, nickel, selenium, lead-210, radium-226+228, thorium-230, natural uranium, and gross alpha minus natural uranium in Table E-1. The wells selected as representative of the maximum concentrations present in the Southwestern Flow Regime are summarized below. The concentration trend plots for the wells representing maximum concentrations (exclusive of anomalous data) are provided in Figures E-1 through E-9. The proposed ACL for each constituent for the Southwestern Flow Regime is presented in Table 1.4. The data used to calculate the proposed ACL for each constituent are provided in Table E-3. The proposed ACL for each constituent is equivalent to the 95 percent UCL of the upper 95th quantile of the representative data set with one exception. Specifically, the ACL for thorium-230 was set equal to the highest observed value at POC Well GW7, because that value exceeded the 95 percent UCL of the upper 95th quantile.

Table 2.9 Results of Geochemical Modeling, Gas Hills Site, Umetco Minerals Corporation, Grand Junction, Colorado

Constituent	Initial Concentration Western Flow Regime	Maximum Modeled Value at POE 0.167 ft/d ¹ / 0.33 ft/d ² 0.167 ft/d ¹ / 0.33 ft/d ²	Initial Concentration Southwestern Flow Regime	Maximum Modeled Value at POE 0.167 ft/d1 / 0.28 ft/d2
Licensed Constituents				
Arsenic (mg/l)	1.8	0.034 / 0.039	1.4	0.016 / 0.017
Beryllium (mg/l)	1.6	0.0050 / 0.0050	1.7	0.0011 / 0.0012
Lead-210 (pCi/l)	35	2.18 / 2.45	47	0.23 / 0.24
Natural Uranium (mg/l)	12	0.0065 / 0.0071	34	0.14 / 0.15
Nickel (mg/l)	13	0.063 / 0.065	9.3	0.015 / 0.016
Radium-226 + 228 (pCi/L)	250	58.9 / 69.5	353	15.7 / 16.9
Selenium (mg/l)	0.16	0.0044 / 0.0048	0.53	0.041 / 0.043
Thorium-230 (pCi/l)	57	0.107 / 0.108	44.8	0.85 / 0.86

Composite parameter Gross Alpha was not modeled.

¹ Representative groundwater velocity based on site hydrologic data.

² Maximum groundwater velocity calculated from stochastic groundwater flow model.

POE Point of Exposure

ft/d feet per day

mg/l milligrams per liter

pCi/l picoCuries per liter

Table 2.10 Summary of Ambient Groundwater Quality, POE Modeled Values, and Class III Groundwater Standards, Gas Hills Site, Umetco Minerals Corporation, Grand Junction, Colorado

Constituent	<u>Western Flow Regime</u>		<u>Southwestern Flow Regime</u>		Class III Wy. Std.
	Background Range	POE Value	Background Range	POE Value	
<u>LICENSED CONSTITUENTS</u>					
Arsenic (mg/l)	0.001 - 0.092	0.039	0.001 - 1.26	0.017	0.2
Beryllium (mg/l)	0.01 - 0.01	0.005	--	0.0012	0.1 ^{Class II}
Gross Alpha (pCi/l)	1.0 - 380	⁽¹⁾	8.6 - 2,670	⁽¹⁾	15
Lead-210 (pCi/l)	-2.8 - 6.1	2.45	-0.80 - 3.5	0.24	--
Natural Uranium (mg/l)	0.0009 - 0.26	0.0071	0.0003 - 5.9	0.15	5.0
Nickel (mg/l)	0.01 - 2.1	0.065	0.01 - 0.28	0.016	0.2 ^{Class II}
Radium ²²⁶⁺²²⁸ (pCi/l)	0.6 - 84	69.5	1.7 - 2,070	16.9	5.0
Selenium (mg/l)	0.01 - 0.01	0.0048	0.001 - 0.097	0.043	0.05
Thorium-230 (pCi/l)	-2.9 - 0.5	0.108	-0.93 - 8.2	0.86	--
<u>NON-LICENSED CONSTITUENTS</u>					
Chloride (mg/l)	1 - 14	76	1 - 138	84	2000
Sulfate (mg/l)	125 - 1920	1715	61 - 1675	730	3000

Notes:

Background ranges taken from Tables A-3, A-4, A-6 and A-7 of Appendix A.

POE values for Licensed Constituents are the highest predicted values listed in Table 2.9 (for the two assumed groundwater flow velocities).

POE values for Non-Licensed Constituents are maximum values resulting from MODFLOW/MT3D model simulations (Appendix C).

⁽¹⁾ Gross Alpha was not modeled because it is a composite parameter.

Table 2.14 Comparison of Wildlife Benchmark Concentrations and Agricultural Standards with Modeled POE Concentrations, Gas Hills Site, Umetco Minerals Corporation, Grand Junction, Colorado

Parameter	Maximum Modeled Value at POE Locations ¹	Groundwater Benchmark for Wildlife Receptors ²	WY DEQ Class II: Agriculture ³	WY DEQ Class III: Livestock ³
<u>Radionuclide Parameters</u>				
Natural Uranium	0.15 mg/l	7 mg/l	5 mg/l	5 mg/l
Thorium-230	0.86 pCi/l	--	--	--
Lead-210	2.45 pCi/l	--	--	--
Ra-226+228	69.5 pCi/l	420 pCi/l	5 pCi/l	5 pCi/l
<u>Inorganic Parameters</u>				
Arsenic	0.039 mg/l	0.3 mg/l	0.1 mg/l	0.2 mg/l
Beryllium	0.005 mg/l	2.8 mg/l	0.1 mg/l	--
Nickel	0.065 mg/l	171 mg/l	0.2 mg/l	--
Selenium	0.043 mg/l	0.086 mg/l	0.02 mg/l	0.05 mg/l
Sulfate	1715 mg/l	--	200 mg/l	3000 mg/l

-- No data available and/or value not determined.

¹The POE concentrations listed above are the highest of those projected for the western and southwestern flow regimes.

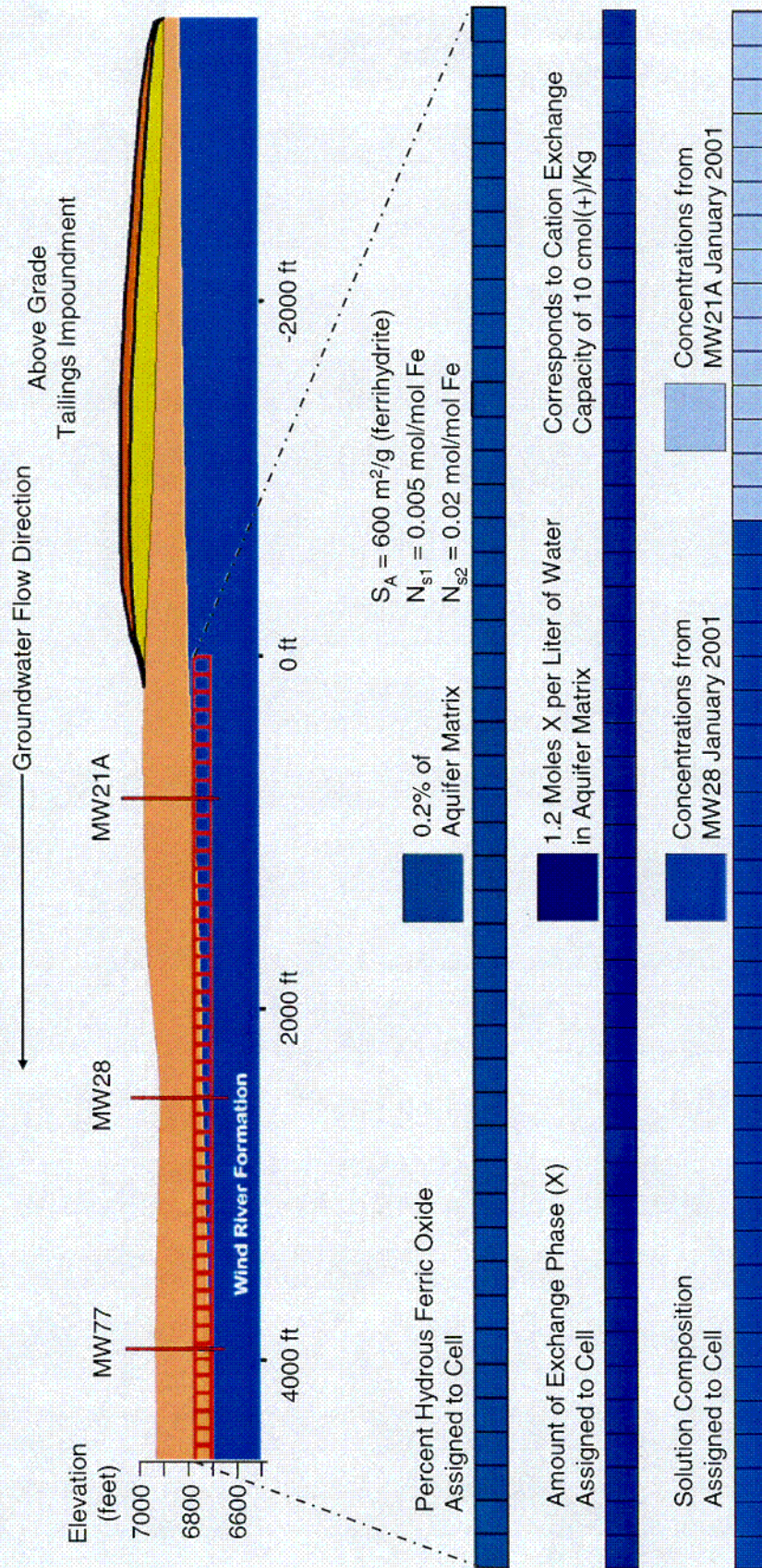
²The radionuclide groundwater benchmark concentrations for wildlife are based on a limiting dose of 100 mrad per day (Higley 1995). The wildlife benchmarks for inorganic constituents are based on No Observed Adverse Effect Levels (NOAELs) derived for white-tailed deer (considered the most sensitive terrestrial receptor for chemical constituents) for DOE's Oak Ridge facility (Sample 1996).

³ Source: Wyoming Department of Environmental Quality (WDEQ) Water Quality Rules and Regulations, Chapter VIII, Table I (WDEQ Water Quality Division, March 1993). In accordance with this document, groundwater classifications are defined as follows:

Class II Groundwater — This water is suitable for agricultural use where soil conditions and other factors are adequate. The ambient quality of underground water of this suitability does not have a concentration in excess of any of the standards for Class II groundwater listed above.

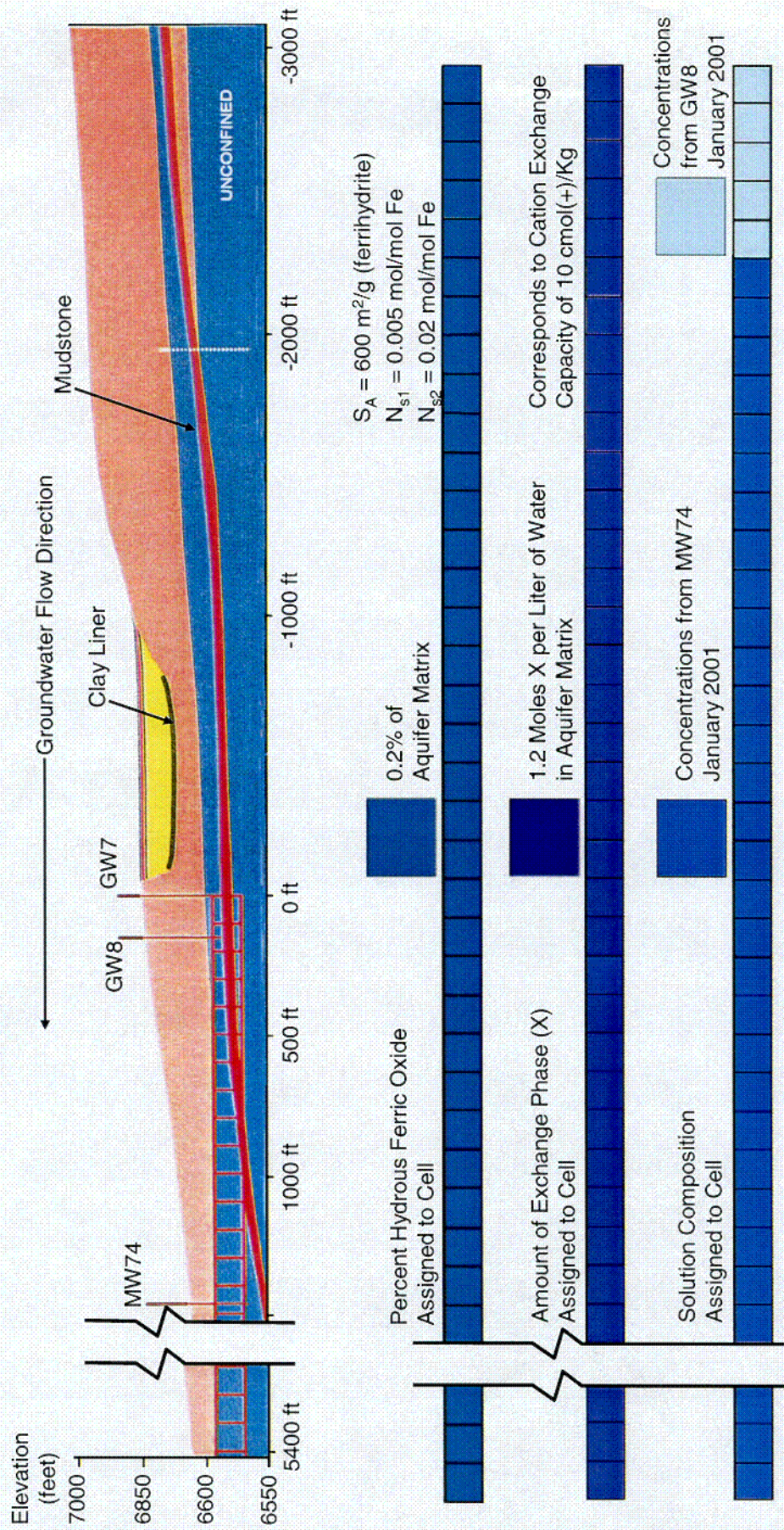
Class III Groundwater — This water is suitable for livestock. The ambient quality of underground water of this suitability does not have a concentration in excess of any of the standards for Class III groundwater listed above.

Figure 2.20 Model Grid for Western Flow Regime (Lower Wind River)

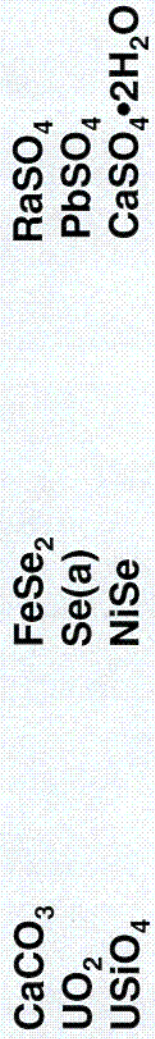


col

Figure 2.21 Model Grid for Southwestern Flow Regime (Upper Wind River)



Minerals Allowed to Precipitate



CO2

Appendix B

Geochemical Model Umetco Gas Hills Site Fremont and Natrona Counties, Wyoming

Umetco Minerals Corporation
2754 Compass Drive, Suite 280
Grand Junction, Colorado 81506

November 2001

Contents

1.0 INTRODUCTION.....	1-1
2.0 CONCEPTUAL GEOCHEMICAL MODEL.....	2-1
2.1 Groundwater Flow Regime.....	2-1
2.2 Uranium Mineralization.....	2-1
2.3 Geochemical Conditions within the Wind River Aquifer.....	2-1
2.4 Sources of Mill-Related Constituents and Interaction with Aquifer Components	2-2
3.0 GEOCHEMICAL COMPUTER CODE - PHREEQC.....	3-1
3.1 PHREEQC Model Database	3-1
3.1.1 Correction of the Gypsum Solubility Constant in the MINTEQ Database	3-1
3.1.2 MINTEQ Database Modification to Include Radium Thermodynamic Data	3-2
3.1.3 MINTEQ Database Modification to Include Thorium Thermodynamic Data...	3-2
3.2 Surface Complexation Modeling	3-3
3.2.1 Surface Area	3-4
3.2.2 Mass of the Adsorbing Surface	3-4
3.2.3 Surface Site Density	3-4
3.3 Ion Exchange Modeling	3-5
4.0 PHREEQC MODEL CONSTRUCTION	4-1
4.1 Initial Model Source Terms	4-1
4.2 Decreasing Model Source Terms.....	4-2
4.3 Model Source Decay Terms.....	4-2
4.4 Model Design for the Western Flow Regime	4-3
4.5 Model Design for the Southwestern Flow Regime.....	4-5
4.6 Advective Transport Parameters for the Modeled Flow Regimes.....	4-5
4.7 Precipitating Minerals and Equilibrium Phases.....	4-5
4.8 Summary of Site-Specific Input Used in the Geochemical Model.....	4-7
5.0 PREDICTIVE SIMULATION RESULTS	5-1
5.1 Reactions Controlling the Attenuation of the Constituents of Concern	5-1
5.1.1 Arsenic.....	5-1
5.1.2 Beryllium.....	5-2
5.1.3 Lead	5-2
5.1.4 Uranium.....	5-2
5.1.5 Nickel	5-2

Contents

5.1.6 Radium	5-2
5.1.7 Selenium.....	5-3
5.1.8 Thorium.....	5-3
5.2 Estimated Gross Alpha Concentrations at the Points of Exposure (POEs):	5-6
6.0 REFERENCES	6-1
7.0 ATTACHMENTS.....	7-1
Source Decay Terms	7-1
Southwestern Flow Regime	7-1
Western Flow Regime.....	7-1
PHREEQC Model Database	7-1

Tables

Table B3.1	Relevant Thermodynamic Equations for Radium.....	2
Table B3.2	Relevant Thermodynamic Equations for Thorium.	3
Table B4.1	PHREEQC Source Decay Terms for the Gas Hills Geochemical Model.....	4
Table B4.2	Site-Specific Data Defined in PHREEQC Modeling.....	7
Table B5.1	Geochemical Model Results for Western Flow Regime. Maximum Modeled Output Concentration at the POE.	4
Table B5.2	Geochemical Model Results for Southwestern Flow Regime. Maximum Modeled Output Concentration at the POE.	5
Table B5.3	Projected Radionuclide Activity Concentrations at the Points of Exposure.....	7

Figures

Figure B.1	1000-Year Arsenic Concentrations Between the Western Flow Regime POC and POE
Figure B.2	1000-Year Beryllium Concentrations Between the Western Flow Regime POC and POE
Figure B.3	1000-Year Lead-210 Concentrations Between the Western Flow Regime POC and POE
Figure B.4	1000-Year Uranium Concentrations Between the Western Flow Regime POC and POE
Figure B.5	1000-Year Nickel Concentrations Between the Western Flow Regime POC and POE
Figure B.6	1000-Year Radium-226+228 Concentrations Between the Western Flow Regime POC and POE

Contents

Figures (continued)

Figure B.7	1000-Year Selenium Concentrations Between the Western Flow Regime POC and POE
Figure B.8	1000-Year Thorium-230 Concentrations Between the Western Flow Regime POC and POE
Figure B.9	Arsenic Concentrations at the POE for the Western Flow Regime With Time
Figure B.11	Lead-210 Concentrations at the POE for the Western Flow Regime With Time
Figure B.12	Uranium Concentrations at the POE for the Western Flow Regime With Time
Figure B.13	Nickel Concentrations at the POE for the Western Flow Regime With Time
Figure B.14	Radium-226+228 Concentrations at the POE for the Western Flow Regime With Time
Figure B.15	Selenium Concentrations at the POE for the Western Flow Regime With Time
Figure B.16	Thorium-230 Concentrations at the POE for the Western Flow Regime With Time
Figure B.17	1000-Year Arsenic Concentrations Between the Southwestern Flow Regime POC and POE
Figure B.18	1000-Year Beryllium Concentrations Between the Southwestern Flow Regime POC and POE
Figure B.19	1000-Year Lead-210 Concentrations Between the Southwestern Flow Regime POC and POE
Figure B.20	1000-Year Uranium Concentrations Between the Southwestern Flow Regime POC and POE
Figure B.21	1000-Year Nickel Concentrations Between the Southwestern Flow Regime POC and POE
Figure B.22	1000-Year Radium-226+228 Concentrations Between the Southwestern Flow Regime POC and POE
Figure B.23	1000-Year Selenium Concentrations Between the Southwestern Flow Regime POC and POE
Figure B.24	1000-Year Thorium-230 Concentrations Between the Southwestern Flow Regime POC and POE
Figure B.25	Arsenic Concentrations at the POE for the Southwestern Flow Regime With Time
Figure B.26	Beryllium Concentrations at the POE for the Southwestern Flow Regime With Time
Figure B.27	Lead-210 Concentrations at the POE for the Southwestern Flow Regime With Time
Figure B.28	Uranium Concentrations at the POE for the Southwestern Flow Regime With Time
Figure B.29	Nickel Concentrations at the POE for the Southwestern Flow Regime With Time
Figure B.30	Radium-226+228 Concentrations at the POE for the Southwestern Flow Regime With Time
Figure B.31	Selenium Concentrations at the POE for the Southwestern Flow Regime With Time
Figure B.32	Thorium-230 Concentrations at the POE for the Southwestern Flow Regime With Time
Figure B.33	Concentration of Adsorbed Arsenic Phases for the Western Flow Regime
Figure B.34	Concentration of Adsorbed Beryllium Phases for the Western Flow Regime

Contents

Figures (continued)

- Figure B.35 Concentration of Adsorbed and Exchangeable Lead-210 Phases for the Western Flow Path
- Figure B.36 Concentration of Precipitated and Adsorbed Uranium Phases for the Western Flow Path
- Figure B.37 Concentration of Adsorbed and Precipitated Nickel Phases for the Western Flow Path
- Figure B.38 Concentration of Exchangeable and Adsorbed Radium Phases for the Western Flow Path
- Figure B.39 Concentration of Precipitated and Adsorbed Selenium Phases for the Western Flow Path
- Figure B.40 Concentration of Adsorbed Thorium-230 Phases for the Western Flow Path
- Figure B.41 Concentration of Adsorbed Arsenic Phases for the Southwestern Flow Path
- Figure B.42 Concentration of Adsorbed Beryllium Phases for the Southwestern Flow Path
- Figure B.43 Concentration of Adsorbed and Exchangeable Lead Phases for the Southwestern Flow Path
- Figure B.44 Concentration of Precipitated and Adsorbed Uranium Phases for the Southwestern Flow Path
- Figure B.45 Concentration of Precipitated and Adsorbed Nickel Phases for the Southwestern Flow Path
- Figure B.46 Concentration of Precipitated and Adsorbed Radium Phases for the Southwestern Flow Path
- Figure B.47 Concentration of Precipitated and Adsorbed Selenium Phases for the Southwestern Flow Path
- Figure B.48 Concentration of Adsorbed Thorium-230 Phases for the Southwestern Flow Path

Acronyms and Abbreviations

<u>Acronym</u>	<u>Definition</u>
ACL	Alternate Concentration Limit
AGTI	Above Grade Tailings Impoundment
As(III)	Arsenite
As(V)	Arsenate
Ba ²⁺	Barium Ion
Ca ²⁺	Calcium Ion
Calcite	CaCO ₃ (s)
CEC	Cation Exchange Capacity
Coffinite	USiO ₄ (s)
Eh	Oxidation/Reduction Potential Relative to Standard Hydrogen Electrode
Fe(OH) ₃	Ferrihydrite
FeSe ₂	Ferroselite
Ft/d	Feet per Day
Gypsum	CaSO ₄ •2H ₂ O
HFO	Hydrous Ferric Oxide
ΔH°	Standard Enthalpy of Reaction
K	Dissociation or Formation Constant
K _{sp}	Solubility Product
Kcal/mol	Kilocalories per Mole
MCL	Maximum Contaminant Level
MnO ₂	Manganese Dioxide
Na ⁺	Sodium Ion
NaOCl ₃	Sodium Chlorate
NiSe	Nickel Selenide
PbX ₂	Exchangeable Lead
pE	Negative Logarithm of Free Electron Activity, -log(e ⁻)
pH	Negative Logarithm of Hydrogen Ion Activity, -log (H ⁺)
POC	Point of Compliance
POE	Point of Exposure
PV	Pore Volume
Pyrite	FeS ₂ (s)
Ra ²⁺	Radium Ion
RaX ₂	Exchangeable Radium

Acronyms and Abbreviations

<u>Acronym</u>	<u>Definition</u>
Redox	Reduction/Oxidation
SO ₄ ²⁻	Sulfate Ion
Sur_sAsO4-2	Respective Arsenic (V) Species Adsorbed to Type 1 Sites
Sur_sH2AsO3	Respective Arsenic (III) Species Adsorbed to Type 1 Sites
Sur_sHAsO4-	Respective Arsenic (V) Species Adsorbed to Type 1 Sites
Sur_sH2AsO4	Respective Arsenic (V) Species Adsorbed to Type 1 Sites
Sur_sOBe+	Beryllium Adsorbed to Type 1 Sites
Sur_sOHAsO4-3	Respective Arsenic (V) Species Adsorbed to Type 1 Sites
Sur_sOHRa+2	Radium Adsorbed to Type 1 Sites
Sur_sOHUO2+2	Respective Uranium (IV) Species Adsorbed to Type 1 Sites
Sur_sONi+	Nickel Adsorbed to Type 1 Sites
Sur_sOPb+	Lead Adsorbed to Type 1 Sites
Sur_wAsO4-2	Respective Arsenic (V) Species Adsorbed to Type 2 Sites
Sur_wHAsO4-	Respective Arsenic (V) Species Adsorbed to Type 2 Sites
Sur_wH2AsO3	Respective Arsenic (III) Species Adsorbed to Type 2 Sites
Sur_wH2AsO4	Respective Arsenic (V) Species Adsorbed to Type 2 Sites
Sur_wOBe+	Beryllium Adsorbed to Type 2 Sites
Sur_wOHAsO4-3	Respective Arsenic (V) Species Adsorbed to Type 2 Sites
Sur_wOHSeO3-	Respective Selenium (III) Species Adsorbed to Type 2 Sites
Sur_wOHSeO4-	Respective Selenium (VI) Species Adsorbed to Type 2 Sites
Sur_wONi+	Nickel Adsorbed to Type 2 Sites
Sur_wOPb+	Lead Adsorbed to Type 2 Sites
Sur_wORa+	Radium Adsorbed to Type 2 Sites
Sur_wOTh+3	Respective Thorium Species Adsorbed to Type 2 Sites
Sur_wOTh(OH)2+	Respective Thorium Species Adsorbed to Type 2 Sites
Sur_wOTh(OH)3	Respective Thorium Species Adsorbed to Type 2 Sites
Sur_wOTh(OH)4-	Respective Thorium Species Adsorbed to Type 2 Sites
Sur_wOUO2+2	Respective U(IV) Species Adsorbed to Type 2 Sites
Sur_wSeO4-	Respective Selenium (VI) Species Adsorbed to Type 2 Sites
Sur_wTh(OH)+2	Respective Thorium Species Adsorbed to Type 2 Sites
Uraninite	UO ₂ (s)

1.0 INTRODUCTION

Application of a dynamic geochemical model at the Gas Hills site can be used to show that the proposed Alternate Concentration Limits (ACLs) are protective of human health and the environment at the Point of Exposure (POE). The model is based on knowledge of groundwater compositions and geochemically reactive aquifer components present at Gas Hills, and utilizes geochemical principles based on the site conceptual geochemical model (Geraghty & Miller, Inc. 1996). The results of the geochemical model are used to predict the 1,000-year concentrations of constituents in the Wind River Aquifer as a function of distance between the Point of Compliance (POC) wells and the POE.

The Umetco Gas Hills site is located in Fremont and Natrona Counties, Wyoming, approximately 60 miles east of Riverton in a remote area of central Wyoming, in the Gas Hills Uranium District of the Wind River Basin. The site consists of approximately 542 acres, including tailings disposal and heap leach areas. Open pit mining occurred within and around the Umetco site from the late 1950s until 1984. The Gas Hills mill was constructed in 1959 and uranium oxide was produced until the mill was decommissioned in 1987. Tailings from the milling process were stored in the Above Grade Tailings Impoundment (AGTI) and the A-9 Repository.

The Wind River Formation lies beneath the facility and is characterized by a network of oxidation-reduction (redox) fronts that contain uranium mineralization. This network is extensive in both the vertical and horizontal directions throughout the stratigraphic section. Open pit and underground mining along the redox fronts exposed ore bodies within the Wind River Formation to oxidizing conditions. Surface water infiltration through the pits and mine spoils produced acidic drainage which subsequently migrated into the shallow aquifer system. Natural uranium mineralization, open pit mines, and mine spoil piles are present throughout and surrounding the site.

2.0 CONCEPTUAL GEOCHEMICAL MODEL

Geochemical conditions within the Wind River Aquifer have been characterized through government and private scientific studies and from Umetco exploration, development, and reclamation activities. The data collected during these studies were used to create the geochemical model to assist in projecting future concentrations of constituents along groundwater flow paths.

The Wind River Formation is differentiated into an upper unit and a lower unit separated by a mudstone aquitard. The majority of the Wind River Aquifer is reducing and has a high neutralization capacity as a result of CaCO_3 (calcite) present in the aquifer. The aquifer materials also contain reactive mineral surfaces capable of adsorbing dissolved groundwater constituents. Therefore, natural attenuation processes associated with the initial geochemical conditions that produced uranium mineralization limit the mobility of constituents from all sources. Thus, elevated concentrations of constituents near source areas do not persist in downgradient areas. The following sections describe the groundwater flow regimes, geochemical conditions, and conceptual geochemical model.

2.1 Groundwater Flow Regime

The regional groundwater flow pattern is northwest toward the Wind River. In the northern portion of the site, local groundwater flow is to the west (Western Flow Regime) and in the southern portion, local flow is to the southwest (Southwestern Flow Regime). Groundwater flowing to the west discharges at seeps and springs located along West Canyon Creek. Groundwater flowing to the southwest continues until reaching the area of the Lucky Mc site (approximately five miles away) where the flow turns north and eventually discharges at seeps and springs along Fraser Draw and Willow Springs Draw.

2.2 Uranium Mineralization

Historically, the Gas Hills district in Central Wyoming has been one of the major uranium-producing regions of the United States. Based on past production and established reserves, the district accounts for about 12 percent of the United States' total uranium reserves (Anderson 1969). Uranium mineralization occurs in an area about five miles wide and 20 miles long, in three north-trending belts known as the East, Central, and West Gas Hills (Figure 2.1). The uranium solution front can be traced for miles along each of these belts and may be mineralized to ore grade continuously for thousands of feet along the front. The thickness of an ore body is constrained by the thickness of the permeable sandstone unit, which is bounded by less-permeable strata. Uranium ore bodies in the Gas Hills can be extensive as seen in the Lucky Mc ore trend that is approximately 2,300 feet long, 600 feet wide, and contains nine ore zones averaging 5 feet in thickness distributed throughout a stratigraphic interval 150 feet thick (USAEC 1959).

2.3 Geochemical Conditions within the Wind River Aquifer

Wyoming roll-front uranium deposits have been comprehensively studied and Gas Hills has been used as a type location for these deposits (King and Austin 1966; Harshman 1974; DeVoto 1978). These studies provided site-specific information on mineral phases found upgradient, downgradient, and within the ore zone. Existing mineral phases control the solubility of

constituents and, therefore, their concentrations in the groundwater. Figure 1.15 depicts a cross-section of an idealized roll-front uranium deposit typical of the Gas Hills and the characteristic mineralogy across an ore deposit.

Above the mudstone aquitard in the vicinity of the AGTI and the A-9 Repository, the Wind River Formation is an oxidizing environment. Roll-front uranium ore deposits are located above the mudstone unit along a redox boundary downgradient of the AGTI and A-9 Repository. Geochemical conditions at the ore deposits and in areas farther downgradient (west of the AGTI and southwest of the A-9 Repository) are pervasively reducing. Beneath the mudstone unit, the Wind River Formation is generally a reducing geochemical environment. Uranium is likely to be enriched in the aquifer matrix as UO_2 (uraninite), USiO_4 (coffinite), or other reduced uranium minerals because of the reducing conditions within the aquifer. Based on the model of a Wyoming roll-front uranium deposit, the portion of the Wind River Formation below the local mudstone corresponds to the downgradient, regionally reduced portion of the aquifer that is in equilibrium with FeS_2 (pyrite) and calcite.

Previous Umetco studies at Gas Hills provided information on specific pH and redox conditions in the vicinity of ore deposits. These parameters vary widely across an ore deposit and influence the transport of constituents in groundwater. For example, many constituents that are mobile in acidic-oxidizing environments are immobile in more neutral and reducing environments. Figure 2.18 summarizes conditions determined by Harshman (1966) for ore deposits at Gas Hills and Shirley Basin, Wyoming. The oxidation-reduction potential (Eh) ranges from near +300 to -300 millivolts. The pH ranges from approximately 8 to less than 4, depending on the location relative to ore deposits.

2.4 Sources of Mill-Related Constituents and Interaction with Aquifer Components

The AGTI and the A-9 Repository are the primary sources of mill-related constituents. Mine pits and spoils are also sources of constituents to groundwater. The source fluids that transport mill-related constituents are oxidizing and acidic. Reagents such as NaClO_3 (sodium chlorate) and MnO_2 (manganese dioxide) were added during the milling process as oxidizing agents to bring the process solution to an Eh between +400 and +425 millivolts (Merrit 1971). The pH of the process solution was generally less than 2.0 due to additions of sulfuric acid (H_2SO_4) during milling.

In the vicinity of the AGTI, the water table occurs beneath the mudstone unit. Seepage from the AGTI is impeded by the low permeability of the mudstone unit, resulting in localized perched conditions. The geochemical environment of the Wind River Formation directly beneath the AGTI and above the mudstone unit is characterized as oxidized and calcite-depleted and corresponds to the hematitic core shown in the idealized cross-section in Figure 1.15. The mill-affected groundwater migrates west into the regionally reduced portion of the Wind River Aquifer. Attenuation of the milling-related constituents occurs through reactions with groundwater and aquifer components.

In the area of the A-9 Repository, the water table occurs above the mudstone unit and tailings seepage mixing with groundwater is restricted to the area above the mudstone, typically less than 50 feet thick. The A-9 Repository was formerly a mine pit. Milling-related constituents in the vicinity of the A-9 Repository mix with constituents derived from mining and ore deposits. Constituents from these commingled sources migrate to the southwest and encounter reducing

conditions. When the constituents, regardless of source, encounter reducing conditions, they are attenuated through reactions with groundwater and aquifer components.

3.0 GEOCHEMICAL COMPUTER CODE – PHREEQC

The Wind River groundwater beneath the Gas Hills contains complex chemical compositions and the aquifer materials include diverse reactive minerals and adsorbing surfaces. To predict changes in solution speciation and mineralogical controls on dissolved constituent concentrations as mill-affected water moves through the aquifer, the computer code used must be capable of solution speciation, mass transfer, and mass transport. PHREEQC (Parkhurst and Appelo 1999) was chosen because it is a well-established code applicable to a wide range of geochemical conditions. PHREEQC was derived from the original PHREEQE code (Parkhurst and others 1980) in use for 20 years. PHREEQC is capable of performing a variety of aqueous geochemical calculations, such as (1) speciation and saturation index calculations; (2) reaction-path and advective-transport calculations involving specified irreversible reactions, mixing of solutions, mineral and gas equilibria, surface complexation reactions, and ion exchange reactions; and (3) inverse modeling to account for chemical changes that occur along a groundwater flow path. Construction of the PHREEQC database and input files is discussed in the following sections, (these files are supplied on disk; see key in Section 7.0).

3.1 PHREEQC Model Database

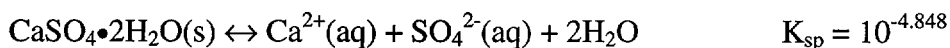
Three different databases are included in the PHREEQC model package: (1) the PHREEQE database (Parkhurst and others 1980), (2) the WATEQ4F database (Ball and Nordstrom 1991), and (3) the MINTEQ database (Allison and others 1991). The MINTEQ database was used for this study because it is an extensive thermodynamic compilation that is adequate for addressing a broad range of geochemical conditions involving metals. While the User's Guide to PHREEQC (Parkhurst and Appelo 1999) states that one limitation of the aqueous model is a lack of internal consistency in the database, this is an inherent property of any geochemical database. The lack of internal consistency results from those equilibrium constants and enthalpies of reaction that are compiled from various literature sources. In fact, no geochemical database exists that contains thermodynamic data derived from a single source. The databases used in contemporary geochemical models (MINTEQ, WATEQ4F, EQ3/6, SOLMNEQ, GEOCHEM) contain thermodynamic data that were compiled from various sources because it would not be feasible for an individual to generate equilibrium constants for the hundreds of reactions contained within any geochemical database.

The original MINTEQ model was developed at Batelle Pacific Northwest Laboratories. Research contributing to the continued development of MINTEQ was supported in part by the Office of Solid Waste at the U. S. Environmental Protection Agency. The current MINTEQ database originated from the "...well-developed thermodynamic database of the U. S. Geological Survey's WATEQ3 model (from Ball and others 1981)" (Allison and others 1991). The following sections describe the modifications made to the MINTEQ database for the site-specific Gas Hills conceptual geochemical model. The modified database is included on the disk provided in Section 7.0.

3.1.1 Correction of the Gypsum Solubility Constant in the MINTEQ Database

Gypsum ($\text{CaSO}_4 \cdot 2\text{H}_2\text{O}$) is an important potential control on the concentration of sulfate in soil solutions and aquifer systems. Therefore, the sulfate concentrations modeled using PHREEQC can be dependent on the gypsum solubility constant used in the MINTEQ database. The gypsum

solubility expression and corresponding solubility constant (K_{sp}) provided in the MINTEQ database are shown below:



Nordstrom and others (1990) presented a revised summary of equilibrium constants for aqueous ion associations and mineral solubilities, and proposed a revised gypsum solubility constant of $10^{-4.58}$. This revised gypsum solubility product is used by both the PHREEQC (Parkhurst and Appelo 1999) and WATEQ4F (Ball and Nordstrom 1991) databases, and is known with high precision based on measurements by previous investigators cited in Nordstrom and others (1990). Therefore, the revised gypsum solubility constant of $10^{-4.58}$ was added to the MINTEQ database and used for the Gas Hills modeling.

3.1.2 MINTEQ Database Modification to Include Radium Thermodynamic Data

Thermodynamic data for radium complexes and solid phases were obtained from Langmuir and Riese (1985) and added to the MINTEQ database. These authors used a comprehensive thermodynamic model based on similarities among calcium, strontium, and barium aqueous complexes and solid compounds to extrapolate the equilibrium constants (K) and standard enthalpies of reaction (ΔH°) for radium solids and solution species. Given the chemical similarities between the radium (Ra^{2+}) and barium (Ba^{2+}) ions, surface complexation constants for barium are assumed to be valid for radium (Langmuir 1997). Therefore, a surface complexation constant for adsorption of radium by hydrous ferric oxide (HFO) was added by using the well-established barium surface complexation data provided by Dzombak and Morel (1990). The radium thermodynamic data added to the MINTEQ database are given in Table B3.1. The values for K indicate that RaSO_4° is the most stable form of the listed aqueous species.

Table B3.1 Relevant Thermodynamic Equations for Radium.

Reaction	log K or log K_{sp}	ΔH° (kcal/mol)
$\text{Ra}^{2+} + \text{OH}^- = \text{Ra}(\text{OH})^+$	0.5	1.1
$\text{Ra}^{2+} + \text{Cl}^- = \text{RaCl}^+$	-0.10	0.50
$\text{Ra}^{2+} + \text{CO}_3^{2-} = \text{RaCO}_3^\circ$	2.5	1.07
$\text{Ra}^{2+} + \text{SO}_4^{2-} = \text{RaSO}_4^\circ$	2.75	1.3
$\text{RaCO}_3(\text{c}) = \text{Ra}^{2+} + \text{CO}_3^{2-}$	-8.3	-2.8
$\text{RaSO}_4(\text{c}) = \text{Ra}^{2+} + \text{SO}_4^{2-}$	-10.26	-9.4
$\text{Hfo_wOH} + \text{Ra}^{2+} = \text{Hfo_wORa}^{2+} + \text{H}^+$	-7.2	-----
$\text{Hfo_sOH} + \text{Ra}^{2+} = \text{Hfo_sOHRa}^{2+}$	5.46	-----

Source: Langmuir and Riese (1985)

3.1.3 MINTEQ Database Modification to Include Thorium Thermodynamic Data

The thermodynamic data for the aqueous thorium complexes and solid phases are those used in the database of the chemical equilibrium model EQ3/6 developed at Lawrence Livermore National Laboratory (Wolery 1992). Surface complexation constants to describe thorium

adsorption onto HFO were obtained from LaFlamme and Murray (1987). Relevant thorium thermodynamic equations for solution species, solid phases, and surface complexes are given in Table B3.2. The data indicate that the aqueous thorium sulfate solution species are the most stable species relative to the other listed complexes.

Table B3.2 Relevant Thermodynamic Equations for Thorium.

Reaction	log K or log K _{sp}	ΔH° (kcal/mol)	Source
$\text{Th}^{+4} + \text{H}_2\text{O} = \text{ThOH}^{+3} + \text{H}^+$	-3.887	-246.2	Wagman and others (1982)
$\text{Th}^{+4} + 2\text{H}_2\text{O} = \text{Th}(\text{OH})_2^{+2} + 2\text{H}^+$	-7.11	-306.5	Langmuir and Herman (1980)
$\text{Th}^{+4} + 3\text{H}_2\text{O} = \text{Th}(\text{OH})_3^+ + 3\text{H}^+$	-11.86	-368.4	Langmuir and Herman (1980)
$\text{Th}^{+4} + 4\text{H}_2\text{O} = \text{Th}(\text{OH})_4 + 4\text{H}^+$	-16.03	-438.4	Langmuir and Herman (1980)
$2\text{Th}^{+4} + 2\text{H}_2\text{O} = \text{Th}_2(\text{OH})_2^{+6} + 2\text{H}^+$	-6.46	-489.4	Langmuir and Herman (1980)
$4\text{Th}^{+4} + 8\text{H}_2\text{O} = \text{Th}_4(\text{OH})_8^{+8} + 8\text{H}^+$	-21.76	-1224.0	Langmuir and Herman (1980)
$6\text{Th}^{+4} + 15\text{H}_2\text{O} = \text{Th}_6(\text{OH})_{15}^{+9} + 15\text{H}^+$	-37.70	-2019.0	Langmuir and Herman (1980)
$\text{Th}^{+4} + \text{Cl}^- = \text{ThCl}^{+3}$	0.954	-223.7	Langmuir and Herman (1980)
$\text{Th}^{+4} + 2\text{Cl}^- = \text{ThCl}_2^{+2}$	0.676	NR	Langmuir and Herman (1980)
$\text{Th}^{+4} + 3\text{Cl}^- = \text{ThCl}_3^+$	1.498	NR	Langmuir and Herman (1980)
$\text{Th}^{+4} + 4\text{Cl}^- = \text{ThCl}_4$	1.073	NR	Langmuir and Herman (1980)
$\text{Th}^{+4} + \text{SO}_4^{-2} = \text{ThSO}_4^{+2}$	5.31	-397.2	Langmuir and Herman (1980)
$\text{Th}^{+4} + 2\text{SO}_4^{-2} = \text{Th}(\text{SO}_4)_2$	9.62	-611.0	Langmuir and Herman (1980)
$\text{Th}^{+4} + 3\text{SO}_4^{-2} = \text{Th}(\text{SO}_4)_3^{-2}$	10.40	NR	Langmuir and Herman (1980)
$\text{Th}^{+4} + 4\text{SO}_4^{-2} = \text{Th}(\text{SO}_4)_4^{-4}$	8.44	NR	Langmuir and Herman (1980)
$\text{Th}(\text{SO}_4)_2(\text{c}) = \text{Th}^{+4} + 2\text{SO}_4^{-2}$	-20.3	-607.7	Wagman and others (1982)
$\text{Th}(\text{OH})_4(\text{c}) + 4\text{H}^+ = \text{Th}^{+4} + 4\text{H}_2\text{O}$	9.65	-423.6	Naumov and others (1974) ¹
$\text{ThO}_2(\text{c}) + 4\text{H}^+ = \text{Th}^{+4} + 2\text{H}_2\text{O}$	1.86	-293.1	Cox and others (1989)
$\text{Hfo_wOH} + \text{Th}^{+4} = \text{Hfo_wOTh}^{+3} + \text{H}^+$	3.5	NR	LaFlamme and Murray (1987)
$\text{Hfo_wOH} + \text{Th}^{+4} + \text{H}_2\text{O} = \text{Hfo_wOTh}(\text{OH})^{+2} + 2\text{H}^+$	0.20	NR	LaFlamme and Murray (1987)
$\text{Hfo_wOH} + \text{Th}^{+4} + 2\text{H}_2\text{O} = \text{Hfo_wOTh}(\text{OH})_2^+ + 3\text{H}^+$	-6.38	NR	LaFlamme and Murray (1987)
$\text{Hfo_wOH} + \text{Th}^{+4} + 3\text{H}_2\text{O} = \text{Hfo_wOTh}(\text{OH})_3 + 4\text{H}^+$	-6.3	NR	LaFlamme and Murray (1987)
$\text{Hfo_wOH} + \text{Th}^{+4} + 4\text{H}_2\text{O} = \text{Hfo_wOTh}(\text{OH})_4 + 5\text{H}^+$	-16.32	NR	LaFlamme and Murray (1987)

NR not reported.

¹ log K for $\text{Th}(\text{OH})_4(\text{c})$ reported by Naumov and others (1974) is consistent with Langmuir and Herman (1980).

3.2 Surface Complexation Modeling

A commonly used surface complexation model was used to represent the attenuation of calcium, sulfate, beryllium, nickel, arsenic, selenium, ²²⁶⁺²²⁸radium, ²³⁰thorium, ²¹⁰lead, and uranium. Many studies have shown adsorption models based on double-layer theory to be successful in predicting the composition of complex solutions in contact with an adsorbing surface (Langmuir 1997). Westall and Hohl (1980) demonstrated that any of five electrostatic models can describe the same set of experimental data equally well. The PHREEQC geochemical model incorporates the Dzombak and Morel (1990) diffuse double-layer and a non-electrostatic surface-complexation model (Davis and Kent 1990). Of the three adsorption models commonly used, (constant capacitance, diffuse double-layer, and triple-layer), the diffuse double-layer model requires the least number of input parameters.

The modeling exercise assumes that the adsorbing surface is HFO. HFO is a naturally dominant adsorbent because of its tendency to be finely dispersed and to exist as both ubiquitous coatings on mineral particles and as discrete oxide particles (Jenne 1968; Dzombak and Morel 1990). The reactive properties of HFO are well characterized. The three most important properties of the adsorbing phase that are used as input to the model are (1) the surface area, (2) the mass of the adsorbing material, and (3) the surface site density.

3.2.1 Surface Area

Laboratory experiments demonstrate that measured surface areas depend on the HFO aging after it is prepared and the specific method used to measure surface area. Tabulating measured surface areas for HFO (21 determinations) shows a range of 159 to 720 square meters per gram (m^2/g). However, the values at the low end of this range are considered to be underestimates due to difficulties in measuring the surface area of HFO with the commonly used nitrogen gas adsorption methods (Dzombak and Morel 1990). The Gas Hills geochemical model used the estimate of $600 \text{ m}^2/\text{g}$ recommended by Davis and co-workers (Davis 1977; Davis and Leckie 1978; Luoma and Davis 1983) and is consistent with the work by Dzombak and Morel (1990).

3.2.2 Mass of the Adsorbing Surface

Analyses of aquifer materials in the Gas Hills area show that iron concentrations in the sediments commonly range from 2 to 3 percent (Lidstone & Anderson, Inc. 1989). The modeling exercise is conservative, assuming that the aquifer sediments contain 2 percent total iron, and that 10 percent of the total iron exists as HFO. The model was shown to be insensitive to total iron concentration when the results were compared using 1, 2, and 3 percent total iron. The mass of HFO used in PHREEQC must be expressed on a per liter basis and was calculated by assuming that the sediments contain 0.2 percent HFO, and by using an estimated aquifer porosity of 15 percent ($5.7 \text{ L soil} / \text{L H}_2\text{O}$), a bulk density of 2.1 g/cm^3 (Umetco Minerals Corporation 1997), and a molecular weight of 107 g/mol for HFO [$\text{Fe}(\text{OH})_3$, (ferrihydrite)]. The resulting value is 45.9 g HFO/L and was calculated as follows:

$$\frac{\text{g HFO}}{\text{L}} = \left(\frac{5.7 \text{ L rock}}{\text{L H}_2\text{O}} \right) \left(\frac{1000 \text{ cm}^3 \text{ rock}}{\text{L rock}} \right) \left(\frac{2.1 \text{ g rock}}{\text{cm}^3 \text{ rock}} \right) \left(\frac{0.2 \text{ g Fe as HFO}}{100 \text{ g rock}} \right) \left(\frac{107 \text{ g HFO}}{55.85 \text{ g Fe}} \right) = \frac{45.9 \text{ g HFO}}{\text{L H}_2\text{O}}$$

3.2.3 Surface Site Density

The PHREEQC adsorption model assumes that the number of active sites on the adsorbing surface (surface site density) is known. Surface densities for adsorption sites are divided into two types, both used in the model. Type 1 sites are a small set of high-energy binding sites. Type 2 sites are determined from experimental sorption maxima. Previous studies showed that measured densities of Type 1 sites on HFO are sufficiently close to justify the use of a single Type 1 site density (0.005 mol/mol Fe) (Dzombak and Morel 1990). The range of estimates for Type 2 site densities on HFO is small (from 0.1 to 0.3 mol/mol Fe) and use of an approximate median Type 2 site density of 0.20 mol/mol Fe is shown to be successful when describing the sorption behavior of HFO (Dzombak and Morel 1990). To calculate the number of adsorption sites, the moles of iron per liter of water must first be calculated from the mass of HFO:

$$\frac{\text{moles Fe}}{LH_2O} = \left(\frac{45.9 \text{ g HFO}}{LH_2O} \right) \left(\frac{\text{mole HFO}}{107 \text{ g HFO}} \right) \left(\frac{1 \text{ mole Fe}}{\text{mole HFO}} \right) = \frac{0.429 \text{ moles Fe}}{LH_2O}$$

Based on this result, it follows that the number of Type 1 and Type 2 sites can be calculated as follows:

$$\frac{\text{moles Type 1 sites}}{LH_2O} = \left(\frac{0.429 \text{ moles Fe}}{LH_2O} \right) \left(\frac{0.005 \text{ moles sites}}{\text{mole Fe}} \right) = \frac{0.002 \text{ moles Type 1 sites}}{LH_2O}$$

$$\frac{\text{moles Type 2 sites}}{LH_2O} = \left(\frac{0.429 \text{ moles Fe}}{LH_2O} \right) \left(\frac{0.2 \text{ moles sites}}{\text{mole Fe}} \right) = \frac{0.086 \text{ moles Type 2 sites}}{LH_2O}$$

3.3 Ion Exchange Modeling

Ion exchange equilibria were included in PHREEQC to model the exchange of calcium, sodium, potassium, magnesium, ²¹⁰Pb, ²²⁶⁺²²⁸Ra, and iron (II) during transport. Ion exchange equilibria are included in PHREEQC through heterogeneous mass-action and mole-balance equations for exchange sites, with mass-action expressions based on half-reactions between aqueous species and unoccupied exchange sites. Values for the exchange coefficients were taken from Appelo and Postma (1993), where the exchange coefficients are expressed using Na⁺ (sodium) as the reference cation, and using equivalent fractions for activities of the exchange species (Gaines-Thomas convention, Gaines and Thomas 1953).

A range in measured cation exchange capacity (CEC) values (3.9 to 14.1 cmol/kg) has been reported for the Wind River Aquifer (Umetco Minerals Corporation 1997). The number of exchange sites (moles X) specified in PHREEQC must be expressed on a per liter of water basis and was calculated using a representative CEC value of 10 cmol/kg, an aquifer porosity of 15 percent (5.7 L soil/ L H₂O), and a bulk density of 2.1 g/cm³ (Umetco Minerals Corporation 1997).

$$\frac{\text{moles X}}{LH_2O} = \left(\frac{5.7 \text{ L rock}}{LH_2O} \right) \left(\frac{1000 \text{ cm}^3 \text{ rock}}{L \text{ rock}} \right) \left(\frac{2.1 \text{ g rock}}{\text{cm}^3 \text{ rock}} \right) \left(\frac{10 \text{ cmol}}{1000 \text{ g rock}} \right) \left(\frac{\text{mol}}{100 \text{ cmol}} \right) = \frac{1.2 \text{ moles X}}{LH_2O}$$

4.0 PHREEQC MODEL CONSTRUCTION

The groundwater flow regime at the Gas Hills site has two distinct components: (1) a southwestern flow in the vicinity of the A-9 Repository, and (2) a deeper, western flow in the vicinity of the AGTI. A mudstone unit separates the two flow regimes. Because unique conditions are present in the two flow regimes, each was modeled separately. Both models used an assumed aquifer porosity of 15 percent, a hydraulic conductivity of 1 foot/day (ft/d) and a hydraulic gradient of 0.025, resulting in a representative groundwater velocity of 0.167 ft/d. The modeling was performed with several conservative attributes:

- Additional modeling exercises were conducted using higher conservative velocities of 0.33 ft/d for the Western Flow Regime and 0.28 ft/d for the Southwestern Flow Regime. These values are upper limits derived from the stochastic groundwater flow modeling effort described in Appendix C.
- Calcite, which acts to neutralize acidic water, was not added to the model cells. Although calcite is known to occur throughout the aquifer system, the native groundwater assigned to specific cells of the model is not in equilibrium with calcite. Therefore, calcite was omitted from the model, because including calcite was found to alter the initial model groundwater compositions such that their compositions were no longer representative of actual site groundwater (Section 4.5).
- Coprecipitation of the hazardous constituents with secondary aquifer minerals, which would normally act to reduce dissolved concentrations, was not simulated in the model. However, coprecipitation of uranium, radium, lead, and thorium with minerals such as calcite, gypsum, and siderite, has been well-documented (Morin and others, 1988; Curti, 1999; Landa, 1999).
- Transport of hazardous constituents is modeled with one-dimensional advective flow, using a conservative longitudinal dispersivity value of 50 m. Values of longitudinal dispersivity as large as 100 m have been used in mathematical simulation studies of the migration of large contaminant plumes in sandy aquifers (Freeze and Cherry 1979). The one-dimensional model does not account for mixing of the source terms with natural groundwater during transport.

4.1 Initial Model Source Terms

The model inflow solutions (source terms) represent the source of constituents entering the Western and Southwestern Flow Regimes. For the Western Flow Regime source term, the model conservatively incorporated the 95 percent upper confidence limit of the upper 95th quantile concentration of the hazardous constituents from data sets collected from monitoring wells screened in the lower portion of the Wind River Aquifer that contain consistently elevated levels of the hazardous constituents. Elevated levels of the hazardous constituents are consistently reported at these locations. Selection for input values is described in Appendix E. For the major ions, the input concentrations from the original ACL application were used (99th percentile of concentrations in first quarter 1997 through fourth quarter 1998 data from MW1 or MW21A, whichever was higher). The oxidation-reduction potential measured in POC Well MW21A corresponded to a negative logarithm of free electron activity (pE) of 5.8. As mentioned earlier, sodium chlorate and manganese dioxide were added to the milling process as oxidizers to bring the solution to an Eh of between +400 and +425 millivolts (Merritt 1971) which corresponds to a

pE of 6.8 to 7.2. Assuming only minor reaction with redox sensitive materials through the thick unsaturated zone beneath the AGTI, the oxidation-reduction potential of the initial solution was therefore set at a pE of 6.

For the Southwestern Flow Regime source term, the model also incorporated the 95 percent upper confidence limit of the upper 95th quantile concentration of constituents from data sets collected from monitoring wells screened within the upper portion of the Wind River Aquifer that contain consistently elevated levels of the hazardous constituents. The only exception was the value for thorium-230, which was the maximum value observed at POC Well GW7. The selection of input values is presented in Appendix E. As for the Western Flow Regime, the Southwestern Flow Regime model is conservative because it uses the 95 percent upper confidence limit of the upper 95th quantile concentration of constituents, and because it also assumes that the source is constant. For the major ions, the input concentrations from the original ACL application were used (99th percentile of concentrations in first quarter 1997 through fourth quarter 1998 data from GW7 or GW8, whichever was higher). A calculated pE of 9, based on site-specific measurements of the $\text{Fe}^{2+}/\text{Fe}^{3+}$ couple collected from POC Well GW7 in August 1998, was used in the model input.

4.2 Decreasing Model Source Terms

Due to dewatering processes within the tailing impoundments, the source term will not be constant, but will instead decrease over time. The source term for each flow regime can be divided into two components: (1) a component that is already in the aquifer system and which is the result of previous tailings seepage to groundwater (*initial source term*), and (2) a second component that consists of continuing tailings seepage that will mix with groundwater beneath the impoundments (*ongoing source term*). Over time, the initial source term will decrease as a result of advective and dispersive processes, in addition to chemical reactions such as adsorption, precipitation, and radioactive decay. The ongoing source term will also decrease because of the declining rate of drainage from the impoundments. Detailed studies have been conducted to characterize the decreasing drainage characteristics from both the AGTI and the A-9 Repository over time (SMI 1997; SMI 1998a). The combined effect of the decreasing source term from both components is considered the source decay term, and is measured as the change in concentration over time at the downgradient edge of the impoundments, or essentially the POCs.

4.3 Model Source Decay Terms

A groundwater flow and transport model was then used to predict the rate that constituent concentrations in groundwater in the vicinity of the impoundments would decrease in response to diminishing tailings seepage (the source decay term; Appendix C). The respective seepage rates for each impoundment were distributed uniformly over the areal extent of the impoundments and the MODFLOW/MT3D model was used to generate concentration profiles for sulfate at each of the POCs (Appendix C). Since sulfate is generally non-reactive, sulfate concentration profiles generated by the flow and transport model were used as a conservative surrogate for the regulated constituents. Utilizing the results of the sulfate decay curves, source concentrations were calculated for five time periods for each flow regime that correspond to 0, 33, 50, 75, and 90 percent reductions in concentration at the POC. Although a 99% reduction is predicted to occur as soon as 175 years for the Western Flow Regime and 120 years for the Southwest Flow Regime, a 90% reduction was the maximum conservative source decay term applied in the model.

The geochemical speciation and mixing model PHREEQC (Parkhurst and Appelo, 1999) was then used to numerically mix the initial source water with adjacent groundwater to produce source/groundwater mixtures that correspond to the 33, 50, 75, and 90 percent reductions in concentration. Although all constituents are assumed to exhibit conservative behavior during mixing, numerical mixing using PHREEQC was necessary to accurately calculate pH, pE, and alkalinity values for the mixtures. The initial source terms for the Western Flow Regime were mixed with representative upgradient groundwater from Well MW-27, and those from the Southwestern Flow Regime were mixed with upgradient water from Well LA-2 (using water quality data from the January 2001 sampling for both upgradient wells). The two PHREEQC input files used to calculate the compositions of the source decay terms are included in the Section 7.0 attachment. The time periods shown in Table B4.1 were derived from the sulfate decay curves (Appendix C), and are arbitrary based on the 33, 50, 75, and 90 percent reductions that were chosen as source decay terms. The time periods were used to calculate the number of pore volumes based on the flow rates used in the model. The number of shifts defined in the transport calculation was calculated by multiplying the number of cells times the number of pore volumes (Section 4.6).

4.4 Model Design for the Western Flow Regime

The model flow path for the Western Flow Regime is one-dimensional, extending from the edge of the AGTI through the POC well MW21A and monitoring well MW28 to the POE, approximately 4,600 feet from the edge of the impoundment (Figure 2.20). The model grid consists of a single row of 46 cells, each representing an aquifer unit 100 feet long. Each of the 46 cells was assigned 0.20 percent HFO (Section 3.2) and an ion exchange assemblage corresponding to a CEC of 10 cmol/kg (Section 3.3). Initially, no mineral solid phases were assigned to the cells. However, the following minerals were allowed to precipitate to equilibrium if oversaturated conditions developed: Calcite, gypsum, uraninite, coffinite, ferroselite (FeSe_2), radium sulfate (RaSO_4), nickel selenide (NiSe), and anglesite (PbSO_4).

The initial solutions in the first 15 cells of the Western Flow Regime model use concentrations (including pH and oxidation-reduction potential measurements) measured during January 2001 in POC Well MW21A located immediately downgradient of the AGTI. Based on analytical data and field measurements, MW21A is within the oxidized, carbonate-depleted halo downgradient of the AGTI. The basis of this is:

- Elevated total dissolved solids (TDS) concentrations (typically ranging between 1,500 to 2,000 mg/l).
- pH values (approximately 6.0) that are transitional between the average pH at the edge of the cell (5.5) and those from Well MW28 (> 6.5), which is located outside of the depleted halo.

The solutions in cells 16-46 of the Western Flow Regime model are also concentrations (including pH and oxidation-reduction potential measurements) measured during January 2001 in monitor Well MW28. Well MW28 appears to be outside the influence of the AGTI since tritium measurements indicate the water in this well is older than uranium milling at Gas Hills (SMI 1998b), as well as consistently low levels (<10 mg/l) of chloride.

Table B4.1 PHREEQC Source Decay Terms for the Gas Hills Geochemical Model.

Western Flow Regime Source Decay Terms ¹						Southwestern Flow Regime Source Decay Terms ¹					
Time (years)	0 to 17	18 to 25	26 to 70	71 to 135	136 to 1,000	Time (years)	0 to 6	7 to 9	10 to 16	17 to 35	36 to 1,000
% Reduction	0	33	50	75	90	% Reduction	0	33	50	75	90
pH	5.50	5.66	5.80	6.18	6.57	pH	4.33	4.47	4.57	4.85	5.27
pE	6	3.9	3.6	3.0	2.2	pE	6	5.6	5.5	5.1	4.4
Ca	456	360	314	242	199	Ca	660	537	478	385	329
Mg	112	80.4	65.3	41.6	27.5	Mg	144	117	104	83.1	70.8
Na	182	136	114	79.5	58.8	Na	61.0	56.9	55.0	51.9	50.0
K	24	19	17	13	11	K	15	16.2	16.8	17.7	18.2
Cl	274	183	140	72.4	31.8	Cl	161	115	92.5	58	37.3
Alkalinity	3.10	3.14	3.16	3.18	3.19	Alkalinity	2.44	4.00	4.73	5.88	6.56
S(6)	3,480	2,434	1,933	1,152	682	S(6)	2,650	1,980	1,660	1,160	861
Fe	86	62	50	31	20	Fe(2)	89	61.8	48	29	17
Th (pCi/l)	57.4	38.1	28.8	14.5	5.89	Th (pCi/l)	44.8	9.11E-07	6.93E-07	3.52E-07	1.47E-07
Pb (pCi/l)	35.4	28.6	22.0	11.6	5.44	Pb (pCi/l)	46.7	31.9	25.0	14.0	7.42
Ra (pCi/l)	250	168	132	73.5	38.8	Ra (pCi/l)	353	239	184	99	47.9
U	11.9	7.89	5.98	2.99	1.20	U	34.1	22.62	17.16	8.62	3.50
As	1.80	1.20	0.91	0.46	0.19	As	1.36	0.90	0.68	0.34	0.14
Se	0.16	0.11	0.08	0.04	0.02	Se	0.53	0.35	0.27	0.13	0.05
Ni	13.00	8.64	6.56	3.30	1.35	Ni	9.34	6.20	4.70	2.36	0.96
Be	1.64	1.09	0.83	0.42	0.17	Be	1.70	1.13	0.85	0.43	0.17
Si	24.0	15.9	12.1	6.03	2.41	Si	56.4	37.4	28.3	14.2	5.66
Transport Parameters-Western Flow Regime						Transport Parameters-Southwestern Flow Regime					
<u>0.167 ft/d</u>						<u>0.167 ft/d</u>					
Years	17	8	45	65	865	Years	6	3	7	19	965
Shifts	10	5	27	40	527	Shifts	4	2	4	12	588
Cells	46	46	46	46	46	Cells	54	54	54	54	54
Pore Volumes	0.23	0.11	0.60	0.86	11.5	Pore Volumes	0.068	0.034	0.079	0.214	10.9
<u>0.330 ft/d</u>						<u>0.280 ft/d</u>					
Years	17	8	45	65	865	Years	6	3	7	19	965
Shifts	20	10	54	78	1042	Shifts	6	3	7	19	987
Cells	46	46	46	46	46	Cells	54	54	54	54	54
Pore Volumes	0.45	0.21	1.18	1.70	22.6	Pore Volumes	0.11	0.06	0.13	0.36	18.38

¹ concentrations expressed as mg/l unless otherwise indicated.

4.5 Model Design for the Southwestern Flow Regime

The model flow path for the Southwestern Flow Regime (Figure 2.21) begins at the toe of the A-9 Repository and extends for 5,400 feet downgradient to the POE. The model grid consists of a single row of 54 cells each representing an aquifer unit 100 feet long. As for the Western Flow Regime, each of the 54 cells was assigned 0.20 percent HFO (Section 3.2) and an ion exchange assemblage corresponding to a CEC of 10 cmol/kg (Section 3.3). Initially, no mineral solid phases were assigned to the cells. However, the following minerals were allowed to precipitate to equilibrium if oversaturated conditions developed: Calcite, gypsum, uraninite, coffinite, ferroselite (FeSe_2), radium sulfate (RaSO_4), nickel selenide (NiSe), and anglesite (PbSO_4).

The initial solutions in the first five cells of the Southwestern Flow Regime model used concentrations (including pH, temperature, and oxidation-reduction measurements) measured during January 2001 in POC Well GW8. It is assumed that as groundwater approaches the PRI ore body, conditions closely resemble those found in the ore body. Well MW74 appears to be outside the influence of the A-9 Repository based on low concentrations of chloride, sulfate, and licensed constituents. Therefore, the initial solutions in the remaining cells (6-54) are those from Well MW74 measured in January 2001.

4.6 Advective Transport Parameters for the Modeled Flow Regimes

Advective transport simulation is one-dimensional transport that incorporates a value of 50 m for longitudinal dispersivity (Freeze and Cherry 1979). Advective transport occurs through a number of "shifts", which is the number of times the solution in each cell will be shifted to the next higher numbered cell. Two flow rates were modeled for the Western Flow Regime: 0.167 ft/d and 0.33 ft/d. For these two flow rates, the model was assigned 644 and 1,242 shifts, respectively. For example, at a flow rate of 0.167 ft/d along the Western Flow Regime, 14 pore volumes (PV) will have moved from the POC to the POE (4,600 feet) in 1,000 years. Therefore, $(14 \text{ PV}) \times (46 \text{ cells}) = 644 \text{ shifts}$.

Similar to the Western Flow Regime, the transport simulations for the Southwestern Flow Regime were also conservatively modeled using simple advective transport that incorporates a value of 50 m for longitudinal dispersivity. Two flow rates were modeled for the Southwestern Flow Regime: 0.167 ft/d and 0.28 ft/d. For these two flow rates, the model was assigned 648 and 1,026 shifts, respectively. For example, at a flow rate of 0.167 ft/d along the Southwestern Flow Regime, 12 PV will have moved from the POC to the POE (5,400 feet) in 1,000 years. Therefore, $(12 \text{ PV}) \times (54 \text{ cells}) = 648 \text{ shifts}$.

4.7 Precipitating Minerals and Equilibrium Phases

A number of minerals have been identified as being associated with Wyoming roll front uranium deposits, in general, and at Gas Hills specifically (Granger and Warren 1974; Harshman 1974; DeVoto 1978; Ludwig and Grauch 1980; U.S. Environmental Services 1996). Of these minerals, calcite is the most potentially reactive mineral present. Calcite will react and dissolve when in contact with acidic mill-affected groundwater, raising the pH to approximately 8.0. The rise in pH will cause many metals and radionuclides to precipitate as various oxide, hydroxide, and carbonate forms. However, preliminary speciation of the groundwater in the model cells (MW21A, MW28, GW8, and MW74) using PHREEQC indicate that these specific waters are undersaturated with respect to calcite. Therefore, when calcite is assigned as an initial phase in

the model, calcite dissolves, the solution pH increases, and certain secondary mineral phases are predicted to precipitate. The end result is that the initial groundwater chemistry is significantly changed prior to the transport calculations, and therefore the modeled groundwater compositions are no longer representative of native groundwater at the site.

Based on these model observations, calcite (and all mineral phases) were conservatively omitted as initial mineral phases in the model cells. However, certain minerals that are known to be associated with Wyoming roll front deposits, and those that precipitate readily from solution, were allowed to precipitate if they became oversaturated in the model. The following minerals were allowed to precipitate to equilibrium upon saturation:

- calcite [CaCO_3]
- gypsum [$\text{CaSO}_4 \cdot 2\text{H}_2\text{O}$]
- uraninite [UO_2]
- coffinite [USiO_4]
- anglesite [PbSO_4]
- ferroselite [FeSe_2]
- radium sulfate [$\text{RaSO}_4(\text{c})$]
- nickel selenide [NiSe]
- selenium (elemental) [$\text{Se}(\text{a})$]

4.8 Summary of Site-Specific Input Used in the Geochemical Model

Site-specific data from the Gas Hills Site were used in the geochemical model to define properties of groundwater, reactive mineral phases, adsorption surfaces, and cation exchange sites. The site-specific data used with the PHREEQC data blocks are summarized in Table B4.2

Table B4.2 Site-Specific Data Defined in PHREEQC Modeling.

Keyword Data Block ¹	Site-Specific Parameter(s)	Comments
SOLUTION	<p><u>Source Water</u> 95% UCL of the 95th quantile from site wells with source decay term applied</p> <p><u>Native Groundwater</u> Well MW28 (W Flow Regime) Well MW74 (SW Flow Regime)</p>	The compositions for these wells can be found in the attached PHREEQC input files. Data include chemical composition and measured redox potential.
EQUILIBRIUM_PHASES	Potential controlling solid phases are $\text{CaSO}_4 \cdot 2\text{H}_2\text{O}$, USiO_4 , UO_2 , CaCO_3 , FeSe_2 , Se(a) , RaSO_4 , NiSe , PbSO_4	$\text{CaSO}_4 \cdot 2\text{H}_2\text{O}$, USiO_4 , UO_2 , FeSe_2 , and Se(a) are known to occur in the Wind River Formation.
SURFACE	A total iron concentration of two percent (Lidstone & Anderson 1989) was used to calculate the mass of the adsorbing phase (45.9 g/l). ²	The value of 2 percent is a conservative value since some samples contained 3 percent iron.
EXCHANGE	A cation exchange capacity of 10 cmol/kg was used to calculate an exchanger concentration of 1.68 mol/l. ²	Measured CEC values ranged from 4 to 14 cmol/kg (Umetco 1997). The value of 10 cmol/kg is within the measured range, and is a typical value for chlorite identified in the Wind River Aquifer.

¹ See the attached PHREEQC input files key in Section 7.0.

² An average bulk density of 2.1 g/cm³ was used to calculate the moles of solid phase per liter of water. Sandstone bulk density was 2.15 g/cm³ and mudstone was 2.00 g/cm³ (Umetco 1997).

5.0 PREDICTIVE SIMULATION RESULTS

The Western Flow Regime model was run using two flow rates across 46 cells (0.167 ft/d or 644 shifts and 0.33 ft/d or 1,242 shifts). These two flow rates correspond to 14 and 27 PV, respectively, and represent 1,000 years of transport time. Examination of chloride data show that in the model, the mill-affected water passes through the POE before 1,000 years. The maximum concentration passing through the POE for each constituent is shown in Table B5.1. Concentration profiles for each constituent along the flow path at 1,000 years of transport are shown in Figures B.1 through B.8, while their concentrations as a function of time at the POE are shown in Figures B.9 through B.16.

The Southwestern Flow Regime model was also run using two flow rates across 54 cells (0.167 ft/d or 648 shifts and 0.28 ft/d or 1,026 shifts). These two flow rates correspond to 12 and 19 PV, respectively, and represent 1,000 years of transport time. Examination of chloride data for the Southwestern Flow Regime also shows that the mill-affected water passes through the POE before 1,000 years. The maximum concentration passing through the POE in the Southwest Flow Regime for each constituent is shown in Table B5.2. Concentration profiles for each constituent along the flow path at 1,000 years of transport are shown in Figures B.17 through B.24, while their concentrations as a function of time at the POE are shown in Figures B.25 through B.32.

5.1 Reactions Controlling the Attenuation of the Constituents of Concern

Attenuation was represented by geochemical reactions defined by the user and then specified in the PHREEQC model input files. Three important geochemical processes were considered for the various constituents in the model: (1) precipitation-dissolution of mineral phases, (2) cation exchange on the surfaces of clay minerals, and (3) adsorption-desorption interactions with HFO. Ion exchange and adsorption to HFO are the dominant mechanisms controlling the mobility of the hazardous constituents in the model. The following sections describe the dominant attenuation mechanisms for the hazardous constituents predicted by the geochemical model. Because geochemical conditions differ between the Western and Southwestern Flow Regimes, there may be differences in the types and amounts of phases predicted to form between the two flow regimes. The types of phases formed are independent of flow rate, however, and therefore only the results for the 0.167 ft/day flow rate are presented for the Western (Figure B.33 through B.40) and Southwestern (B.41 through B.48) Flow Regimes.

5.1.1 Arsenic

Under oxidizing and mildly reducing conditions such as those encountered in the Western and Southwestern Flow Regimes, dissolved arsenic concentrations are typically controlled by adsorption rather than mineral precipitation (Clement and Faust 1981). The model does not consider arsenic minerals to be initially present nor are any arsenic minerals allowed to precipitate. Rather, the model calculates the distribution of aqueous arsenic species according to the equations in the MINTEQ database, and then allows for arsenic concentrations to be controlled by adsorption to HFO. Surface complexation constants for arsenic(V) (arsenate) and arsenic(III) (arsenite) were taken from Dzombak and Morel (1990). The model predicts that adsorption of arsenate will be the dominant attenuation mechanism for arsenic within the Western (Figure B.33) and Southwestern (Figure B.41) Flow Regimes.

5.1.2 Beryllium

Beryllium is strongly bound by organic matter and clays and therefore is relatively immobile in soils and sediments (Kabata-Pendias and Pendias 1992). No thermodynamic data were available in the MINTEQA database to allow for precipitation of discrete beryllium mineral phases. However, beryllium is an alkaline earth metal whose chemical behavior in groundwater systems is similar to calcium, magnesium, barium, strontium, and radium. Therefore, attenuation of beryllium was modeled by allowing for adsorption to the surface of HFO. Beryllium surface complexation constants were obtained from Dzombak and Morel (1990). Consequently, the modeled beryllium attenuation for the Western (Figure B.34) and Southwestern (Figure B.42) Flow Regimes result from adsorption to HFO.

5.1.3 Lead

Aqueous speciation of lead is generally dominated by the free lead ion (Pb^{2+}) in neutral to acidic solutions with lead carbonate solution species becoming important at higher pH values (Rai and others 1987). Under these conditions, lead will form adsorbed surface complexes with available clay minerals and iron hydroxide. Therefore, lead attenuation was modeled using ion-exchange (Appelo and Postma 1993) and surface-complexation equilibria (Dzombak and Morel 1990). The mineral PbSO_4 (anglesite) was also specified as a potential solid phase due to its low solubility, but anglesite was not predicted to precipitate along either flow path. The model predicts that adsorption, and to a lesser extent ion exchange, will be the attenuation mechanisms for lead along the Western (Figure B.35) and Southwestern (Figure B.43) Flow Regimes.

5.1.4 Uranium

Distribution of uranium solution species was calculated according to the equations in the MINTEQA database that allow for the formation of aqueous complexes with carbonate, hydroxide, and sulfate ions. Uraninite and coffinite are the important uranium minerals in the Gas Hills ore, and although the model allowed for precipitation of these minerals upon saturation, neither of these minerals reached oversaturation. The geochemical model predicts that adsorption to HFO is the primary attenuation mechanism for uranium in both the Western (Figure B.36) and Southwestern (Figure B.44) Flow Regimes.

5.1.5 Nickel

Dissolved nickel species in groundwater are typically dominated by the free nickel ion $[\text{Ni}^{2+}(\text{aq})]$ and by association with sulfate to form $\text{NiSO}_4^0(\text{aq})$. In most groundwater systems, adsorption is the primary mechanism of nickel attenuation. Therefore, nickel attenuation was modeled using established surface complexation constants for HFO (Dzombak and Morel 1990). Nickel was also allowed to precipitate as NiSe (nickel selenide) (Masscheleyn and others 1991), although saturation with respect to NiSe was not predicted. Attenuation resulted from adsorption to HFO for the Western (Figure B.37) and Southwestern (Figure B.45) Flow Regimes.

5.1.6 Radium

Distribution of solution radium species was calculated according to the equations given in Table B3.1 (Langmuir and Riese 1985). Radium concentrations in groundwater are generally limited by adsorption or solid solution formation, because radium concentrations in both natural waters and waters associated with uranium mining are usually not high enough to reach saturation with $\text{RaSO}_4(\text{c})$ (Langmuir and Riese 1985). Results of the modeling indicated that the groundwater

was undersaturated with respect to $\text{RaCO}_3(\text{c})$ (radium carbonate) and the less soluble $\text{RaSO}_4(\text{c})$ (radium sulfate). Barium surface-complexation (Dzombak and Morel 1990) and ion-exchange (Appelo and Postma 1993) constants for HFO were used to model radium attenuation because these constants are considered to be valid for radium (Langmuir 1997). Although the model predicts some interaction of radium with HFO, ion exchange was the dominant model attenuation mechanism for radium in both the Western (Figure B.38) and Southwestern (B.46) Flow Regimes.

5.1.7 Selenium

Distribution of dissolved selenium species was calculated based on both the equations for selenium aqueous complex formation in the MINTEQ database and also according to a set of redox conditions that are defined in the PHREEQC input files. The Se(III) (selenite) species are strongly adsorbed by HFO, while the Se(VI) (selenate) species are also adsorbed, but to a lesser extent (Neal 1990). The reduction of selenate and selenite species to Se(a) (amorphous selenium) is usually microbially mediated and occurs under anaerobic conditions; with further reduction and in the presence of iron, Se(-II) (selenide) can precipitate as ferroselite (Weres and others 1989; Garbisu and others 1996). The model input files allowed for precipitation of ferroselite, elemental selenium, and nickel selenide if these phases became oversaturated. In addition, selenium adsorption was modeled using the surface complexation constants for selenite and selenate taken from Dzombak and Morel (1990). Adsorption of selenite onto HFO was predicted to be the dominant attenuation mechanism for both the Western (Figure B.39) and the Southwestern (Figure B.47) Flow Regimes.

5.1.8 Thorium

Distribution of thorium species was calculated according to the equations given in Table B3.2. Results indicated that the modeled groundwater was undersaturated with minerals that might be expected to control thorium concentrations in groundwater, namely Th(OH)_4 (thorium hydroxide) and ThO_2 (thorium oxide) (Langmuir 1997). However, thorium concentrations in groundwater are also controlled by adsorption. Complete adsorption of thorium has been observed in laboratory studies on FeOOH (goethite) when carbonate alkalinities are low enough (<100 meq/l) to prevent both complexation with, and desorption of, thorium by carbonate (LaFlamme and Murray 1987). Because the modeled groundwater contains carbonate alkalinities ≤ 3 meq/l, thorium attenuation was modeled with adsorption using the surface complexation constants for aqueous Th^{4+} (without carbonate complexes) provided by LaFlamme and Murray (1987). The model results indicated that thorium attenuation will occur as a result of surface complexation in both the Western (Figure B.40) and Southwestern (Figure B.48) Flow Regimes. The modeled thorium results are consistent with observed adsorption characteristics of thorium in natural systems. Maximum thorium adsorption occurs above pH values of 5.5 to 6.5, and the tendency of thorium to be strongly adsorbed by clays and oxyhydroxides in neutral to alkaline solutions causes thorium to be naturally concentrated in sediments. Thorium-230 activities up to 22,000 pCi/l have been measured in acidic waste milling solutions discharged from the Highland Uranium Mill in Wyoming, which may be contrasted with a thorium-230 activity of 110 pCi/l in alkaline ($\text{pH} \geq 10$) leach solutions discharged from the Humeca Uranium Mill (Langmuir and Herman 1980).

Table B5.1 Geochemical Model Results for Western Flow Regime. Maximum Modeled Output Concentration at the POE.

Parameter		Maximum Source Concentration	Modeled Flow Rate 0.167 ft/d	Modeled Flow Rate 0.330 ft/d
Licensed Constituents				
Arsenic	(mg/l)	1.8	0.034	0.039
Beryllium	(mg/l)	1.64	0.005	0.005
Selenium	(mg/l)	0.161	0.0044	0.0048
Nickel	(mg/l)	13	0.063	0.065
Uranium	(mg/l)	12	0.0065	0.0071
²¹⁰ Pb	(pCi/l)	35.4	2.18	2.45
²²⁶⁺²²⁸ Ra	(pCi/l)	250	58.9	69.5
²³⁰ Th	(pCi/l)	57.4	0.107	0.108
Non-Licensed Constituents				
Calcium	(mg/l)	460	400	460
Magnesium	(mg/l)	110	75.2	86.1
Sodium	(mg/l)	180	115	120
Potassium	(mg/l)	24	13.7	14.4
Bicarbonate	(mg/l)	3.1	4.9	5.4
TDS	(mg/l)	4,500	2,500	2,600

Note: Chloride and Sulfate addressed in Appendix C.

Table B5.2 Geochemical Model Results for Southwestern Flow Regime. Maximum Modeled Output Concentration at the POE.

Parameter	Maximum Source Concentration	Modeled Flow Rate 0.167 ft/d	Modeled Flow Rate 0.280 ft/d
Licensed Constituents			
Arsenic (mg/l)	1.36	0.016	0.017
Beryllium (mg/l)	1.70	0.0011	0.0012
Selenium (mg/l)	0.53	0.041	0.043
Nickel (mg/l)	9.34	0.015	0.016
Uranium (mg/l)	34.1	0.14	0.15
²¹⁰ Pb (pCi/l)	47.7	0.23	0.24
²²⁶⁺²²⁸ Ra (pCi/l)	353	15.7	16.9
²³⁰ Th (pCi/l)	44.8	0.85	0.86
Non-Licensed Constituents			
Calcium (mg/l)	660	433	455
Magnesium (mg/l)	140	69	72
Sodium (mg/l)	60	49	50
Potassium (mg/l)	15	17	17
Bicarbonate (mg/l)	2.4	119	125
TDS (mg/l)	3,700	2,400	2,440

Note: Chloride and Sulfate addressed in Appendix C.

5.2 Estimated Gross Alpha Concentrations at the Points of Exposure (POEs):

The gross alpha concentrations at the POEs for the Western and Southwestern Flow Regimes were calculated using geochemical modeling results assuming flow rates of 0.167 ft/d and 0.33 ft/d for the Western Flow Regime, and 0.167 ft/d and 0.28 ft/d for the Southwestern Flow Regime. The gross alpha concentration at the POE is the sum of the activity concentrations of the individual alpha emitters. The calculations for the projected specific radionuclide concentrations at the Western and Southwestern POEs, attributable to the Gas Hills Facility, are given in Table B5.3. Radon-222 and Rn-220 and their short-lived decay products were not included in the calculations.

Radium-228 is a beta emitter. However, the activity of Ra-228 was included in calculating the gross alpha concentration since its decay product, Ra-224 is an alpha emitter. While the immediate parent of Ra-224, Th-228, is also an alpha emitter, it would not be transported at the same rate as the radium isotopes. Estimating the contribution of Ra-228 to the gross alpha concentration is difficult; however, it is not likely to constitute a significant fraction of the radium in the source term because it is a decay product of Th-232 and is not part of the U-238 decay series. Therefore, uncertainty in estimating the contribution from Ra-228 is not likely to add significantly to the uncertainty in the calculated gross alpha concentration.

The calculated gross alpha concentrations, excluding uranium isotopes, at the POEs for the Western flow regime were 61 and 72 picoCuries per liter (pCi/l) for modeled flow rates of 0.167 feet per day and 0.33 feet per day respectively. For the Southwestern flow regime, the calculated gross alpha concentrations excluding uranium isotopes, at the POEs were 16.8 and 18.0 pCi/l for modeled flow rates of 0.167 ft/d and 0.28 ft/d respectively. In comparison, the gross alpha maximum contaminant level (MCL) for drinking water is 15 pCi/l, excluding uranium and radon.

It is inappropriate to evaluate health and safety impacts on the basis of gross alpha concentrations since the tap water ingestion risk coefficient is different for each of the radionuclides. The mortality risk coefficients in lifetime risk per unit activity ingested (Bq^{-1}) from Federal Guidance Report No. 13 (EPA, 1999) are given below for each of the radionuclides listed in the table:

U-238:	1.13 E-9 Bq^{-1}	Th-228:	1.82 E-9 Bq^{-1}
U-235:	1.21 E-9 Bq^{-1}	Po-210:	3.53 E-8 Bq^{-1}
U-234:	1.24 E-9 Bq^{-1}	Ra-224:	2.74 E-9 Bq^{-1}
Th-230:	1.67 E-9 Bq^{-1}	Ra-228:	2.00 E-8 Bq^{-1}

The risk coefficients vary by more than an order of magnitude. Therefore, health risk evaluations should be performed only on the basis of specific radionuclide activity concentrations. Uranium decay products Th-234, Pa-234m, and Bi-210 were not considered in this analysis since they are beta emitters. Polonium-210, the alpha-emitting decay product of Bi-210, is accounted for in the analysis by assuming that the decay of Pb-210 results in the emission of one alpha.

Table B5.3 Projected Radionuclide Activity Concentrations at the Points of Exposure.

Radionuclide	Proposed ACL (pCi/l)	WFR OE Conc. (pCi/l)	WFR POE Conc. (pCi/l)	Proposed ACL (pCi/l)	SW POE Conc. (pCi/l)	SW POE Conc. (pCi/l)
	WFR	0.167 ft/d	0.33 ft/d	SWFR	0.167 ft/d	0.33 ft/d
U-238 ¹						
mg/l	12	6.5×10^{-3}	7.1×10^{-3}	34	0.14	0.15
pCi/l	3,960	2.1	2.3	11,220	46	50
U-235	178	0.09	0.10	505	2.1	2.3
U-234	3,960	2.1	2.3	11,220	46	50
Th-230	57	0.107	0.108	27	0.85	0.86
Ra-226+228 ²	250	58.9	69.5	353	15.7	16.9
Pb-210 ³	35	2.18	2.45	47	0.23	0.24
Total	NA	65.5	76.8	NA	111	120
Total excluding uranium	NA	61.2	72.1	NA	16.8	18.0

¹ The ACL for uranium is 12 mg/l for the WFR and 34 mg/l for the SWFR. The U-238 concentrations for the ACLs and the POEs (pCi/l) were calculated from the mass concentrations in mg/l as follows:
 $[U-238 \text{ (pCi/l)}] = [U-238 \text{ (mg/l)}](330 \text{ pCi/mg})$

Western Flow Regime

$$\text{ACL} = (12 \text{ mg/l})(330 \text{ pCi/mg}) = 3,960 \text{ pCi/l}$$

$$\text{POE [0.167 ft/d]} = (3.7 \times 10^{-5} \text{ mg/l})(330 \text{ pCi/mg}) = 0.012 \text{ pCi/l}$$

$$\text{POE [0.33 ft/d]} = (5.2 \times 10^{-5} \text{ mg/l})(330 \text{ pCi/mg}) = 0.017 \text{ pCi/l}$$

Southwestern POE

$$\text{ACL} = (34 \text{ mg/l})(330 \text{ pCi/mg}) = 1.12 \times 10^4 \text{ pCi/l}$$

$$\text{POE [0.167 ft/d]} = (4.7 \times 10^{-5} \text{ mg/l})(330 \text{ pCi/mg}) = 0.015 \text{ pCi/l}$$

$$\text{POE [0.28 ft/d]} = (2.7 \times 10^{-5} \text{ mg/l})(330 \text{ pCi/mg}) = 0.009 \text{ pCi/l}$$

The uranium isotopes were assumed to be in equilibrium in the groundwater so that the activity concentration of U-234 is equal to the activity concentration of U-238. The activity concentration of U-235 is 4.5 percent of the U-238.

² Ra-228 is a beta emitter; however, its shorter-lived decay products, Th-228 (1.9 years) and Ra-224 (3.7 days), are alpha emitters and could be in equilibrium with the Ra-228 depending on the residence time. Therefore, the gross alpha concentration for the combined Ra-226+228 activity concentration would be somewhat greater than the a factor of one times the combined activity concentration. The Ra-226 was assumed to comprise nearly all of the combined activity. Therefore, the relative error in assuming one alpha per disintegration of the combined Ra-226+228 would be small.

³ Pb-210 is a beta emitter but decays to Po-210, which is an alpha emitter. Therefore, the Pb-210 was assumed to emit one alpha per disintegration.

6.0 REFERENCES

- Allison, J.D., D.S. Brown, and K.J. Novo-Gradac. 1991. "MINTEQA2/PRODEFA2, A Geochemical Assessment Model for Environmental Systems," Version 3.0 *User's Manual*. Environmental Research Laboratory, Office of Research and Development, U.S. Environmental Protection Agency, Athens, Georgia. 106 pages.
- Anderson, D.A. 1969. "Uranium Deposits of the Gas Hills," *Contributions to Geology of Wyoming*, Uranium Issue, Volume 8, Number 2, page 93.
- Appelo, C.A.J. and D. Postma. 1993. *Geochemistry, Groundwater, and Pollution*. A.A. Balkema, Rotterdam. 536 pages.
- Ball, J.W., E.A. Jenne, and M.W. Cantrell. 1981. "WATEQ3: A Geochemical Model with Uranium Added". *U.S. Geological Survey Open File Report 81-1183*. Washington, D.C.
- Ball, J.W. and D.K. Nordstrom. 1991. "WATEQ4F – User's Manual with Revised Thermodynamic Database and Test Cases for Calculating Speciation of Major, Trace, and Redox Elements in Natural Waters". *U.S. Geological Survey Open-File Report 90-129*. 185 pages.
- Clement, W.H. and S.D. Faust. 1981. "The Release of Arsenic from Contaminated Muds and Sediments." *Journal of Environmental Science and Health*, A16:87-122.
- Cox, J.D., D.D. Wagman, and V.A. Medvedev. 1989. *Codata Key Values for Thermodynamics*. Hemisphere Publications, New York. 271 pages.
- Curti, E. 1999. Coprecipitation of radionuclides with calcite: estimation of partition coefficients based on review of laboratory investigations and geochemical data. *Applied Geochemistry*. 14:433-445.
- Davis, J.A. 1977. *Adsorption of Trace Metals and Complexing Ligands at the Oxide/Water Interface*. Ph.D. Thesis, Stanford University, Stanford, California.
- Davis, J.A. and D.B. Kent. 1990. "Surface Complexation Modeling in Aqueous Chemistry," in M.F. Hochella and A.F. White (eds.), *Mineral-Water Interface Geochemistry, Reviews in Mineralogy*, Volume 23, Chapter 5, pages 177-260. Mineralogical Society of America, Washington, D.C.
- Davis, J.A. and J.O. Leckie. 1978. "Surface Ionization and Complexation at the Oxide/Water Interface. II, Surface Properties of Amorphous Iron Oxyhydroxide and Adsorption of Metal Ions," *Journal of Colloid and Interface Science*, 67:90-107.
- DeVoto, R.H. 1978. *Uranium Geology and Exploration*, Lecture Notes and References. Colorado School of Mines, Golden, Colorado. 396 pages.
- Dzombak, D.A. and F.M.M. Morel. 1990. *Surface Complexation Modeling-Hydrous Ferric Oxide*. John Wiley & Sons, New York. 393 pages.

- Freeze, R.A. and J.A. Cherry. 1979. *Groundwater*. Prentice-Hall, Inc., New Jersey. 604 pages.
- Gaines, G.L. and H.C. Thomas. 1953. "Adsorption studies on clay minerals II, A formulation of the thermodynamics of exchange adsorption." *Journal of Chemical Physics*, 21:714-718.
- Garbisu, C., T. Ishii, T. Leighton, and B.B. Buchanan. 1996. "Bacterial Reduction of Selenite to Elemental Selenium." *Chemical Geology*, Volume 132, pages 199-204.
- Geraghty & Miller, Inc. 1996. *Preliminary Site Conceptual Model and Proposed Groundwater Compliance Program, Umetco Uranium Mill Site, Gas Hills, Wyoming*. Prepared for Umetco Minerals Corporation, Grand Junction, Colorado, by Geraghty & Miller, Inc., Albuquerque, NM.
- Granger, H.C. and C.G. Warren. 1974. *Zoning in the Altered Tongue Associated With Uranium Deposits, in Formation Of Uranium Ore Deposits*, proceedings of a symposium, Athens, 6-10 May 1974. International Atomic Energy Agency, Vienna. 748 pages.
- Harshman, E.N. 1966. *Genetic Implications of Some Elements Associated with Uranium Deposits, Shirley Basin, Wyoming*. U.S. Geological Survey Professional Paper 550-C.
- Harshman, E.N. 1974. *Distribution of Elements in Some Roll-type Uranium Deposits, in Formation of Uranium Ore Deposits*, proceedings of a symposium, Athens, 6-10 May 1974. International Atomic Energy Agency, Vienna. 748 pages.
- Jenne, E.A. 1968. "Controls on Mn, Fe, Co, Ni, Cu, and Zn Concentrations in Soils and Water: The Significant Role of Hydrous Mn and Fe Oxides." *American Chemical Society Advances in Chemistry Series*, 73:337-387.
- Kabata-Pendias and Pendias. 1992. *Trace Elements in Soils and Plants*, Second Edition. CRC Press, Boca Raton. 365 pages.
- King, J.W. and S.R. Austin. 1966. "Some Characteristics of Roll-type Uranium Deposits at Gas Hills, Wyoming." *Mining Engineering*, Volume 18, Number 5, pages 73-80.
- LaFlamme, B.D. and J.M. Murray. 1987. "Solid/Solution Interaction: The Effect of Carbonate Alkalinity on Adsorbed Thorium." *Geochimica et Cosmochimica Acta*, 51:243-250.
- Landa, E.R. 1999. Geochemical and Biogeochemical Controls on Element Mobility In and Around Uranium Mill Tailings. In *The Environmental Geochemistry of Mineral Deposits. Part B: Case Studies and Research Topics. Reviews in Economic Geology, Volume 6B*. Pages 527-538.
- Langmuir, D. and J.S. Herman. 1980. "The Mobility of Thorium in Natural Waters at Low Temperatures." *Geochimica et Cosmochimica Acta*, 44:1753-1766.
- Langmuir, D. and A.C. Riese. 1985. "The Thermodynamic Properties of Radium." *Geochimica et Cosmochimica Acta*, 49:1593-1601.

- Langmuir, D. 1997. *Aqueous Environmental Chemistry*. Prentice-Hall, Inc., New Jersey. 599 pages.
- Lidstone & Anderson, Inc. 1989. *Ground-Water Investigation of the East Gas Hills. AML 16-E*. Prepared for Worthington, Lenhart, & Carpenter, Casper, Wyoming, by Lidstone & Anderson, Inc., Fort Collins, Colorado.
- Ludwig, K.R. and R.I. Grauch. 1980. "Coexisting Coffinite and Uraninite in Some Sandstone-host Uranium Ores of Wyoming." *Economic Geology*, Volume 75, pages 296-302.
- Luoma, S.N. and J.A. Davis. 1983. "Requirements for Modeling Trace Metal Partitioning in Oxidized Estuarine Sediments." *Marine Chemistry*, 12:159-181.
- Masscheleyn, P.H., R.D. Delaune, and W.H. Patrick, Jr. 1991. "Arsenic and selenium chemistry as affected by sediment redox potential and pH." *Journal of Environmental Quality*, 20:522-527.
- Merritt, R.C. 1971. *The Extractive Metallurgy of Uranium*. Prepared Under Contract with the U.S. Atomic Energy Commission by the Colorado School of Mines Research Institute.
- Morin, K.A., J.A. Cherry, N.K. Dave, T.P. Lim, and A.J. Vivyurka. 1988. Migration of acidic groundwater seepage from uranium tailings impoundments, 2. Geochemical behavior of radionuclides in groundwater. *Journal of Contaminant Hydrology*. 2:305-322.
- Naumov, G.B., B.N. Ryzhenko, and I.L. Khodakovsky. 1974. *Handbook of Thermodynamic Data*. U.S.G.S. WRD-74-001. 328 pages.
- Neal, R.H. 1990. "Selenium," pages 237-260, in B.J. Alloway (ed.) *Heavy Metals in Soils*. John Wiley & Sons, Inc. New York. 339 pages.
- Nordstrom, D.K., L.N. Plummer, D. Langmuir, E. Busenberg, H.M. May, B.F. Jones, and D.L. Parkhurst. 1990. "Revised chemical equilibrium data for major water-mineral reactions and their limitations," pages 398-413, in D.C. Melchior and R.L. Bassett (eds.) *Chemical Modeling of Aqueous Systems II*. American Chemical Society, Washington, D.C.
- Parkhurst, D.L. and C.A.J. Appelo. 1999. "User's Guide to PHREEQC (Version 2)-A Computer Program for Speciation, Batch-Reaction, One-Dimensional Transport, and Inverse Geochemical Calculations." *U.S. Geological Survey Water-Resources Investigations Report* 99-4259.
- Parkhurst, D.L., D.C. Thorstenson, and L.N. Plummer. 1980. "PHREEQE - A Computer Program For Geochemical Calculations." *U.S. Geological Survey Water-Resources Investigations Report* 80-96. Revised and Reprinted August, 1990.
- Rai, D., C.C. Ainsworth, L.E. Eary, S.V. Mattigod, and D.R. Jackson. 1987. *Inorganic and Organic Constituents in Fossil Fuel Combustion Residues, Volume 1: A Critical Review*. EA-5176, Electric Power Research Institute, Palo Alto, California.

- SMI (Shepherd Miller, Inc.). 1997. *Evaluation of Drainage of Gas Hills Tailing Impoundment*. Prepared for Umetco Minerals Corporation, Grand Junction, Colorado, by Shepherd Miller, Inc., Fort Collins, Colorado.
- SMI. 1998a. Evaluation of Drainage from the A-9 Repository. Prepared for Umetco Minerals Corporation, Grand Junction, Colorado, by Shepherd Miller, Inc., Fort Collins, Colorado.
- SMI. 1998b. *Evaluation of Background Groundwater Quality for the Umetco Gas Hills Uranium Mill Site, Fremont and Natrona Counties, Wyoming*. Prepared for Umetco Minerals Corporation, Grand Junction, Colorado, by Shepherd Miller, Inc., Fort Collins, Colorado.
- Umetco Minerals Corporation. 1997. *Site Characterization Report, East Gas Hills Reclamation Project, Gas Hills, Wyoming*.
- USAEC (Atomic Energy Commission). 1959. *Guidebook to Uranium Deposits of the Western United States*. Prepared by the Production Evaluation Division of the Grand Junction Operations Office.
- USEPA (Environmental Protection Agency). 1999. "Cancer Risk Coefficients for Environmental Exposure to Radionuclides." *Federal Guidance Report Number 13*. EPA 402-R-99-001.
- U.S. Environmental Services. 1996. *Drilling and Construction of Monitoring Wells MW75, MW76, and MW77, East Gas Hills, Wyoming*, unpublished report prepared for Umetco Minerals Corporation, May, 1997.
- Wagman, D.D., W.H. Evans, V.B. Parker, R.H. Schumm, I. Halow, S.M. Bailey, K.L. Churney, and R.L. Nutall. 1982. "The NBS Tables of Chemical Thermodynamic Properties. Selected Values for Inorganic and C1 and C2 Organic Substances in SI Units." *Journal of Physical and Chemical Reference Data*. Volume 11, Supplement Number 2. 392 pages.
- Weres, O., A.R. Jaouni, and L. Tsao. 1989. "The Distribution, Speciation and Geochemical Cycling of Selenium in a Sedimentary Environment, Kesterson Reservoir, California, U.S.A." *Applied Geochemistry*, Volume 4, pages 543-563.
- Westall, J.C. and H. Hohl. 1980. "A Comparison of Electrostatic Models for the Oxide/Solution Interface." *Advanced Colloid Interface Science*, 12:265-294.
- Wolery, T.J. 1992. *EQ3/6. A Software Package for Geochemical Modeling of Aqueous Systems: Package Overview and Installation Guide, Version 7*. UCRL-MA-11062 Part I, Lawrence Livermore National Laboratory.

7.0 ATTACHMENTS

The PHREEQC input files and the modified MINTEQ database used for the Gas Hills geochemical model are on the disk included with this attachment. A key to the filenames on the disk is provided below.

Source Decay Terms

- SWFRSources.in Mixing of A-9 Source Term with LA-2
- WFRSources.in Mixing of AGTI Source Term with MW-27

Southwestern Flow Regime

- SWFR1d.in Southwestern Flow Regime (0.167 ft/d). Concentration vs Distance (1000 yr)
- SWFR2d.in Southwestern Flow Regime (0.280 ft/d). Concentration vs Distance (1000 yr)
- SWFR1td.in Southwestern Flow Regime (0.167 ft/d). Concentration vs Time at the POE
- SWFR2td.in Southwestern Flow Regime (0.280 ft/d). Concentration vs Time at the POE

Western Flow Regime

- WFR1d.in Western Flow Regime (0.167 ft/d). Concentration vs Distance (1000 yr)
- WFR2d.in Western Flow Regime (0.330 ft/d). Concentration vs Distance (1000 yr)
- WFR1td.in Western Flow Regime (0.167 ft/d). Concentration vs Time at the POE
- WFR2td.in Western Flow Regime (0.330 ft/d). Concentration vs Time at the POE

PHREEQC Model Database

- Umetco.dat Modified MINTEQ Database Used in the Gas Hills Modeling

from diskette
Unmetco geochemical input files — 10 files in ASCII DOS

TITLE A-9 area (SW flow regime). FILE: SWFR1d.in
#Using flow rate of 0.167 ft/d - DECREASING SOURCE TERM TO 90% REDUCTION
#Dispersivity = 50
#SOLID PHASES ALLOWED

KNOBS

-iterations 100
-tolerance 1.00E-13
-step_size 100
-pe_step_size 10
-diagonal_scale TRUE
-debug_prep FALSE
-debug_set FALSE
-debug_model FALSE
-debug_inverse FALSE
-logfile FALSE

SOLUTION 0 # Initial Source Term

units	ppm
pe	8
pH	4.33
Th	2.22e-6
Pb	6.02e-10
Be	1.7
Ca	660
Mg	144
Na	61
K	15
Fe(2)	89
Cl	161
As	1.36
Ni	9.34
Se	0.53
Si	56.4
U	34.1
Alkalinity	2.44 as HCO ₃
S(6)	2650
Ra	3.57e-7

SOLUTION 1-5 GW8 January 2001

units	ppm
pe	7
pH	4.73
S(6)	1540
Cl	97
Alkalinity	2.0 as HCO ₃
Ca	418

Na	30.6
Mg	70.8
K	17.6
Fe(2)	127
As	0.007
Be	0.076
Th	7.97e-8
Pb	2.58e-10
Ra	6.25e-8
Ni	1.31
Se	0.001
U	10.3

SOLUTION 6-54 MW-74 January 2001

units	ppm
pe	6
pH	6.69
S(6)	24.1
Cl	9.1
Alkalinity	35 as HCO3
Ca	17.7
Na	6.3
Mg	2.9
K	4.2
Fe(2)	0.1
As	0.0019
Be	0.001 # 1/2 DL
Th	3.77e-8
Pb	1.68e-11
Ra	4.55e-10
Ni	0.005 # 1/2 DL
Se	0.012
U	0.0139
S(-2)	0.033

EQUILIBRIUM_PHASES 1-54

Calcite	0.0	0.0
Gypsum	0.0	0.0
Uraninite	0.0	0.0
USiO4(c)	0.0	0.0
Ferroselite	0.0	0.0
Se(A)	0.0	0.0
RaSO4	0.0	0.0
NiSe	0.0	0.0
Anglesite	0.0	0.0

SURFACE 1-5

-equilibrate 1		
Hfo_wOH	0.086	600 45.9
Hfo_sOH	0.0021	

SURFACE 6-54
-equilibrate 6
Hfo_wOH 0.086 600 45.9
Hfo_sOH 0.0021

EXCHANGE 1-5
-equilibrate 1
X 1.2

EXCHANGE 6-54
-equilibrate 6
X 1.2

TRANSPORT
-lengths 54*30.5
-dispersivities 54*50
-cells 54
-shifts 4

PRINT
-reset false

END

SOLUTION 0 #33% REDUCTION

units	ppm
pe	5.6
pH	4.47
Th	1.47e-6
Pb	4.12E-10
Ra	2.41E-07
U	22.62
Be	1.13
Ca	536.7
Mg	116.7
Na	57
K	16.2
Fe(2)	61.8
Cl	114.6
As	0.90
Ni	6.20
Se	0.35
Si	37.4
Alkalinity	4.0 as HCO3
S(6)	1980.5

TRANSPORT
-lengths 54*30.5

-dispersivities 54*50
 -cells 54
 -shifts 2

END

SOLUTION 0 #50% Reduction

units	ppm
pe	5.5
pH	4.57
Th	1.12e-6
Pb	3.22E-10
Ra	1.86E-07
U	17.16
Be	0.85
Ca	477.5
Mg	103.6
Na	55
K	16.8
Fe(2)	48.9
Cl	92.5
As	0.68
Ni	4.7
Se	0.27
Si	28.31
Alkalinity	4.73 as HCO3
S(6)	1661

TRANSPORT

-lengths 54*30.5
 -dispersivities 54*50
 -cells 54
 -shifts 4

END

SOLUTION 0 #75% Reduction

units	ppm
pe	5.1
pH	4.85
Th	5.65e-07
Pb	1.81E-10
Ra	1.0E-07
U	8.62
Be	0.43
Ca	384.9
Mg	83.1
Na	51.9
K	17.7

Fe(2)	28.7
Cl	58
As	0.34
Ni	2.36
Se	0.13
Si	14.2
Alkalinity 5.88 as HCO3	
S(6)	1161

TRANSPORT

-lengths	54*30.5
-dispersivities	54*50
-cells	54
-shifts	12

END

SOLUTION 0 #90% Reduction

units	ppm
pe	4.4
pH	5.27
Th	2.33E-07
Pb	9.58e-11
Ra	4.84e-8
U	3.5
Be	0.17
Ca	329.4
Mg	70.8
Na	50
K	18.2
Fe(2)	16.5
Cl	37.3
As	0.14
Ni	0.96
Se	0.05
Si	5.66
Alkalinity 6.56 as HCO3	
S(6)	860.7

TRANSPORT

-lengths	54*30.5
-dispersivities	54*50
-cells	54
-shifts	588
-punch_frequency	588

SELECTED_OUTPUT

-file P:\100040-7\phreeqc\SWFR1d.dat

USER_PUNCH

```
-headings As Be Cl Pb U Ni Se SO4 Th Ra sOPb+
-headings wOPb+ PbX2 Anglesite sOHUO2+2
-headings wOUO2+ USiO4(C) Uraninite sONi+ wONi+
-headings NiSe sOHRa+2 wORa+ RaX2 RaSO4 wSeO4-
-headings wOHSeO4-2 wSeO3- wOHSeO3-2 Se(A)
-headings FeSe2 sSO4- wSO4- sOHsO4-2 wOHsO4-2
-headings gypsum wOTh+3 wOTh(OH)+2 wOTh(OH)2+
-headings wOTh(OH)3 wOTh(OH)4- sH2AsO3 wH2AsO3
-headings sH2AsO4 wH2AsO4 sHAsO4- wHAsO4- sAsO4-2
-headings wAsO4-2 sOHAsO4-3 wOHAsO4-3 sOBe+ wOBe+
-headings Calcite Ca Mg Na K HCO3 SO4 Cl TDS
-start
10 REM Convert to ppm and show molalities
20 PUNCH TOT("As")*74.9216*1000
30 PUNCH TOT("Be")*9.0122*1000
40 PUNCH TOT("Cl")*35.453*1000
50 PUNCH TOT("Pb")*207.19*1000/1.29e-11
60 PUNCH TOT("U")*238.029*1000
70 PUNCH TOT("Ni")*58.71*1000
80 PUNCH TOT("Se")*78.96*1000
90 PUNCH TOT("S(6)")*96.0616*1000
100 PUNCH TOT("Th")*232.038*1000/4.96e-8
110 PUNCH TOT("Ra")*226*1000/1.01e-9
120 PUNCH MOL("Hfo_sOPb+")
130 PUNCH MOL("Hfo_wOPb+")
140 PUNCH MOL("PbX2")
150 PUNCH EQUI("Anglesite")
160 PUNCH MOL("Hfo_sOHUO2+2")
170 PUNCH MOL("Hfo_wOUO2+")
180 PUNCH EQUI("USiO4(C)")
190 PUNCH EQUI("Uraninite")
200 PUNCH MOL("Hfo_sONi+")
210 PUNCH MOL("Hfo_wONi+")
220 PUNCH EQUI("NiSe")
230 PUNCH MOL("Hfo_sOHRa+2")
240 PUNCH MOL("Hfo_wORa+")
250 PUNCH MOL("RaX2")
260 PUNCH EQUI("RaSO4")
270 PUNCH MOL("Hfo_wSeO4-")
280 PUNCH MOL("Hfo_wOHSeO4-2")
290 PUNCH MOL("Hfo_wSeO3-")
300 PUNCH MOL("Hfo_wOHSeO3-2")
310 PUNCH EQUI("Se(A)")
320 PUNCH EQUI("Ferroselite")
330 PUNCH MOL("Hfo_sSO4-")
340 PUNCH MOL("Hfo_wSO4-")
350 PUNCH MOL("Hfo_sOHsO4-2")
```

```

360 PUNCH MOL("Hfo_wOHSO4-2")
370 PUNCH EQUI("gypsum")
380 PUNCH MOL("Hfo_wOTh+3")
390 PUNCH MOL("Hfo_wOTh(OH)+2")
400 PUNCH MOL("Hfo_wOTh(OH)2+")
410 PUNCH MOL("Hfo_wOTh(OH)3")
420 PUNCH MOL("Hfo_wOTh(OH)4-")
430 PUNCH MOL("Hfo_sH2AsO3")
440 PUNCH MOL("Hfo_wH2AsO3")
450 PUNCH MOL("Hfo_sH2AsO4")
460 PUNCH MOL("Hfo_wH2AsO4")
470 PUNCH MOL("Hfo_sHAsO4-")
480 PUNCH MOL("Hfo_wHAsO4-")
490 PUNCH MOL("Hfo_sAsO4-2")
500 PUNCH MOL("Hfo_wAsO4-2")
510 PUNCH MOL("Hfo_sOHasO4-3")
520 PUNCH MOL("Hfo_wOHasO4-3")
530 PUNCH MOL("Hfo_sOBe+")
540 PUNCH MOL("Hfo_wOBe+")
550 PUNCH EQUI("Calcite")
560 PUNCH TOT("Ca")*40.08*1000
570 PUNCH TOT("Mg")*24.312*1000
580 PUNCH TOT("Na")*22.9898*1000
590 PUNCH TOT("K")*39.102*1000
600 PUNCH TOT("C(4)")*61.018*1000
610 PUNCH TOT("S(6)")*96.0616*1000
620 PUNCH TOT("Cl")*35.453*1000
630 A = (TOT("Ca")*40.08*1000)+(TOT("Mg")*24.312*1000)
640 B = (TOT("Na")*22.9898*1000)+(TOT("K")*39.102*1000)
650 C = TOT("C(4)")*61.018*1000
660 D = TOT("S(6)")*96.0616*1000
670 E = TOT("Cl")*35.453*1000
680 PUNCH A+B+C+D+E
-end

```

END

TITLE A-9 area (SW flow regime). FILE: SWFR1td.in CONC vs TIME
#Using flow rate of 0.167 ft/d - DECREASING SOURCE TERM TO 90% REDUCTION
#DISPERSIVITY = 50
#SOLID PHASES ALLOWED

PRINT

-reset false

KNOBS

-iterations 100
-tolerance 1.00E-13
-step_size 100
-pe_step_size 10
-diagonal_scale TRUE
-debug_prep FALSE
-debug_set FALSE
-debug_model FALSE
-debug_inverse FALSE
-logfile FALSE

SELECTED_OUTPUT

-file P:\100040-7\phreeqc\SWFR1td.dat

USER_PUNCH

-headings As Be Cl Pb U Ni Se SO4 Th Ra sOPb+
-headings wOPb+ PbX2 Anglesite sOHUO2+2
-headings wOUO2+ USiO4(C) Uraninite sONi+ wONi+
-headings NiSe sOHRa+2 wORa+ RaX2 RaSO4 wSeO4-
-headings wOHSeO4-2 wSeO3- wOHSeO3-2 Se(A)
-headings FeSe2 sSO4- wSO4- sOHSeO4-2 wOHSeO4-2
-headings gypsum wOTh+3 wOTh(OH)+2 wOTh(OH)2+
-headings wOTh(OH)3 wOTh(OH)4- sH2AsO3 wH2AsO3
-headings sH2AsO4 wH2AsO4 sHAsO4- wHAsO4- sAsO4-2
-headings wAsO4-2 sOHAsO4-3 wOHAsO4-3 sOBe+ wOBe+
-headings Calcite Ca Mg Na K HCO3 SO4 Cl TDS
-start
10 REM Convert to ppm and show molalities
20 PUNCH TOT("As")*74.9216*1000
30 PUNCH TOT("Be")*9.0122*1000
40 PUNCH TOT("Cl")*35.453*1000
50 PUNCH TOT("Pb")*207.19*1000/1.29e-11
60 PUNCH TOT("U")*238.029*1000
70 PUNCH TOT("Ni")*58.71*1000
80 PUNCH TOT("Se")*78.96*1000
90 PUNCH TOT("S(6)")*96.0616*1000
100 PUNCH TOT("Th")*232.038*1000/4.96e-8
110 PUNCH TOT("Ra")*226*1000/1.01e-9
120 PUNCH MOL("Hfo_sOPb+")

130 PUNCH MOL("Hfo_wOPb+")
140 PUNCH MOL("PbX2")
150 PUNCH EQUI("Anglesite")
160 PUNCH MOL("Hfo_sOHUO2+2")
170 PUNCH MOL("Hfo_wOUO2+")
180 PUNCH EQUI("USiO4(C)")
190 PUNCH EQUI("Uraninite")
200 PUNCH MOL("Hfo_sONi+")
210 PUNCH MOL("Hfo_wONi+")
220 PUNCH EQUI("NiSe")
230 PUNCH MOL("Hfo_sOHRa+2")
240 PUNCH MOL("Hfo_wORa+")
250 PUNCH MOL("RaX2")
260 PUNCH EQUI("RaSO4")
270 PUNCH MOL("Hfo_wSeO4-")
280 PUNCH MOL("Hfo_wOHSeO4-2")
290 PUNCH MOL("Hfo_wSeO3-")
300 PUNCH MOL("Hfo_wOHSeO3-2")
310 PUNCH EQUI("Se(A)")
320 PUNCH EQUI("Ferroselite")
330 PUNCH MOL("Hfo_sSO4-")
340 PUNCH MOL("Hfo_wSO4-")
350 PUNCH MOL("Hfo_sOHSO4-2")
360 PUNCH MOL("Hfo_wOHSO4-2")
370 PUNCH EQUI("gypsum")
380 PUNCH MOL("Hfo_wOTh+3")
390 PUNCH MOL("Hfo_wOTh(OH)+2")
400 PUNCH MOL("Hfo_wOTh(OH)2+")
410 PUNCH MOL("Hfo_wOTh(OH)3")
420 PUNCH MOL("Hfo_wOTh(OH)4-")
430 PUNCH MOL("Hfo_sH2AsO3")
440 PUNCH MOL("Hfo_wH2AsO3")
450 PUNCH MOL("Hfo_sH2AsO4")
460 PUNCH MOL("Hfo_wH2AsO4")
470 PUNCH MOL("Hfo_sHAsO4-")
480 PUNCH MOL("Hfo_wHAsO4-")
490 PUNCH MOL("Hfo_sAsO4-2")
500 PUNCH MOL("Hfo_wAsO4-2")
510 PUNCH MOL("Hfo_sOHAsO4-3")
520 PUNCH MOL("Hfo_wOHAsO4-3")
530 PUNCH MOL("Hfo_sOBe+")
540 PUNCH MOL("Hfo_wOBe+")
550 PUNCH EQUI("Calcite")
560 PUNCH TOT("Ca")*40.08*1000
570 PUNCH TOT("Mg")*24.312*1000
580 PUNCH TOT("Na")*22.9898*1000
590 PUNCH TOT("K")*39.102*1000
600 PUNCH MOL("HCO3-")*61.018*1000
610 PUNCH TOT("S(6)")*96.0616*1000
620 PUNCH TOT("Cl")*35.453*1000

```

630 A = (TOT("Ca")*40.08*1000)+(TOT("Mg")*24.312*1000)
640 B = (TOT("Na")*22.9898*1000)+(TOT("K")*39.102*1000)
650 C = MOL("HCO3-")*61.018*1000
660 D = TOT("S(6)")*96.0616*1000
670 E = TOT("Cl")*35.453*1000
680 PUNCH A+B+C+D+E
-end

```

```

PRINT
-selected_output      false

```

SOLUTION 0 # Initial Source Term

units	ppm
pe	8
pH	4.33
Th	2.22e-6
Pb	6.02e-10
Be	1.7
Ca	660
Mg	144
Na	61
K	15
Fe(2)	89
Cl	161
As	1.36
Ni	9.34
Se	0.53
Si	56.4
U	34.1
Alkalinity	2.44 as HCO3
S(6)	2650
Ra	3.57e-7

SOLUTION 1-5 GW8 January 2001

units	ppm
pe	7
pH	4.73
S(6)	1540
Cl	97
Alkalinity	2.0 as HCO3
Ca	418
Na	30.6
Mg	70.8
K	17.6
Fe(2)	127
As	0.007
Be	0.076

Th	7.97e-8
Pb	2.58e-10
Ra	6.25e-8
Ni	1.31
Se	0.001
U	10.3

SOLUTION 6-54 MW-74 January 2001

units	ppm
pe	6
pH	6.69
S(6)	24.1
Cl	9.1
Alkalinity	35 as HCO3
Ca	17.7
Na	6.3
Mg	2.9
K	4.2
Fe(2)	0.1
As	0.0019
Be	0.001 # 1/2 DL
Th	3.77e-8
Pb	1.68e-11
Ra	4.55e-10
Ni	0.005 # 1/2 DL
Se	0.012
U	0.0139
S(-2)	0.033

EQUILIBRIUM_PHASES 1-54

Calcite	0.0	0.0
Gypsum	0.0	0.0
Uraninite	0.0	0.0
USiO4(c)	0.0	0.0
Ferroselite	0.0	0.0
Se(A)	0.0	0.0
RaSO4	0.0	0.0
NiSe	0.0	0.0
Anglesite	0.0	0.0

SURFACE 1-5

-equilibrate 1		
Hfo_wOH	0.086	600 45.9
Hfo_sOH	0.0021	

SURFACE 6-54

-equilibrate 6		
Hfo_wOH	0.086	600 45.9
Hfo_sOH	0.0021	

EXCHANGE 1-5
-equilibrate 1
X 1.2

EXCHANGE 6-54
-equilibrate 6
X 1.2

TRANSPORT
-lengths 54*30.5
-dispersivities 54*50
-cells 54
-shifts 4
-punch_cells 54

PRINT
-selected_output true

END

PRINT
-selected_output false

SOLUTION 0 #33% REDUCTION

units	ppm
pe	5.6
pH	4.47
Th	1.47e-6
Pb	4.12E-10
Ra	2.41E-07
U	22.62
Be	1.13
Ca	536.7
Mg	116.7
Na	57
K	16.2
Fe(2)	61.8
Cl	114.6
As	0.90
Ni	6.20
Se	0.35
Si	37.4
Alkalinity	4.0 as HCO3
S(6)	1980.5

TRANSPORT
-lengths 54*30.5
-dispersivities 54*50
-cells 54

```
-shifts      2
-punch_cells 54

PRINT
  -selected_output  true
```

END

```
PRINT
  -selected_output  false
```

SOLUTION 0 #50% Reduction

units	ppm
pe	5.5
pH	4.57
Th	1.12e-6
Pb	3.22E-10
Ra	1.86E-07
U	17.16
Be	0.85
Ca	477.5
Mg	103.6
Na	55
K	16.8
Fe(2)	48.9
Cl	92.5
As	0.68
Ni	4.7
Se	0.27
Si	28.31
Alkalinity	4.73 as HCO3
S(6)	1661

```
TRANSPORT
  -lengths      54*30.5
  -dispersivities 54*50
  -cells        54
  -shifts       4
  -punch_cells  54
```

```
PRINT
  -selected_output  true
```

END

```
PRINT
  selected_output  false
```

SOLUTION 0 #75% Reduction

units	ppm
pe	5.1
pH	4.85
Th	5.65E-07
Pb	1.81E-10
Ra	1.0E-07
U	8.62
Be	0.43
Ca	384.9
Mg	83.1
Na	51.9
K	17.7
Fe(2)	28.7
Cl	58
As	0.34
Ni	2.36
Se	0.13
Si	14.2
Alkalinity	5.88 as HCO3
S(6)	1161

TRANSPORT

-lengths	54*30.5
-dispersivities	54*50
-cells	54
-shifts	12
-punch_cells	54

PRINT

selected_output	true
-----------------	------

END

PRINT

selected_output	false
-----------------	-------

SOLUTION 0 #90% Reduction

units	ppm
pe	4.4
pH	5.27
Th	2.33E-07
Pb	9.58e-11
Ra	4.84e-8
U	3.5
Be	0.17
Ca	329.4
Mg	70.8
Na	50
K	18.2

Fe(2)	16.5
Cl	37.3
As	0.14
Ni	0.96
Se	0.05
Si	5.66
Alkalinity	6.56 as HCO ₃
S(6)	860.7

TRANSPORT

-lengths	54*30.5
-dispersivities	54*50
-cells	54
-shifts	588
-punch_cells	54

PRINT

-selected_output	true
------------------	------

END

PRINT

selected_output	false
-----------------	-------

TITLE A-9 area (SW flow regime). FILE: SWFR2d.in
#Using flow rate of 0.280 ft/d - DECREASING SOURCE TERM TO 90% REDUCTION
#dispersivity = 50
#SOLID PHASES ALLOWED

KNOBS

-iterations 100
-tolerance 1.00E-13
-step_size 100
-pe_step_size 10
-diagonal_scale TRUE
-debug_prep FALSE
-debug_set FALSE
-debug_model FALSE
-debug_inverse FALSE
-logfile FALSE

SOLUTION 0 # Initial Source Term

units	ppm
pe	8
pH	4.33
Th	2.22e-6
Pb	6.02e-10
Be	1.7
Ca	660
Mg	144
Na	61
K	15
Fe(2)	89
Cl	161
As	1.36
Ni	9.34
Se	0.53
Si	56.4
U	34.1
Alkalinity	2.44 as HCO3
S(6)	2650
Ra	3.57e-7

SOLUTION 1-5 GW8 January 2001

units	ppm
pe	7
pH	4.73
S(6)	1540
Cl	97
Alkalinity	2.0 as HCO3
Ca	418

Na	30.6
Mg	70.8
K	17.6
Fe(2)	127
As	0.007
Be	0.076
Th	7.97e-8
Pb	2.58e-10
Ra	6.25e-8
Ni	1.31
Se	0.001
U	10.3

SOLUTION 6-54 MW-74 January 2001

units	ppm
pe	6
pH	6.69
S(6)	24.1
Cl	9.1
Alkalinity	35 as HCO3
Ca	17.7
Na	6.3
Mg	2.9
K	4.2
Fe(2)	0.1
As	0.0019
Be	0.001 # 1/2 DL
Th	3.77e-8
Pb	1.68e-11
Ra	4.55e-10
Ni	0.005 # 1/2 DL
Se	0.012
U	0.0139
S(-2)	0.033

EQUILIBRIUM_PHASES 1-54

Calcite	0.0	0.0
Gypsum	0.0	0.0
Uraninite	0.0	0.0
USiO4(c)	0.0	0.0
Ferroselite	0.0	0.0
Se(A)	0.0	0.0
RaSO4	0.0	0.0
NiSe	0.0	0.0
Anglesite	0.0	0.0

SURFACE 1-5

-equilibrate 1		
Hfo_wOH	0.086	600 45.9
Hfo_sOH	0.0021	

SURFACE 6-54
-equilibrate 6
Hfo_wOH 0.086 600 45.9
Hfo_sOH 0.0021

EXCHANGE 1-5
-equilibrate 1
X 1.2

EXCHANGE 6-54
-equilibrate 6
X 1.2

TRANSPORT
-lengths 54*30.5
-dispersivities 54*50
-cells 54
-shifts 6

PRINT
-reset false

END

SOLUTION 0 #33% REDUCTION

units	ppm
pe	5.6
pH	4.47
Th	1.47e-6
Pb	4.12E-10
Ra	2.41E-07
U	22.62
Be	1.13
Ca	536.7
Mg	116.7
Na	57
K	16.2
Fe(2)	61.8
Cl	114.6
As	0.90
Ni	6.20
Se	0.35
Si	37.4
Alkalinity	4.0 as HCO3
S(6)	1980.5

TRANSPORT
-lengths 54*30.5

-dispersivities 54*50
 -cells 54
 -shifts 3

END

SOLUTION 0 #50% Reduction

units	ppm
pe	5.5
pH	4.57
Th	1.12e-6
Pb	3.22E-10
Ra	1.86E-07
U	17.16
Be	0.85
Ca	477.5
Mg	103.6
Na	55
K	16.8
Fe(2)	48.9
Cl	92.5
As	0.68
Ni	4.7
Se	0.27
Si	28.31
Alkalinity	4.73 as HCO3
S(6)	1661

TRANSPORT

-lengths 54*30.5
 -dispersivities 54*50
 -cells 54
 -shifts 7

END

SOLUTION 0 #75% Reduction

units	ppm
pe	5.1
pH	4.85
Th	5.65E-07
Pb	1.81E-10
Ra	1.0E-07
U	8.62
Be	0.43
Ca	384.9
Mg	83.1
Na	51.9
K	17.7

Fe(2)	28.7
Cl	58
As	0.34
Ni	2.36
Se	0.13
Si	14.2
Alkalinity 5.88 as HCO3	
S(6)	1161

TRANSPORT

-lengths	54*30.5
-dispersivities	54*50
-cells	54
-shifts	19

END

SOLUTION 0 #90% Reduction

units	ppm
pe	4.4
pH	5.27
Th	2.33E-07
Pb	9.58e-11
Ra	4.84e-8
U	3.5
Be	0.17
Ca	329.4
Mg	70.8
Na	50
K	18.2
Fe(2)	16.5
Cl	37.3
As	0.14
Ni	0.96
Se	0.05
Si	5.66
Alkalinity 6.56 as HCO3	
S(6)	860.7

TRANSPORT

-lengths	54*30.5
-dispersivities	54*50
-cells	54
-shifts	987
-punch_frequency	987

SELECTED_OUTPUT

-file P:\100040-7\phreeqc\SWFR2d.dat

USER_PUNCH

-headings As Be Cl Pb U Ni Se SO4 Th Ra sOPb+
-headings wOPb+ PbX2 Anglesite sOHUO2+2
-headings wOUO2+ USiO4(C) Uraninite sONi+ wONi+
-headings NiSe sOHRa+2 wORa+ RaX2 RaSO4 wSeO4-
-headings wOHSeO4-2 wSeO3- wOHSeO3-2 Se(A)
-headings FeSe2 sSO4- wSO4- sOHSO4-2 wOHSO4-2
-headings gypsum wOTh+3 wOTh(OH)+2 wOTh(OH)2+
-headings wOTh(OH)3 wOTh(OH)4- sH2AsO3 wH2AsO3
-headings sH2AsO4 wH2AsO4 sHAsO4- wHAsO4- sAsO4-2
-headings wAsO4-2 sOHAsO4-3 wOHAsO4-3 sOBe+ wOBe+
-headings Calcite Ca Mg Na K HCO3 SO4 Cl TDS
-start
10 REM Convert to ppm and show molalities
20 PUNCH TOT("As")*74.9216*1000
30 PUNCH TOT("Be")*9.0122*1000
40 PUNCH TOT("Cl")*35.453*1000
50 PUNCH TOT("Pb")*207.19*1000/1.29e-11
60 PUNCH TOT("U")*238.029*1000
70 PUNCH TOT("Ni")*58.71*1000
80 PUNCH TOT("Se")*78.96*1000
90 PUNCH TOT("S(6)")*96.0616*1000
100 PUNCH TOT("Th")*232.038*1000/4.96e-8
110 PUNCH TOT("Ra")*226*1000/1.01e-9
120 PUNCH MOL("Hfo_sOPb+")
130 PUNCH MOL("Hfo_wOPb+")
140 PUNCH MOL("PbX2")
150 PUNCH EQUI("Anglesite")
160 PUNCH MOL("Hfo_sOHUO2+2")
170 PUNCH MOL("Hfo_wOUO2+")
180 PUNCH EQUI("USiO4(C)")
190 PUNCH EQUI("Uraninite")
200 PUNCH MOL("Hfo_sONi+")
210 PUNCH MOL("Hfo_wONi+")
220 PUNCH EQUI("NiSe")
230 PUNCH MOL("Hfo_sOHRa+2")
240 PUNCH MOL("Hfo_wORa+")
250 PUNCH MOL("RaX2")
260 PUNCH EQUI("RaSO4")
270 PUNCH MOL("Hfo_wSeO4-")
280 PUNCH MOL("Hfo_wOHSeO4-2")
290 PUNCH MOL("Hfo_wSeO3-")
300 PUNCH MOL("Hfo_wOHSeO3-2")
310 PUNCH EQUI("Se(A)")
320 PUNCH EQUI("Ferroselite")
330 PUNCH MOL("Hfo_sSO4-")
340 PUNCH MOL("Hfo_wSO4-")
350 PUNCH MOL("Hfo_sOHSO4-2")
360 PUNCH MOL("Hfo_wOHSO4-2")

```

370 PUNCH EQUI("gypsum")
380 PUNCH MOL("Hfo_wOTh+3")
390 PUNCH MOL("Hfo_wOTh(OH)+2")
400 PUNCH MOL("Hfo_wOTh(OH)2+")
410 PUNCH MOL("Hfo_wOTh(OH)3")
420 PUNCH MOL("Hfo_wOTh(OH)4-")
430 PUNCH MOL("Hfo_sH2AsO3")
440 PUNCH MOL("Hfo_wH2AsO3")
450 PUNCH MOL("Hfo_sH2AsO4")
460 PUNCH MOL("Hfo_wH2AsO4")
470 PUNCH MOL("Hfo_sHAsO4-")
480 PUNCH MOL("Hfo_wHAsO4-")
490 PUNCH MOL("Hfo_sAsO4-2")
500 PUNCH MOL("Hfo_wAsO4-2")
510 PUNCH MOL("Hfo_sOHAsO4-3")
520 PUNCH MOL("Hfo_wOHAsO4-3")
530 PUNCH MOL("Hfo_sOBe+")
540 PUNCH MOL("Hfo_wOBe+")
550 PUNCH EQUI("Calcite")
560 PUNCH TOT("Ca")*40.08*1000
570 PUNCH TOT("Mg")*24.312*1000
580 PUNCH TOT("Na")*22.9898*1000
590 PUNCH TOT("K")*39.102*1000
600 PUNCH TOT("C(4)")*61.018*1000
610 PUNCH TOT("S(6)")*96.0616*1000
620 PUNCH TOT("Cl")*35.453*1000
630 A = (TOT("Ca")*40.08*1000)+(TOT("Mg")*24.312*1000)
640 B = (TOT("Na")*22.9898*1000)+(TOT("K")*39.102*1000)
650 C = TOT("C(4)")*61.018*1000
660 D = TOT("S(6)")*96.0616*1000
670 E = TOT("Cl")*35.453*1000
680 PUNCH A+B+C+D+E
-end

```

END

TITLE A-9 area (SW flow regime). FILE: SWFR2td.in CONC VS TIME

#Using flow rate of 0.280 ft/d - DECREASING SOURCE TERM TO 90% REDUCTION
#SOLID PHASES ALLOWED

PRINT

-reset false

KNOBS

-iterations 100
-tolerance 1.00E-13
-step_size 100
-pe_step_size 10
-diagonal_scale TRUE
-debug_prep FALSE
-debug_set FALSE
-debug_model FALSE
-debug_inverse FALSE
-logfile FALSE

SELECTED_OUTPUT

-file P:\100040-7\phreeqc\SWFR2td.dat

USER_PUNCH

-headings As Be Cl Pb U Ni Se SO4 Th Ra sOPb+
-headings wOPb+ PbX2 Anglesite sOHUO2+2
-headings wOUO2+ USiO4(C) Uraninite sONi+ wONi+
-headings NiSe sOHRa+2 wORa+ RaX2 RaSO4 wSeO4-
-headings wOHSeO4-2 wSeO3- wOHSeO3-2 Se(A)
-headings FeSe2 sSO4- wSO4- sOHSO4-2 wOHSO4-2
-headings gypsum wOTH+3 wOTH(OH)+2 wOTH(OH)2+
-headings wOTH(OH)3 wOTH(OH)4- sH2AsO3 wH2AsO3
-headings sH2AsO4 wH2AsO4 sHAsO4- wHAsO4- sAsO4-2
-headings wAsO4-2 sOHAsO4-3 wOHAsO4-3 sOBe+ wOBe+
-headings Calcite Ca Mg Na K HCO3 SO4 Cl TDS
-start
10 REM Convert to ppm and show molalities
20 PUNCH TOT("As")*74.9216*1000
30 PUNCH TOT("Be")*9.0122*1000
40 PUNCH TOT("Cl")*35.453*1000
50 PUNCH TOT("Pb")*207.19*1000/1.29e-11
60 PUNCH TOT("U")*238.029*1000
70 PUNCH TOT("Ni")*58.71*1000
80 PUNCH TOT("Se")*78.96*1000
90 PUNCH TOT("S(6)")*96.0616*1000
100 PUNCH TOT("Th")*232.038*1000/4.96e-8
110 PUNCH TOT("Ra")*226*1000/1.01e-9
120 PUNCH MOL("Hfo_sOPb+")
130 PUNCH MOL("Hfo_wOPb+")

140 PUNCH MOL("PbX2")
 150 PUNCH EQUI("Anglesite")
 160 PUNCH MOL("Hfo_sOHUO2+2")
 170 PUNCH MOL("Hfo_wOUO2+")
 180 PUNCH EQUI("USiO4(C)")
 190 PUNCH EQUI("Uraninite")
 200 PUNCH MOL("Hfo_sONi+")
 210 PUNCH MOL("Hfo_wONi+")
 220 PUNCH EQUI("NiSe")
 230 PUNCH MOL("Hfo_sOHRa+2")
 240 PUNCH MOL("Hfo_wORa+")
 250 PUNCH MOL("RaX2")
 260 PUNCH EQUI("RaSO4")
 270 PUNCH MOL("Hfo_wSeO4-")
 280 PUNCH MOL("Hfo_wOHSeO4-2")
 290 PUNCH MOL("Hfo_wSeO3-")
 300 PUNCH MOL("Hfo_wOHSeO3-2")
 310 PUNCH EQUI("Se(A)")
 320 PUNCH EQUI("Ferroselite")
 330 PUNCH MOL("Hfo_sSO4-")
 340 PUNCH MOL("Hfo_wSO4-")
 350 PUNCH MOL("Hfo_sOHSO4-2")
 360 PUNCH MOL("Hfo_wOHSO4-2")
 370 PUNCH EQUI("gypsum")
 380 PUNCH MOL("Hfo_wOTh+3")
 390 PUNCH MOL("Hfo_wOTh(OH)+2")
 400 PUNCH MOL("Hfo_wOTh(OH)2+")
 410 PUNCH MOL("Hfo_wOTh(OH)3")
 420 PUNCH MOL("Hfo_wOTh(OH)4-")
 430 PUNCH MOL("Hfo_sH2AsO3")
 440 PUNCH MOL("Hfo_wH2AsO3")
 450 PUNCH MOL("Hfo_sH2AsO4")
 460 PUNCH MOL("Hfo_wH2AsO4")
 470 PUNCH MOL("Hfo_sHAsO4-")
 480 PUNCH MOL("Hfo_wHAsO4-")
 490 PUNCH MOL("Hfo_sAsO4-2")
 500 PUNCH MOL("Hfo_wAsO4-2")
 510 PUNCH MOL("Hfo_sOHAAsO4-3")
 520 PUNCH MOL("Hfo_wOHAAsO4-3")
 530 PUNCH MOL("Hfo_sOBe+")
 540 PUNCH MOL("Hfo_wOBe+")
 550 PUNCH EQUI("Calcite")
 560 PUNCH TOT("Ca")*40.08*1000
 570 PUNCH TOT("Mg")*24.312*1000
 580 PUNCH TOT("Na")*22.9898*1000
 590 PUNCH TOT("K")*39.102*1000
 600 PUNCH MOL("HCO3-")*61.018*1000
 610 PUNCH TOT("S(6)")*96.0616*1000
 620 PUNCH TOT("Cl")*35.453*1000
 630 A = (TOT("Ca")*40.08*1000)+(TOT("Mg")*24.312*1000)


```

640 B = (TOT("Na")*22.9898*1000)+(TOT("K")*39.102*1000)
650 C = MOL("HCO3-")*61.018*1000
660 D = TOT("S(6)")*96.0616*1000
670 E = TOT("Cl")*35.453*1000
680 PUNCH A+B+C+D+E
-end

```

PRINT

```
-selected_output      false
```

SOLUTION 0 # Initial Source Term

units	ppm
pe	8
pH	4.33
Th	2.22e-6
Pb	6.02e-10
Be	1.7
Ca	660
Mg	144
Na	61
K	15
Fe(2)	89
Cl	161
As	1.36
Ni	9.34
Se	0.53
Si	56.4
U	34.1
Alkalinity 2.44	as HCO3
S(6)	2650
Ra	3.57e-7

SOLUTION 1-5 GW8 January 2001

units	ppm
pe	7
pH	4.73
S(6)	1540
Cl	97
Alkalinity 2.0	as HCO3
Ca	418
Na	30.6
Mg	70.8
K	17.6
Fe(2)	127
As	0.007
Be	0.076
Th	7.97e-8
Pb	2.58e-10

Ra	6.25e-8
Ni	1.31
Se	0.001
U	10.3

SOLUTION 6-54 MW-74 January 2001

units	ppm
pe	6
pH	6.69
S(6)	24.1
Cl	9.1
Alkalinity	35 as HCO3
Ca	17.7
Na	6.3
Mg	2.9
K	4.2
Fe(2)	0.1
As	0.0019
Be	0.001 # 1/2 DL
Th	3.77e-8
Pb	1.68e-11
Ra	4.55e-10
Ni	0.005 # 1/2 DL
Se	0.012
U	0.0139
S(-2)	0.033

EQUILIBRIUM_PHASES 1-54

Calcite	0.0	0.0
Gypsum	0.0	0.0
Uraninite	0.0	0.0
USiO4(c)	0.0	0.0
Ferroselite	0.0	0.0
Se(A)	0.0	0.0
RaSO4	0.0	0.0
NiSe	0.0	0.0
Anglesite	0.0	0.0

SURFACE 1-5

-equilibrate 1			
Hfo_wOH	0.086	600	45.9
Hfo_sOH	0.0021		

SURFACE 6-54

-equilibrate 6			
Hfo_wOH	0.086	600	45.9
Hfo_sOH	0.0021		

EXCHANGE 1-5

-equilibrate 1	
----------------	--

X 1.2

EXCHANGE 6-54

-equilibrate 6

X 1.2

TRANSPORT

-lengths 54*30.5

-dispersivities 54*50

-cells 54

-shifts 6

-punch_cells 54

PRINT

-selected_output true

END

PRINT

-selected_output false

SOLUTION 0 #33% REDUCTION

units	ppm
-------	-----

pe	5.6
----	-----

pH	4.47
----	------

Th	1.47e-6
----	---------

Pb	4.12E-10
----	----------

Ra	2.41E-07
----	----------

U	22.62
---	-------

Be	1.13
----	------

Ca	536.7
----	-------

Mg	116.7
----	-------

Na	57
----	----

K	16.2
---	------

Fe(2)	61.8
-------	------

Cl	114.6
----	-------

As	0.90
----	------

Ni	6.20
----	------

Se	0.35
----	------

Si	37.4
----	------

Alkalinity 4.0 as HCO3	
------------------------	--

S(6)	1980.5
------	--------

TRANSPORT

-lengths 54*30.5

-dispersivities 54*50

-cells 54

-shifts 3

-punch_cells 54

```
PRINT
    -selected_output    true
```

```
END
```

```
PRINT
    -selected_output    false
```

```
SOLUTION 0 #50% Reduction
```

units	ppm
pe	5.5
pH	4.57
Th	1.12e-6
Pb	3.22E-10
Ra	1.86E-07
U	17.16
Be	0.85
Ca	477.5
Mg	103.6
Na	55
K	16.8
Fe(2)	48.9
Cl	92.5
As	0.68
Ni	4.7
Se	0.27
Si	28.31
Alkalinity	4.73 as HCO3
S(6)	1661

```
TRANSPORT
    -lengths            54*30.5
    -dispersivities    54*50
    -cells              54
    -shifts             7
    -punch_cells       54
```

```
PRINT
    -selected_output    true
```

```
END
```

```
PRINT
    -selected_output    false
```

```
SOLUTION 0 #75% Reduction
```

units	ppm
pe	5.1
pH	4.85
Th	5.65E-07
Pb	1.81E-10
Ra	1.0E-07
U	8.62
Be	0.43
Ca	384.9
Mg	83.1
Na	51.9
K	17.7
Fe(2)	28.7
Cl	58
As	0.34
Ni	2.36
Se	0.13
Si	14.2
Alkalinity	5.88 as HCO3
S(6)	1161

TRANSPORT

-lengths	54*30.5
-dispersivities	54*50
-cells	54
-shifts	19
-punch_cells	54

PRINT

-selected_output	true
------------------	------

END

PRINT

-selected_output	false
------------------	-------

SOLUTION 0 #90% Reduction

units	ppm
pe	4.4
pH	5.27
Th	2.33E-07
Pb	9.58e-11
Ra	4.84e-8
U	3.5
Be	0.17
Ca	329.4
Mg	70.8
Na	50
K	18.2
Fe(2)	16.5

Cl	37.3
As	0.14
Ni	0.96
Se	0.05
Si	5.66
Alkalinity	6.56 as HCO ₃
S(6)	860.7

TRANSPORT

-lengths	54*30.5
-dispersivities	54*50
-cells	54
-shifts	987
-punch_cells	54

PRINT

-selected_output	true
------------------	------

END

PRINT

-selected_output	false
------------------	-------

#pH and Alkalinity for Source Terms: FILE: SWFRsources.in
 #Mixing of A-9 Tailing Waters With LA-2

SOLUTION 1 A-9 Water

units	ppm
pe	8
pH	4.33
Ca	660
Mg	144
Na	61.00
K	15.0
Cl	161.0
Alkalinity	2.44 as HCO3
S(6)	2650
Fe(2)	89
Th	2.22e-6
Pb	6.02e-10
Ra	3.57e-7
U	34.1
As	1.36
Se	0.53
Ni	9.34
Be	1.7
Si	56.4

END

SOLUTION 2 LA-2

units	ppm	
pe	6	
pH	6.8	
Ca	292	
Mg	62.5	
Na	48.7	
K	18.5	
Cl	23.4	
Alkalinity	7.02 as HCO3	
S(6)	660	
Fe(2)	8.41	
Th	1.09e-8	#neg value + uncertainty
Pb	3.93e-11	
Ra	1.4e-8	
U	0.0817	
As	0.00025	#1/2 DL
Se	0.0005	#1/2 DL
Ni	0.02	
Be	0.001	#1/2 DL

END

SELECTED_OUTPUT

-file P:\100040-7\phreeqc\SWFRsources.dat

USER_PUNCH

-headings Ca Mg Na K Cl SO4 Fe Th Pb Ra U As Se Ni Be Si
-headings USiO4(c) Uraninite RaSO4 Th(OH)4(am)

10 PUNCH TOT("Ca")*40.08*1000
20 PUNCH TOT("Mg")*24.312*1000
30 PUNCH TOT("Na")*22.9898*1000
40 PUNCH TOT("K")*39.102*1000
50 PUNCH TOT("Cl")*35.453*1000
60 PUNCH TOT("S(6)")*96.0616*1000
70 PUNCH TOT("Fe")*55.847*1000
80 PUNCH TOT("Th")*232.038*1000
90 PUNCH TOT("Pb")*207.19*1000
100 PUNCH TOT("Ra")*226*1000
110 PUNCH TOT("U")*238.029*1000
120 PUNCH TOT("As")*74.9216*1000
130 PUNCH TOT("Se")*78.96*1000
140 PUNCH TOT("Ni")*58.71*1000
150 PUNCH TOT("Be")*9.0122*1000
160 PUNCH TOT("Si")*96.1155*1000
170 PUNCH SI("USiO4(c)")
180 PUNCH SI("Uraninite")
190 PUNCH SI("RaSO4")
200 PUNCH SI("Th(OH)4(am)")

MIX 1 #33% Reduction

1	0.66
2	0.34

END

MIX 2 #50% Reduction

1	0.50
2	0.50

END

MIX 3 #75% Reduction

1	0.25
2	0.75

END

MIX 4 #90% Reduction

1	0.10
2	0.90

END

TITLE AGTI area (Western flow regime). FILE: WFR1d.in
#Using flow rate of 0.167 ft/d - DECREASING SOURCE TERM TO 90% REDUCTION
#Dispersivity = 50
#SOLID PHASES ALLOWED

KNOBS

-iterations 200
-tolerance 1.00E-13
-step_size 100
-pe_step_size 10
-diagonal_scale TRUE
-debug_prep FALSE
-debug_set FALSE
-debug_model FALSE
-debug_inverse FALSE
-logfile FALSE

SOLUTION 0 # SOURCE (ACL's) AGTI

pH	5.5
pe	6
units	mg/l
density	1
S(6)	3480
Cl	274
Alkalinity	3.1 as HCO ₃
Ca	456
Na	182
Mg	112
K	24
As	1.8
Fe	86
Be	1.64
Ni	13.0
Se	0.16
Si	24
U	11.9
Th	2.85e-6
Pb	4.57e-10
Ra	2.48e-7

SOLUTION 1-15 #MW-21A January 2001

units	ppm
pe	5.8
pH	6.12
S(6)	1220
Cl	50
Alkalinity	2.4 as HCO ₃

Ca	272
Na	79.6
Mg	80.4
K	13.2
Fe	95
As	0.0463
Be	0.014
Th	9.92e-10
Pb	2.19e-11
Ra	8.99e-9
Ni	0.30
Se	0.002
U	0.00112

SOLUTION 16-46 #MW-28 January 2001

units	ppm
pe	3.9
pH	6.86
S(6)	540
Cl	7.5
Alkalinity	2.8 as HCO3
Ca	150
Na	82
Mg	29
K	9.6
Fe	14
As	0.012
Be	0.005 #1/2 DL
Th	5e-9 #this value estimated
Pb	1.55e-11
Ra	1.81e-8
Ni	0.062
Se	0.0025 #1/2 DL
U	0.0045

EQUILIBRIUM_PHASES 1-46

Calcite	0.0	0.0
Gypsum	0.0	0.0
Uraninite	0.0	0.0
USiO4(c)	0.0	0.0
Ferroselite	0.0	0.0
Se(A)	0.0	0.0
RaSO4	0.0	0.0
NiSe	0.0	0.0
Anglesite	0.0	0.0

SURFACE 1-15

-equilibrate 1			
Hfo_wOH	0.086	600	45.9

Hfo_sOH 0.0021

SURFACE 16-46

-equilibrate 16

Hfo_wOH 0.086 600 45.9

Hfo_sOH 0.0021

EXCHANGE 1-15

-equilibrate 1

X 1.2

EXCHANGE 16-46

-equilibrate 16

X 1.2

TRANSPORT

-lengths 46*30.5

-dispersivities 46*50

-cells 46

-shifts 10

PRINT

-reset false

END

SOLUTION 0 #33% REDUCTION

units ppm

pH 5.66

pe 3.9

Ca 360.2

Mg 80.40

Na 136.0

K 19

Cl 183.0

Alkalinity 3.14 as HCO₃

S(6) 2434

Fe 61.50

Th 1.89E-06

Pb 3.69E-10

Ra 1.70E-07

U 7.89

As 1.20

Se 0.11

Ni 8.64

Be 1.09

Si 15.90

TRANSPORT

-lengths 46*30.5
-dispersivities 46*50
-cells 46
-shifts 5

END

SOLUTION 0 #50% Reduction

units	ppm
pH	5.80
pe	3.6
Ca	314.1
Mg	65.30
Na	114.0
K	17
Cl	140.0
Alkalinity	3.16 as HCO ₃
S(6)	1933
Fe	49.70
Th	1.43E-06
Pb	2.84E-10
Ra	1.33E-07
U	5.98
As	0.91
Se	0.08
Ni	6.56
Be	0.83
Si	12.10

TRANSPORT

-lengths 46*30.5
-dispersivities 46*50
-cells 46
-shifts 27

END

SOLUTION 0 #75% Reduction

units	ppm
pH	6.18
pe	3.0
Ca	242.1
Mg	41.60
Na	79.5
K	13
Cl	72.4
Alkalinity	3.18
S(6)	1152
Fe	31.40

Th	7.20E-07
Pb	1.50E-10
Ra	7.42E-08
U	2.99
As	0.46
Se	0.04
Ni	3.30
Be	0.42
Si	6.03

TRANSPORT

-lengths	46*30.5
-dispersivities	46*50
-cells	46
-shifts	40

END

SOLUTION 0 #90% Reduction

units	ppm
pH	6.57
pe	2.2
Ca	198.9
Mg	27.50
Na	58.8
K	11
Cl	31.8
Alkalinity	3.19 as HCO3
S(6)	682.8
Fe	20.40
Th	2.92E-07
Pb	7.02E-11
Ra	3.92E-08
U	1.20
As	0.19
Se	0.02
Ni	1.35
Be	0.17
Si	2.41

TRANSPORT

-lengths	46*30.5
-dispersivities	46*50
-cells	46
-shifts	527
-punch_frequency	527

SELECTED_OUTPUT

-file P:\100040-7\phreeqc\WFR1d.dat

USER_PUNCH

-headings As Be Cl Pb U Ni Se SO4 Th Ra sOPb+
-headings wOPb+ PbX2 Anglesite sOHUO2+2
-headings wOUO2+ USiO4(C) Uraninite sONi+ wONi+
-headings NiSe sOHRa+2 wORa+ RaX2 RaSO4 wSeO4-
-headings wOHSeO4-2 wSeO3- wOHSeO3-2 Se(A)
-headings FeSe2 sSO4- wSO4- sOHSO4-2 wOHSO4-2
-headings gypsum wOTh+3 wOTh(OH)+2 wOTh(OH)2+
-headings wOTh(OH)3 wOTh(OH)4- sH2AsO3 wH2AsO3
-headings sH2AsO4 wH2AsO4 sHAsO4- wHAsO4- sAsO4-2
-headings wAsO4-2 sOHasO4-3 wOHasO4-3 sOBe+ wOBe+
-headings Calcite Ca Mg Na K HCO3 SO4 Cl TDS
-start
10 REM Convert to ppm and show molalities
20 PUNCH TOT("As")*74.9216*1000
30 PUNCH TOT("Be")*9.0122*1000
40 PUNCH TOT("Cl")*35.453*1000
50 PUNCH TOT("Pb")*207.19*1000/1.29e-11
60 PUNCH TOT("U")*238.029*1000
70 PUNCH TOT("Ni")*58.71*1000
80 PUNCH TOT("Se")*78.96*1000
90 PUNCH TOT("S(6)")*96.0616*1000
100 PUNCH TOT("Th")*232.038*1000/4.96e-8
110 PUNCH TOT("Ra")*226*1000/1.01e-9
120 PUNCH MOL("Hfo_sOPb+")
130 PUNCH MOL("Hfo_wOPb+")
140 PUNCH MOL("PbX2")
150 PUNCH EQUI("Anglesite")
160 PUNCH MOL("Hfo_sOHUO2+2")
170 PUNCH MOL("Hfo_wOUO2+")
180 PUNCH EQUI("USiO4(C)")
190 PUNCH EQUI("Uraninite")
200 PUNCH MOL("Hfo_sONi+")
210 PUNCH MOL("Hfo_wONi+")
220 PUNCH EQUI("NiSe")
230 PUNCH MOL("Hfo_sOHRa+2")
240 PUNCH MOL("Hfo_wORa+")
250 PUNCH MOL("RaX2")
260 PUNCH EQUI("RaSO4")
270 PUNCH MOL("Hfo_wSeO4-")
280 PUNCH MOL("Hfo_wOHSeO4-2")
290 PUNCH MOL("Hfo_wSeO3-")
300 PUNCH MOL("Hfo_wOHSeO3-2")
310 PUNCH EQUI("Se(A)")
320 PUNCH EQUI("Ferroselite")
330 PUNCH MOL("Hfo_sSO4-")
340 PUNCH MOL("Hfo_wSO4-")
350 PUNCH MOL("Hfo_sOHSO4-2")

```

360 PUNCH MOL("Hfo_wOHSO4-2")
370 PUNCH EQUI("gypsum")
380 PUNCH MOL("Hfo_wOTh+3")
390 PUNCH MOL("Hfo_wOTh(OH)+2")
400 PUNCH MOL("Hfo_wOTh(OH)2+")
410 PUNCH MOL("Hfo_wOTh(OH)3")
420 PUNCH MOL("Hfo_wOTh(OH)4-")
430 PUNCH MOL("Hfo_sH2AsO3")
440 PUNCH MOL("Hfo_wH2AsO3")
450 PUNCH MOL("Hfo_sH2AsO4")
460 PUNCH MOL("Hfo_wH2AsO4")
470 PUNCH MOL("Hfo_sHAsO4-")
480 PUNCH MOL("Hfo_wHAsO4-")
490 PUNCH MOL("Hfo_sAsO4-2")
500 PUNCH MOL("Hfo_wAsO4-2")
510 PUNCH MOL("Hfo_sOHAAsO4-3")
520 PUNCH MOL("Hfo_wOHAAsO4-3")
530 PUNCH MOL("Hfo_sOBe+")
540 PUNCH MOL("Hfo_wOBe+")
550 PUNCH EQUI("Calcite")
560 PUNCH TOT("Ca")*40.08*1000
570 PUNCH TOT("Mg")*24.312*1000
580 PUNCH TOT("Na")*22.9898*1000
590 PUNCH TOT("K")*39.102*1000
600 PUNCH TOT("C(4)")*61.018*1000
610 PUNCH TOT("S(6)")*96.0616*1000
620 PUNCH TOT("Cl")*35.453*1000
630 A = (TOT("Ca")*40.08*1000)+(TOT("Mg")*24.312*1000)
640 B = (TOT("Na")*22.9898*1000)+(TOT("K")*39.102*1000)
650 C = TOT("C(4)")*61.018*1000
660 D = TOT("S(6)")*96.0616*1000
670 E = TOT("Cl")*35.453*1000
680 PUNCH A+B+C+D+E
-end

```

END

TITLE AGTI area (Western flow regime). FILE: WFR2d.in
#Using flow rate of 0.330 ft/d - DECREASING SOURCE TERM TO 90% REDUCTION
#Dispersivity = 50
#SOLID PHASES ALLOWED

KNOBS

-iterations 200
-tolerance 1.00E-13
-step_size 100
-pe_step_size 10
-diagonal_scale TRUE
-debug_prep FALSE
-debug_set FALSE
-debug_model FALSE
-debug_inverse FALSE
-logfile FALSE

SOLUTION 0 # SOURCE (ACL's) AGTI

pH	5.5
pe	6
units	mg/l
density	1
S(6)	3480
Cl	274
Alkalinity	3.1 as HCO ₃
Ca	456
Na	182
Mg	112
K	24
As	1.8
Fe	86
Be	1.64
Ni	13.0
Se	0.16
Si	24
U	11.9
Th	2.85e-6
Pb	4.57e-10
Ra	2.48e-7

SOLUTION 1-15 #MW-21A January 2001

units	ppm
pe	5.8
pH	6.12
S(6)	1220
Cl	50
Alkalinity	2.4 as HCO ₃

Ca	272
Na	79.6
Mg	80.4
K	13.2
Fe	95
As	0.0463
Be	0.014
Th	9.92e-10
Pb	2.19e-11
Ra	8.99e-9
Ni	0.30
Se	0.002
U	0.00112

SOLUTION 16-46 #MW-28 January 2001

units	ppm
pe	3.9
pH	6.86
S(6)	540
Cl	7.5
Alkalinity	2.8 as HCO3
Ca	150
Na	82
Mg	29
K	9.6
Fe	14
As	0.012
Be	0.005 #1/2 DL
Th	5e-9 #this value estimated
Pb	1.55e-11
Ra	1.81e-8
Ni	0.062
Se	0.0025 #1/2 DL
U	0.0045

EQUILIBRIUM_PHASES 1-46

Calcite	0.0	0.0
Gypsum	0.0	0.0
Uraninite	0.0	0.0
USiO4(c)	0.0	0.0
Ferroselite	0.0	0.0
Se(A)	0.0	0.0
RaSO4	0.0	0.0
NiSe	0.0	0.0
Anglesite	0.0	0.0

SURFACE 1-15

-equilibrate 1			
Hfo_wOH	0.086	600	45.9

Hfo_sOH 0.0021

SURFACE 16-46

-equilibrate 16

Hfo_wOH 0.086 600 45.9

Hfo_sOH 0.0021

EXCHANGE 1-15

-equilibrate 1

X 1.2

EXCHANGE 16-46

-equilibrate 16

X 1.2

TRANSPORT

-lengths 46*30.5

-dispersivities 46*50

-cells 46

-shifts 20

PRINT

-reset false

END

SOLUTION 0 #33% REDUCTION

units ppm

pH 5.66

pe 3.9

Ca 360.2

Mg 80.40

Na 136.0

K 19

Cl 183.0

Alkalinity 3.14 as HCO₃

S(6) 2434

Fe 61.50

Th 1.89E-06

Pb 3.69E-10

Ra 1.70E-07

U 7.89

As 1.20

Se 0.11

Ni 8.64

Be 1.09

Si 15.90

TRANSPORT

-lengths 46*30.5
-dispersivities 46*50
-cells 46
-shifts 10

END

SOLUTION 0 #50% Reduction

units	ppm
pH	5.80
pe	3.6
Ca	314.1
Mg	65.30
Na	114.0
K	17
Cl	140.0
Alkalinity	3.16 as HCO ₃
S(6)	1933
Fe	49.70
Th	1.43E-06
Pb	2.84E-10
Ra	1.33E-07
U	5.98
As	0.91
Se	0.08
Ni	6.56
Be	0.83
Si	12.10

TRANSPORT

-lengths 46*30.5
-dispersivities 46*50
-cells 46
-shifts 54

END

SOLUTION 0 #75% Reduction

units	ppm
pH	6.18
pe	3.0
Ca	242.1
Mg	41.60
Na	79.5
K	13
Cl	72.4
Alkalinity	3.18
S(6)	1152
Fe	31.40

Th	7.20E-07
Pb	1.50E-10
Ra	7.42E-08
U	2.99
As	0.46
Se	0.04
Ni	3.30
Be	0.42
Si	6.03

TRANSPORT

-lengths	46*30.5
-dispersivities	46*50
-cells	46
-shifts	78

END

SOLUTION 0 #90% Reduction

units	ppm
pH	6.57
pe	2.2
Ca	198.9
Mg	27.50
Na	58.8
K	11
Cl	31.8
Alkalinity	3.19 as HCO3
S(6)	682.8
Fe	20.40
Th	2.92E-07
Pb	7.02E-11
Ra	3.92E-08
U	1.20
As	0.19
Se	0.02
Ni	1.35
Be	0.17
Si	2.41

TRANSPORT

-lengths	46*30.5
-dispersivities	46*50
-cells	46
-shifts	1042
-punch_frequency	1042

SELECTED_OUTPUT

-file P:\100040-7\phreeqc\WFR2d.dat

USER_PUNCH

-headings As Be Cl Pb U Ni Se SO4 Th Ra sOPb+
-headings wOPb+ PbX2 Anglesite sOHUO2+2
-headings wOUO2+ USiO4(C) Uraninite sONi+ wONi+
-headings NiSe sOHRa+2 wORa+ RaX2 RaSO4 wSeO4-
-headings wOHSeO4-2 wSeO3- wOHSeO3-2 Se(A)
-headings FeSe2 sSO4- wSO4- sOHSO4-2 wOHSO4-2
-headings gypsum wOTh+3 wOTh(OH)+2 wOTh(OH)2+
-headings wOTh(OH)3 wOTh(OH)4- sH2AsO3 wH2AsO3
-headings sH2AsO4 wH2AsO4 sHAsO4- wHAsO4- sAsO4-2
-headings wAsO4-2 sOHAsO4-3 wOHAsO4-3 sOBe+ wOBe+
-headings Calcite Ca Mg Na K HCO3 SO4 Cl TDS
-start
10 REM Convert to ppm and show molalities
20 PUNCH TOT("As")*74.9216*1000
30 PUNCH TOT("Be")*9.0122*1000
40 PUNCH TOT("Cl")*35.453*1000
50 PUNCH TOT("Pb")*207.19*1000/1.29e-11
60 PUNCH TOT("U")*238.029*1000
70 PUNCH TOT("Ni")*58.71*1000
80 PUNCH TOT("Se")*78.96*1000
90 PUNCH TOT("S(6)")*96.0616*1000
100 PUNCH TOT("Th")*232.038*1000/4.96e-8
110 PUNCH TOT("Ra")*226*1000/1.01e-9
120 PUNCH MOL("Hfo_sOPb+")
130 PUNCH MOL("Hfo_wOPb+")
140 PUNCH MOL("PbX2")
150 PUNCH EQUI("Anglesite")
160 PUNCH MOL("Hfo_sOHUO2+2")
170 PUNCH MOL("Hfo_wOUO2+")
180 PUNCH EQUI("USiO4(C)")
190 PUNCH EQUI("Uraninite")
200 PUNCH MOL("Hfo_sONi+")
210 PUNCH MOL("Hfo_wONi+")
220 PUNCH EQUI("NiSe")
230 PUNCH MOL("Hfo_sOHRa+2")
240 PUNCH MOL("Hfo_wORa+")
250 PUNCH MOL("RaX2")
260 PUNCH EQUI("RaSO4")
270 PUNCH MOL("Hfo_wSeO4-")
280 PUNCH MOL("Hfo_wOHSeO4-2")
290 PUNCH MOL("Hfo_wSeO3-")
300 PUNCH MOL("Hfo_wOHSeO3-2")
310 PUNCH EQUI("Se(A)")
320 PUNCH EQUI("Ferroselite")
330 PUNCH MOL("Hfo_sSO4-")
340 PUNCH MOL("Hfo_wSO4-")
350 PUNCH MOL("Hfo_sOHSO4-2")

```

360 PUNCH MOL("Hfo_wOHSO4-2")
370 PUNCH EQUI("gypsum")
380 PUNCH MOL("Hfo_wOTh+3")
390 PUNCH MOL("Hfo_wOTh(OH)+2")
400 PUNCH MOL("Hfo_wOTh(OH)2+")
410 PUNCH MOL("Hfo_wOTh(OH)3")
420 PUNCH MOL("Hfo_wOTh(OH)4-")
430 PUNCH MOL("Hfo_sH2AsO3")
440 PUNCH MOL("Hfo_wH2AsO3")
450 PUNCH MOL("Hfo_sH2AsO4")
460 PUNCH MOL("Hfo_wH2AsO4")
470 PUNCH MOL("Hfo_sHAsO4-")
480 PUNCH MOL("Hfo_wHAsO4-")
490 PUNCH MOL("Hfo_sAsO4-2")
500 PUNCH MOL("Hfo_wAsO4-2")
510 PUNCH MOL("Hfo_sOHAsO4-3")
520 PUNCH MOL("Hfo_wOHAsO4-3")
530 PUNCH MOL("Hfo_sOBe+")
540 PUNCH MOL("Hfo_wOBe+")
550 PUNCH EQUI("Calcite")
560 PUNCH TOT("Ca")*40.08*1000
570 PUNCH TOT("Mg")*24.312*1000
580 PUNCH TOT("Na")*22.9898*1000
590 PUNCH TOT("K")*39.102*1000
600 PUNCH TOT("C(4)")*61.018*1000
610 PUNCH TOT("S(6)")*96.0616*1000
620 PUNCH TOT("Cl")*35.453*1000
630 A = (TOT("Ca")*40.08*1000)+(TOT("Mg")*24.312*1000)
640 B = (TOT("Na")*22.9898*1000)+(TOT("K")*39.102*1000)
650 C = TOT("C(4)")*61.018*1000
660 D = TOT("S(6)")*96.0616*1000
670 E = TOT("Cl")*35.453*1000
680 PUNCH A+B+C+D+E
-end

```

END

TITLE AGTI area (Western flow regime). FILE: WFR2td.in CONC VS TIME
#Using flow rate of 0.330 ft/d - DECREASING SOURCE TERM TO 90% REDUCTION
#Dispersivities = 50
#SOLID PHASES ALLOWED

KNOBS

-iterations 200
-tolerance 1.00E-13
-step_size 100
-pe_step_size 10
-diagonal_scale TRUE
-debug_prep FALSE
-debug_set FALSE
-debug_model FALSE
-debug_inverse FALSE
-logfile FALSE

PRINT

-reset false

SELECTED_OUTPUT

-file P:\100040-7\phreeqc\WFR2td.dat

USER_PUNCH

-headings As Be Cl Pb U Ni Se SO4 Th Ra sOPb+
-headings wOPb+ PbX2 Anglesite sOHUO2+2
-headings wOUO2+ USiO4(C) Uraninite sONi+ wONi+
-headings NiSe sOHRa+2 wORa+ RaX2 RaSO4 wSeO4-
-headings wOHSeO4-2 wSeO3- wOHSeO3-2 Se(A)
-headings FeSe2 sSO4- wSO4- sOHSeO4-2 wOHSeO4-2
-headings gypsum wOTh+3 wOTh(OH)+2 wOTh(OH)2+
-headings wOTh(OH)3 wOTh(OH)4- sH2AsO3 wH2AsO3
-headings sH2AsO4 wH2AsO4 sHAsO4- wHAsO4- sAsO4-2
-headings wAsO4-2 sOHAsO4-3 wOHAsO4-3 sOBe+ wOBe+
-headings Calcite Ca Mg Na K HCO3 SO4 Cl TDS
-start
10 REM Convert to ppm and show molalities
20 PUNCH TOT("As")*74.9216*1000
30 PUNCH TOT("Be")*9.0122*1000
40 PUNCH TOT("Cl")*35.453*1000
50 PUNCH TOT("Pb")*207.19*1000/1.29e-11
60 PUNCH TOT("U")*238.029*1000
70 PUNCH TOT("Ni")*58.71*1000
80 PUNCH TOT("Se")*78.96*1000
90 PUNCH TOT("S(6)")*96.0616*1000
100 PUNCH TOT("Th")*232.038*1000/4.96e-8
110 PUNCH TOT("Ra")*226*1000/1.01e-9
120 PUNCH MOL("Hfo_sOPb+")

130 PUNCH MOL("Hfo_wOPb+")
140 PUNCH MOL("PbX2")
150 PUNCH EQUI("Anglesite")
160 PUNCH MOL("Hfo_sOHUO2+2")
170 PUNCH MOL("Hfo_wOUO2+")
180 PUNCH EQUI("USiO4(C)")
190 PUNCH EQUI("Uraninite")
200 PUNCH MOL("Hfo_sONi+")
210 PUNCH MOL("Hfo_wONi+")
220 PUNCH EQUI("NiSe")
230 PUNCH MOL("Hfo_sOHRa+2")
240 PUNCH MOL("Hfo_wORa+")
250 PUNCH MOL("RaX2")
260 PUNCH EQUI("RaSO4")
270 PUNCH MOL("Hfo_wSeO4-")
280 PUNCH MOL("Hfo_wOHSeO4-2")
290 PUNCH MOL("Hfo_wSeO3-")
300 PUNCH MOL("Hfo_wOHSeO3-2")
310 PUNCH EQUI("Se(A)")
320 PUNCH EQUI("Ferroselite")
330 PUNCH MOL("Hfo_sSO4-")
340 PUNCH MOL("Hfo_wSO4-")
350 PUNCH MOL("Hfo_sOHSO4-2")
360 PUNCH MOL("Hfo_wOHSO4-2")
370 PUNCH EQUI("gypsum")
380 PUNCH MOL("Hfo_wOTh+3")
390 PUNCH MOL("Hfo_wOTh(OH)+2")
400 PUNCH MOL("Hfo_wOTh(OH)2+")
410 PUNCH MOL("Hfo_wOTh(OH)3")
420 PUNCH MOL("Hfo_wOTh(OH)4-")
430 PUNCH MOL("Hfo_sH2AsO3")
440 PUNCH MOL("Hfo_wH2AsO3")
450 PUNCH MOL("Hfo_sH2AsO4")
460 PUNCH MOL("Hfo_wH2AsO4")
470 PUNCH MOL("Hfo_sHAsO4-")
480 PUNCH MOL("Hfo_wHAsO4-")
490 PUNCH MOL("Hfo_sAsO4-2")
500 PUNCH MOL("Hfo_wAsO4-2")
510 PUNCH MOL("Hfo_sOHAsO4-3")
520 PUNCH MOL("Hfo_wOHAsO4-3")
530 PUNCH MOL("Hfo_sOBe+")
540 PUNCH MOL("Hfo_wOBe+")
550 PUNCH EQUI("Calcite")
560 PUNCH TOT("Ca")*40.08*1000
570 PUNCH TOT("Mg")*24.312*1000
580 PUNCH TOT("Na")*22.9898*1000
590 PUNCH TOT("K")*39.102*1000
600 PUNCH MOL("HCO3-")*61.018*1000
610 PUNCH TOT("S(6)")*96.0616*1000
620 PUNCH TOT("Cl")*35.453*1000

```

630 A = (TOT("Ca")*40.08*1000)+(TOT("Mg")*24.312*1000)
640 B = (TOT("Na")*22.9898*1000)+(TOT("K")*39.102*1000)
650 C = MOL("HCO3-")*61.018*1000
660 D = TOT("S(6)")*96.0616*1000
670 E = TOT("Cl")*35.453*1000
680 PUNCH A+B+C+D+E
-end

```

SOLUTION 0 # SOURCE (ACL's) AGTI

pH	5.5
pe	6
units	mg/l
density	1
S(6)	3480
Cl	274
Alkalinity	3.1 as HCO3
Ca	456
Na	182
Mg	112
K	24
As	1.8
Fe	86
Be	1.64
Ni	13.0
Se	0.16
Si	24
U	11.9
Th	2.85e-6
Pb	4.57e-10
Ra	2.48e-7

SOLUTION 1-15 #MW-21A January 2001

units	ppm
pe	5.8
pH	6.12
S(6)	1220
Cl	50
Alkalinity	2.4 as HCO3
Ca	272
Na	79.6
Mg	80.4
K	13.2
Fe	95
As	0.0463
Be	0.014
Th	9.92e-10
Pb	2.19e-11
Ra	8.99e-9

Ni	0.30
Se	0.002
U	0.00112

SOLUTION 16-46 #MW-28 January 2001

units	ppm
pe	3.9
pH	6.86
S(6)	540
Cl	7.5
Alkalinity	2.8 as HCO3
Ca	150
Na	82
Mg	29
K	9.6
Fe	14
As	0.012
Be	0.005 #1/2 DL
Th	5e-9 #this value estimated
Pb	1.55e-11
Ra	1.81e-8
Ni	0.062
Se	0.0025 #1/2 DL
U	0.0045

EQUILIBRIUM_PHASES 1-46

Calcite	0.0	0.0
Gypsum	0.0	0.0
Uraninite	0.0	0.0
USiO4(c)	0.0	0.0
Ferroselite	0.0	0.0
Se(A)	0.0	0.0
RaSO4	0.0	0.0
NiSe	0.0	0.0
Anglesite	0.0	0.0

SURFACE 1-15

-equilibrate 1		
Hfo_wOH	0.086	600 45.9
Hfo_sOH	0.0021	

SURFACE 16-46

-equilibrate 16		
Hfo_wOH	0.086	600 45.9
Hfo_sOH	0.0021	

EXCHANGE 1-15

-equilibrate 1	
X	1.2

EXCHANGE 16-46

-equilibrate 16

X 1.2

TRANSPORT

-lengths 46*30.5

-dispersivities 46*50

-cells 46

-shifts 20

-punch_cells 46

PRINT

-selected_output true

END

PRINT

-selected_output false

SOLUTION 0 #33% REDUCTION

units ppm

pH 5.66

pe 3.9

Ca 360.2

Mg 80.40

Na 136.0

K 19

Cl 183.0

Alkalinity 3.14 as HCO₃

S(6) 2434

Fe 61.50

Th 1.89E-06

Pb 3.69E-10

Ra 1.70E-07

U 7.89

As 1.20

Se 0.11

Ni 8.64

Be 1.09

Si 15.90

TRANSPORT

-lengths 46*30.5

-dispersivities 46*50

-cells 46

-shifts 10

-punch_cells 46

PRINT

-selected_output true

END

PRINT

-selected_output false

SOLUTION 0 #50% Reduction

units	ppm
pH	5.80
pe	3.6
Ca	314.1
Mg	65.30
Na	114.0
K	17
Cl	140.0
Alkalinity	3.16 as HCO ₃
S(6)	1933
Fe	49.70
Th	1.43E-06
Pb	2.84E-10
Ra	1.33E-07
U	5.98
As	0.91
Se	0.08
Ni	6.56
Be	0.83
Si	12.10

TRANSPORT

-lengths 46*30.5
-dispersivities 46*50
-cells 46
-shifts 54
-punch_cells 46

PRINT

-selected_output true

END

PRINT

-selected_output false

SOLUTION 0 #75% Reduction

units	ppm
pH	6.18
pe	3.0

Ca	242.1
Mg	41.60
Na	79.5
K	13
Cl	72.4
Alkalinity	3.18
S(6)	1152
Fe	31.40
Th	7.20E-07
Pb	1.50E-10
Ra	7.42E-08
U	2.99
As	0.46
Se	0.04
Ni	3.30
Be	0.42
Si	6.03

TRANSPORT

-lengths	46*30.5
-dispersivities	46*50
-cells	46
-shifts	78
-punch_cells	46

PRINT

-selected_output	true
------------------	------

END

PRINT

-selected_output	false
------------------	-------

SOLUTION 0 #90% Reduction

units	ppm
pH	6.57
pe	2.2
Ca	198.9
Mg	27.50
Na	58.8
K	11
Cl	31.8
Alkalinity	3.19 as HCO3
S(6)	682.8
Fe	20.40
Th	2.92E-07
Pb	7.02E-11
Ra	3.92E-08
U	1.20

As	0.19
Se	0.02
Ni	1.35
Be	0.17
Si	2.41

TRANSPORT

-lengths	46*30.5
-dispersivities	46*50
-cells	46
-shifts	1042
-punch_cells	46

PRINT

-selected_output	true
------------------	------

END

PRINT

-selected_output	false
------------------	-------

TITLE AGTI area (Western flow regime). FILE: WFR1td.in CONC VS TIME
#Using flow rate of 0.167 ft/d - DECREASING SOURCE TERM TO 90% REDUCTION
#Dispersion = 50
#SOLID PHASES ALLOWED

KNOBS

-iterations 200
-tolerance 1.00E-13
-step_size 100
-pe_step_size 10
-diagonal_scale TRUE
-debug_prep FALSE
-debug_set FALSE
-debug_model FALSE
-debug_inverse FALSE
-logfile FALSE

PRINT

-reset false

SELECTED_OUTPUT

-file P:\100040-7\phreeqc\WFR1td.dat

USER_PUNCH

-headings As Be Cl Pb U Ni Se SO4 Th Ra sOPb+
-headings wOPb+ PbX2 Anglesite sOHUO2+2
-headings wOUO2+ USiO4(C) Uraninite sONi+ wONi+
-headings NiSe sOHRa+2 wORa+ RaX2 RaSO4 wSeO4-
-headings wOHSeO4-2 wSeO3- wOHSeO3-2 Se(A)
-headings FeSe2 sSO4- wSO4- sOHSO4-2 wOHSO4-2
-headings gypsum wOTH+3 wOTH(OH)+2 wOTH(OH)2+
-headings wOTH(OH)3 wOTH(OH)4- sH2AsO3 wH2AsO3
-headings sH2AsO4 wH2AsO4 sHAsO4- wHAsO4- sAsO4-2
-headings wAsO4-2 sOHAsO4-3 wOHAsO4-3 sOBe+ wOBe+
-headings Calcite Ca Mg Na K HCO3 SO4 Cl TDS
-start
10 REM Convert to ppm and show molalities
20 PUNCH TOT("As")*74.9216*1000
30 PUNCH TOT("Be")*9.0122*1000
40 PUNCH TOT("Cl")*35.453*1000
50 PUNCH TOT("Pb")*207.19*1000/1.29e-11
60 PUNCH TOT("U")*238.029*1000
70 PUNCH TOT("Ni")*58.71*1000
80 PUNCH TOT("Se")*78.96*1000
90 PUNCH TOT("S(6)")*96.0616*1000
100 PUNCH TOT("Th")*232.038*1000/4.96e-8
110 PUNCH TOT("Ra")*226*1000/1.01e-9

120 PUNCH MOL("Hfo_sOPb+")
130 PUNCH MOL("Hfo_wOPb+")
140 PUNCH MOL("PbX2")
150 PUNCH EQUI("Anglesite")
160 PUNCH MOL("Hfo_sOHUO2+2")
170 PUNCH MOL("Hfo_wOUO2+")
180 PUNCH EQUI("USiO4(C)")
190 PUNCH EQUI("Uraninite")
200 PUNCH MOL("Hfo_sONi+")
210 PUNCH MOL("Hfo_wONi+")
220 PUNCH EQUI("NiSe")
230 PUNCH MOL("Hfo_sOHRa+2")
240 PUNCH MOL("Hfo_wORa+")
250 PUNCH MOL("RaX2")
260 PUNCH EQUI("RaSO4")
270 PUNCH MOL("Hfo_wSeO4-")
280 PUNCH MOL("Hfo_wOHSeO4-2")
290 PUNCH MOL("Hfo_wSeO3-")
300 PUNCH MOL("Hfo_wOHSeO3-2")
310 PUNCH EQUI("Se(A)")
320 PUNCH EQUI("Ferroselite")
330 PUNCH MOL("Hfo_sSO4-")
340 PUNCH MOL("Hfo_wSO4-")
350 PUNCH MOL("Hfo_sOHSO4-2")
360 PUNCH MOL("Hfo_wOHSO4-2")
370 PUNCH EQUI("gypsum")
380 PUNCH MOL("Hfo_wOTh+3")
390 PUNCH MOL("Hfo_wOTh(OH)+2")
400 PUNCH MOL("Hfo_wOTh(OH)2+")
410 PUNCH MOL("Hfo_wOTh(OH)3")
420 PUNCH MOL("Hfo_wOTh(OH)4-")
430 PUNCH MOL("Hfo_sH2AsO3")
440 PUNCH MOL("Hfo_wH2AsO3")
450 PUNCH MOL("Hfo_sH2AsO4")
460 PUNCH MOL("Hfo_wH2AsO4")
470 PUNCH MOL("Hfo_sHAsO4-")
480 PUNCH MOL("Hfo_wHAsO4-")
490 PUNCH MOL("Hfo_sAsO4-2")
500 PUNCH MOL("Hfo_wAsO4-2")
510 PUNCH MOL("Hfo_sOHAsO4-3")
520 PUNCH MOL("Hfo_wOHAsO4-3")
530 PUNCH MOL("Hfo_sOBe+")
540 PUNCH MOL("Hfo_wOBe+")
550 PUNCH EQUI("Calcite")
560 PUNCH TOT("Ca")*40.08*1000
570 PUNCH TOT("Mg")*24.312*1000
580 PUNCH TOT("Na")*22.9898*1000
590 PUNCH TOT("K")*39.102*1000
600 PUNCH MOL("HCO3-")*61.018*1000
610 PUNCH TOT("S(6)")*96.0616*1000

```

620 PUNCH TOT("Cl")*35.453*1000
630 A = (TOT("Ca")*40.08*1000)+(TOT("Mg")*24.312*1000)
640 B = (TOT("Na")*22.9898*1000)+(TOT("K")*39.102*1000)
650 C = MOL("HCO3-")*61.018*1000
660 D = TOT("S(6)")*96.0616*1000
670 E = TOT("Cl")*35.453*1000
680 PUNCH A+B+C+D+E
-end

```

SOLUTION 0 # SOURCE (ACL's) AGTI

pH	5.5
pe	6
units	mg/l
density	1
S(6)	3480
Cl	274
Alkalinity	3.1 as HCO3
Ca	456
Na	182
Mg	112
K	24
As	1.8
Fe	86
Be	1.64
Ni	13.0
Se	0.16
Si	24
U	11.9
Th	2.85e-6
Pb	4.57e-10
Ra	2.48e-7

SOLUTION 1-15 #MW-21A January 2001

units	ppm
pe	5.8
pH	6.12
S(6)	1220
Cl	50
Alkalinity	2.4 as HCO3
Ca	272
Na	79.6
Mg	80.4
K	13.2
Fe	95
As	0.0463
Be	0.014
Th	9.92e-10
Pb	2.19e-11

Ra	8.99e-9
Ni	0.30
Se	0.002
U	0.00112

SOLUTION 16-46 #MW-28 January 2001

units	ppm
pe	3.9
pH	6.86
S(6)	540
Cl	7.5
Alkalinity	2.8 as HCO3
Ca	150
Na	82
Mg	29
K	9.6
Fe	14
As	0.012
Be	0.005 #1/2 DL
Th	5e-9 #this value estimated
Pb	1.55e-11
Ra	1.81e-8
Ni	0.062
Se	0.0025 #1/2 DL
U	0.0045

EQUILIBRIUM_PHASES 1-46

Calcite	0.0	0.0
Gypsum	0.0	0.0
Uraninite	0.0	0.0
USiO4(c)	0.0	0.0
Ferroselite	0.0	0.0
Se(A)	0.0	0.0
RaSO4	0.0	0.0
NiSe	0.0	0.0
Anglesite	0.0	0.0

SURFACE 1-15

-equilibrate 1			
Hfo_wOH	0.086	600	45.9
Hfo_sOH	0.0021		

SURFACE 16-46

-equilibrate 16			
Hfo_wOH	0.086	600	45.9
Hfo_sOH	0.0021		

EXCHANGE 1-15

-equilibrate 1	
----------------	--

```

X      1.2

EXCHANGE 16-46
-equilibrate 16
X      1.2

TRANSPORT
-lengths          46*30.5
-dispersivities 46*50
-cells           46
-shifts          10
-punch_cells     46

PRINT
-selected_output  true

END

PRINT
-selected_output  false

SOLUTION 0 #33% REDUCTION

units  ppm
pH     5.66
pe     3.9
Ca     360.2
Mg     80.40
Na     136.0
K       19
Cl     183.0
Alkalinity 3.14 as HCO3
S(6)   2434
Fe     61.50
Th     1.89E-06
Pb     3.69E-10
Ra     1.70E-07
U       7.89
As     1.20
Se     0.11
Ni     8.64
Be     1.09
Si     15.90

TRANSPORT
-lengths          46*30.5
-dispersivities 46*50
-cells           46
-shifts          5
-punch_cells     46

```

```
PRINT
    -selected_output    true
```

```
END
```

```
PRINT
    -selected_output    false
```

```
SOLUTION 0 #50% Reduction
```

units	ppm
pH	5.80
pe	3.6
Ca	314.1
Mg	65.30
Na	114.0
K	17
Cl	140.0
Alkalinity	3.16 as HCO ₃
S(6)	1933
Fe	49.70
Th	1.43E-06
Pb	2.84E-10
Ra	1.33E-07
U	5.98
As	0.91
Se	0.08
Ni	6.56
Be	0.83
Si	12.10

```
TRANSPORT
    -lengths            46*30.5
    -dispersivities    46*50
    -cells              46
    -shifts            27
    -punch_cells       46
```

```
PRINT
    -selected_output    true
```

```
END
```

```
PRINT
    -selected_output    false
```

```
SOLUTION 0 #75% Reduction
```

units	ppm
pH	6.18

pe	3.0
Ca	242.1
Mg	41.60
Na	79.5
K	13
Cl	72.4
Alkalinity	3.18
S(6)	1152
Fe	31.40
Th	7.20E-07
Pb	1.50E-10
Ra	7.42E-08
U	2.99
As	0.46
Se	0.04
Ni	3.30
Be	0.42
Si	6.03

TRANSPORT

-lengths	46*30.5
-dispersivities	46*50
-cells	46
-shifts	40
-punch_cells	46

PRINT

-selected_output	true
------------------	------

END

PRINT

-selected_output	false
------------------	-------

SOLUTION 0 #90% Reduction

units	ppm
pH	6.57
pe	2.2
Ca	198.9
Mg	27.50
Na	58.8
K	11
Cl	31.8
Alkalinity	3.19 as HCO3
S(6)	682.8
Fe	20.40
Th	2.92E-07
Pb	7.02E-11
Ra	3.92E-08

U	1.20
As	0.19
Se	0.02
Ni	1.35
Be	0.17
Si	2.41

TRANSPORT

-lengths	46*30.5
-dispersivities	46*50
-cells	46
-shifts	527
-punch_cells	46

PRINT

-selected_output	true
------------------	------

END

PRINT

-selected_output	false
------------------	-------

#pH and Alkalinity for Source Terms: FILE: WFRsources.in
#Mixing of AGTI Tailing Waters With MW-27

SOLUTION 1 AGTI Water

units	ppm
pe	6
pH	5.50
Ca	456
Mg	112
Na	182
K	24
Cl	274
Alkalinity	3.10 as HCO ₃
S(6)	3480
Fe(2)	86
Th	2.85e-6
Pb	5.48e-10
Ra	2.48e-7
U	11.9
As	1.80
Se	0.16
Ni	13
Be	1.64
Si	24

END

SOLUTION 2 MW-27

units	ppm	
pe	4	
pH	6.99	
Ca	170	
Mg	18	
Na	45.0	
K	9.6	
Cl	4.7	
Alkalinity	3.20 as HCO ₃	
S(6)	370	
Fe(2)	13.0	
Th	0	
Pb	1.68e-11	
Ra	1.59e-8	
U	0.0045	
As	0.005	#1/2 DL
Se	0.0025	#1/2 DL
Ni	0.049	
Be	0.005	#1/2 DL

END

SELECTED_OUTPUT

-file P:\100040-7\phreeqc\WFRsources.dat

USER_PUNCH

-headings Ca Mg Na K Cl SO4 Fe Th Pb Ra U As Se Ni Be Si
-headings USiO4(c) Uraninite RaSO4 Th(OH)4(am)

10 PUNCH TOT("Ca")*40.08*1000
20 PUNCH TOT("Mg")*24.312*1000
30 PUNCH TOT("Na")*22.9898*1000
40 PUNCH TOT("K")*39.102*1000
50 PUNCH TOT("Cl")*35.453*1000
60 PUNCH TOT("S(6)")*96.0616*1000
70 PUNCH TOT("Fe")*55.847*1000
80 PUNCH TOT("Th")*232.038*1000
90 PUNCH TOT("Pb")*207.19*1000
100 PUNCH TOT("Ra")*226*1000
110 PUNCH TOT("U")*238.029*1000
120 PUNCH TOT("As")*74.9216*1000
130 PUNCH TOT("Se")*78.96*1000
140 PUNCH TOT("Ni")*58.71*1000
150 PUNCH TOT("Be")*9.0122*1000
160 PUNCH TOT("Si")*96.1155*1000
170 PUNCH SI("USiO4(c)")
180 PUNCH SI("Uraninite")
190 PUNCH SI("RaSO4")
200 PUNCH SI("Th(OH)4(am)")

MIX 1 #33% Reduction

1	0.66
2	0.34

END

MIX 2 #50% Reduction

1	0.50
2	0.50

END

MIX 3 #75% Reduction

1	0.25
2	0.75

END

MIX 4 #90% Reduction

1	0.10
2	0.90

END